THERAPEUTIC TARGETING OF INTRINSICALLY DISORDERED ANDROGEN RECEPTOR FUNCTIONAL DOMAINS IN PROSTATE CANCER

A DISSERTATION SUBMITTED TO THE FACULTY OF THE UNIVERSITY OF MINNESOTA BY

LUCAS J. BRAND

IN PARTIAL FULFILLMENT OF THE REQUIREMENTS FOR THE DEGREE OF DOCTOR OF PHILOSOPHY

SCOTT M. DEHM, ADVISOR

APRIL 2015

ACKNOWLEDGEMENTS

I would like to fervently thank my advisor, Dr. Scott Dehm, for his years of guidance, patience, and support. It has been my sincere honor to be mentored by such a respected and brilliant scientist, and more importantly, a great person.

Thanks are also due to past and present members of the Dehm lab: Dr. Yingming Li, Dr. Siu Chiu Chan, Dr. Michael Nyquist, and Ms. Sarita Mutha. For their technical expertise, advice, assistance, and camaraderie, I extend my warmest gratitude.

I would also acknowledge the assistance and mentorship of my thesis committee: Dr. Christopher Pennell, Dr. Carol Lange, Dr. Kaylee Schwertfeger, and Dr. Vivian Bardwell. Further thanks to Dr. Lange for providing breast cancer models and experimental conditions for experiments in Chapter 2.

This work received financial support from the National Institutes of Health, the United States Department of Defense, the American Cancer Society, the Prostate Cancer Foundation, and the University of Minnesota.

Experimental assistance in these studies was provided by the Masonic Cancer Center Analytical Biochemistry Core Facility at the University of Minnesota and the University of Texas Southwestern Medical Center tissue management shared resource, which are both supported by the National Cancer Institute.

DEDICATION

This work is dedicated foremost to my parents, John and Lola, for their many sacrifices and their lessons on hard work, honesty, integrity, and perseverance. I have often fallen short of those ideals, but without them I could never have come this far. This work is as much yours as it is mine, and I am proud to be your son.

For Mike, Bryce, and Jake, who supported me in my moments of despair (both warranted and unwarranted), and were always first in line to cheer me on no matter the occasion: I can't thank you enough for your friendship.

And finally, to my MICaB classmates: Kristin, Adam, Jeff, Ryan, Kristen, Casey, and Cara. It was a pleasure to learn with you, and I wish you all the best in your careers.

ABSTRACT

Prostate cancer (PCa) is a leading cause of morbidity and mortality in the United States, and contributes to a significant healthcare burden due to an overall lack of curative interventions for advanced-stage disease. Because PCa is largely insensitive to cytotoxic chemotherapy, the androgen receptor (AR) has long been the primary therapeutic target for the clinical management of locally advanced and metastatic PCa. Problematically, targeting AR signaling via androgen deprivation or treatment with AR antagonists is associated with progression to lethal, castration-resistant prostate cancer (CRPC) via a variety of molecular mechanisms that alter AR expression and function. However, CRPC is marked by a continued reliance on AR expression and activity. Thus, new modes of intervention with ability to durably repress AR activity in advanced CRPC are an unmet clinical need. In Chapter 1, we review the problem of castration resistance through a new paradigm of genetic rearrangements that produce truncated AR variants (ARV), which confer resistance to all current forms of AR-based PCa therapy. In Chapter 2, we discuss a novel AR inhibitor that directly targets the AR NH2-terminal transcriptional activation domain (NTD), but with significant off-target effects due to the lack of specificity for the intrinsically disordered NTD. In Chapter 3, we characterize the differences in NTD utilization between full length AR and ARV. Finally, in Chapter 4, we discuss a brief history of AR targeting in PCa, and offer a perspective on how future translational

studies can approach the problem of intrinsic disorder in the NTD to develop new interventions with more durable and lasting mechanisms of action.

TABLE OF CONTENTS

LIST OF TABLES

LIST OF FIGURES

LIST OF PUBLICATIONS

Brand LJ, Olson ME, Ravindranathan P, Guo H, Kempema AM, Andrews TE, Chen X, Raj GV, Harki DA, and Dehm SM. EPI-001 is a selective peroxisome proliferator activated receptor-gamma modulator with inhibitory effects on androgen receptor expression and activity in prostate cancer. Oncotarget 2015; In Press.

Brand LJ and Dehm SM. Androgen receptor gene rearrangements: new perspectives on prostate cancer progression. Current Drug Targets 2013; 14:441-9.

Bohrer LR, Liu P, Zhong J, Pan Y, Angstman J, Brand LJ, Dehm SM, Huang H. FOXO1 binds to the TAU5 motif and inhibits constitutively active androgen receptor splice variants. Prostate 2013; 73:1017-27.

Li Y, Chan SC, Brand LJ, Hwang TH, Silverstein KA, and Dehm SM. Androgen receptor splice variants mediate enzalutamide resistance in castration-resistant prostate cancer cell lines. Cancer Research 2013; 73:483-9.

CHAPTER 1

ANDROGEN RECEPTOR GENE REARRANGEMENTS: NEW PERSPECTIVES ON PROSTATE CANCER PROGRESSION

OVERVIEW

The androgen receptor (AR) is a master regulator transcription factor in normal and cancerous prostate cells. Canonical AR activation requires binding of androgen ligand to the AR ligand binding domain, translocation to the nucleus, and transcriptional activation of AR target genes. This regulatory axis is targeted for systemic therapy of advanced prostate cancer. However, a new paradigm for AR activation in castration-resistant prostate cancer (CRPC) has emerged wherein alternative splicing of AR mRNA promotes synthesis of constitutively active AR variants that lack the AR ligand binding domain (LBD). Recent work has indicated that structural alteration of the AR gene locus represents a key mechanism by which alterations in AR mRNA splicing arise. In this review, we examine the role of truncated AR variants (ARVs) and their corresponding genomic origins in models of prostate cancer progression, as well as the challenges they pose to the current standard of prostate cancer therapies targeting the AR ligand binding domain. Since ARVs lack the COOH-terminal LBD, the genesis of these AR gene rearrangements and their resulting ARVs provides strong rationale for the pursuit of new avenues of therapeutic intervention targeted at the AR NH_2-terminal domain. We further suggest that

genomic events leading to ARV expression could act as novel biomarkers of disease progression that may guide the optimal use of current and next-generation AR-targeted therapy.

INTRODUCTION

The AR is a 110 kDa protein with a modular domain organization found in members of the steroid hormone receptor superfamily [1,2]. The NH_2-terminal domain (NTD), also referred to as transcriptional activation function (AF)-1, is a potent transcriptional activation domain in isolation and is responsible for the majority of AR transcriptional activity through the recruitment of diverse co-regulatory proteins. The central domain of the AR is the DNA binding domain (DBD), which is comprised of two zinc-finger motifs. The first zinc finger is responsible for making direct contact with the DNA major groove of an androgen response element (ARE) half-site, while the second zinc finger mediates dimerization with a second AR molecule bound to an adjacent ARE half-site [3]. The DBD is followed by a short, flexible hinge region which contains the bipartite nuclear localization signal. The COOH-terminal domain (CTD) of the AR houses both the ligand binding domain (LBD) and a secondary transcriptional activation domain termed AF-2.

The primary role of the AR is to sense and respond to circulating androgens, the most abundant of which are testosterone and dihydrotestosterone (DHT) [4,5]. In the absence of ligand stimulation, AR is

cytoplasmic, bound in a chaperone complex of heat shock proteins and high molecular weight immunophilins, which maintains AR protein in an inactive conformation with a high affinity for ligand binding [6]. Following ligand binding, the AR undergoes a conformational change, causing dissociation of a subset of chaperone proteins and exposing the nuclear localization signal in the hinge region. Upon translocation of the AR/DHT complex to the nucleus, the AR DBD engages with genomic AREs [7], mediating chromosomal looping and structural reorganization of the genome [8-10]. In order for productive gene transcription to occur, the AR is reliant on interactions with a wide variety of transcriptional co-regulators, of which nearly 200 have been identified to date [11]. These transcriptional co-regulators form large complexes that result in recruitment of the basal transcriptional machinery and a finely-tuned level of androgen-responsive gene transcription [12,13]. In healthy prostate tissue, these androgen-responsive genes are important for normal prostate architecture, homeostasis, and physiological function. In prostate cancer (PCa), these target genes support ongoing proliferation and survival of tumor cells.

Structure and Function of the AR COOH-Terminal Domain

The CTD of the AR is the best understood functional domain by virtue of its structural homology and regulatory similarities with other steroid receptors [14]. The AR gene locus, located at Xq11-12, is approximately 180 kilobases in length and consists of eight coding exons separated by intronic segments of varying length. Exon 1 codes for the entire AR NTD, or approximately 60% of the

total protein, while exons 2 and 3 code for the two zinc finger domains of the AR DBD. Exons 4-8 are located in close proximity to one another in the AR gene locus, and code for the hinge region and CTD/LBD of the AR (Figure 1.1). Importantly, all AR-targeted therapeutics currently approved for clinical use modulate AR activity by exerting action on this domain [15]. The CTD contains 11 α-helices that form the binding pocket of the AR LBD, while a twelfth helix

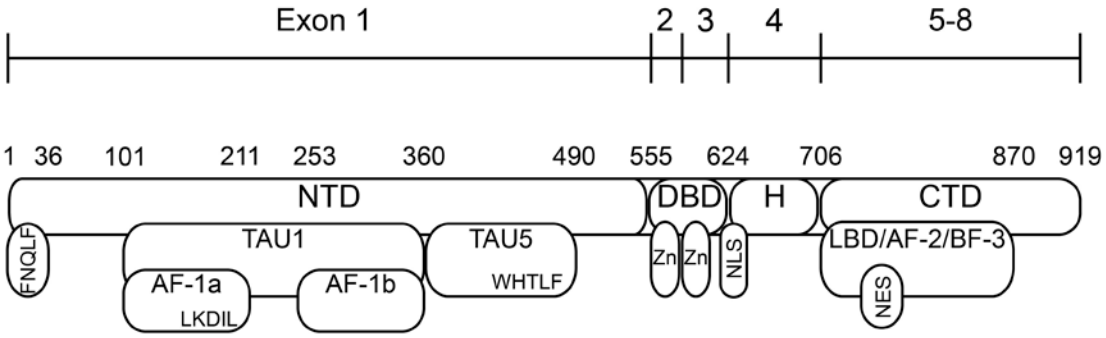

Figure 1.1: Androgen Receptor Functional Domains. The AR possesses a modular domain organization common to members of the steroid hormone receptor family of nuclear receptor transcription factors. The amino-terminal domain (NTD) harbors transcriptional activation units (TAU)-1 and TAU-5. Transcriptional activation function (AF)-1a and AF-1b are subdomains of TAU-1. The DNA binding domain (DBD) is comprised of two zinc finger motifs (Zn), and a flexible hinge (H) region containing the AR nuclear localization signal (NLS). The COOH-terminal domain (CTD) harbors the ligand binding domain (LBD), a ligand-regulated nuclear export signal (NES), and the protein interaction domains AF-2 and binding function (BF)-3.

forms a “kickstand” which locks into place upon androgen binding [16-18]. This upswing of helix 12 stabilizes AR binding to DHT and forms the AF-2 protein interaction interface [19,20]. AF-2 has been shown to exert transcriptional activity in the presence of bound agonist by binding to nuclear receptor (NR)-box motifs in coactivators, such as SRC-2 [19], and is also capable of mediating intramolecular interaction with FxxLF or WxxLF motifs in the AR NTD [21].

Furthermore, the CTD contains a ligand-regulated nuclear export signal which is dominant over the AR nuclear localization signal but is inhibited by ligand binding [22].

Recent work has provided evidence for a second protein interaction domain within the CTD, termed binding function (BF)-3, which communicates allosterically with AF-2 [23,24]. Interestingly, a host of mutations identified in both PCa and androgen insensitivity syndrome map to BF-3, supporting the concept that this domain may play an important role in allosteric regulation of AR function [25]. Another recent study provided evidence that FKBP52, a co-chaperone protein critical for maintaining AR in a conformation competent for ligand binding, may interact with AR through the BF-3 domain [26]. Importantly, these critical AF-2/BF-3 mediated functions are amenable to targeting with small molecules [23,26-28] which could potentially lead to new avenues of AR-targeted therapy.

Therapeutic Targeting of the COOH-Terminal Domain in Prostate Cancer

PCa is the most frequently diagnosed male cancer and second leading cause of cancer deaths [29]. For tumors that are relapsed, locally advanced, and/or metastatic, the current standard of care is androgen deprivation therapy (ADT), achieved by suppression of AR signaling through the use of AR antagonists such as bicalutamide or flutamide, or by preventing production of testosterone by the testes using gonadotropin releasing hormone agonists such as leuprolide [15]. ADT initially provides a robust therapeutic benefit by blocking tumor cell proliferation and inducing apoptosis, resulting in clinical regression.

Invariably, however, AR signaling is eventually reactivated via diverse mechanisms including AR amplification and/or AR protein overexpression, gain of function AR mutations [30,31], enhanced uptake and conversion of adrenal androgens, or *de novo* androgen synthesis by tumor cells [32]. These mechanisms have been reviewed in detail elsewhere [33-35]. These molecular events mark a transition from the initial androgen-dependent PCa to a lethal form of the disease, referred to as “castration-resistant PCa” (CRPC). Enzalutamide (formerly MDV3100), which is an AR antagonist that excludes AR from the nucleus, and abiraterone acetate, which blocks peripheral androgen synthesis by inhibiting CYP17, were developed to address these mechanisms of disease progression [36,37]. In Phase III trials, abiraterone and enzalutamide increased overall survival CRPC patients by 3.9 and 4.8 months, respectively [38,39]. Clinical trials have demonstrated that both drugs provide significant therapeutic benefit to a high proportion of patients [38-40], but a subset of patients continue to experience disease progression, either through acquired resistance or through *de novo* insensitivity prior to treatment. Currently, it is of major interest to identify mechanisms that may drive these types of resistance to help develop next-generation AR-targeted therapies. Importantly, unlike other steroid hormone receptors in which AF-2 is the dominant transactivation domain, the AR NTD is responsible for the majority of AR transactivation [19]. Therefore, recent work describing the discovery and characterization of constitutively active AR splice variants which lack the CTD regulatory domain have generated significant interest, as these species may be capable of restoring AR signaling in PCa

tissues following ADT through a mechanism of constitutive AR NTD transcriptional activity.

CONSTITUTIVELY ACTIVE AR SPLICE VARIANTS PROMOTE CASTRATION RESISTANCE IN PROSTATE TUMORS

Splice variants of the AR have been recognized for over two decades in the context of loss-of-function splicing alterations in androgen insensitivity syndrome, which is a topic that has been reviewed in detail elsewhere [41]. The first gain-of-function AR splice variant (ARV) was identified in 22Rv1 cells due to the presence of a smaller, 75-80 kDa AR immunoreactive species on western blot that was initially thought to be a proteolytic degradation fragment of full length AR [42]. This AR subspecies was shown to lack a ligand binding domain and was constitutively active in both the presence and absence of androgen. Similarly, a subsequently identified Q640Stop mutation resulted in premature truncation and constitutive AR signaling in bone metastases from a patient who relapsed following ADT with luprorelin and flutamide [43]. It was initially postulated that the smaller band observed in the 22Rv1 cell line resulted from calpain-mediated cleavage of full length AR at a consensus calpain recognition site in the AR hinge region [44]. However, later work demonstrated that RNA interference (RNAi) targeted against AR exon 7 (Figure 1.1) had no effect on expression levels of the smaller species, despite robust ablation of full length AR. Conversely, RNAi targeted against AR exon 1 led to ablation of both the full

length and the truncated species [45]. These data strongly suggested that the truncated ARV was not a product of full length AR mRNA or protein, but instead derived from an alternate mRNA species. The ability to differentially target full-length vs. truncated ARV species with discrete RNAi reagents further revealed that the constitutive activity of the truncated ARV was the driving force behind the androgen independent proliferation of 22Rv1 cells.

Since their initial identification, nearly a dozen different ARV mRNA species have been identified in PCa cell lines, xenografts, and clinical samples [41]. ARVs arise as a result of the incorporation of alternative, or cryptic, exons coded for in the AR gene locus [45-48], or through an exon skipping mechanism in which non-contiguous AR exons are spliced together [49]. Characterization of these novel ARV mRNAs has revealed multiple alternative, or “cryptic” exons in the AR locus, most of which flank AR exon 3. For example, alternative exon 2b (also termed cryptic exon 4, or “CE4”) is located upstream of exon 3, whereas many others are within AR intron 3 (CE1, CE2, CE3, CE5, and exon 3'). The products of these splicing aberrations generally incorporate canonical AR exons 1-3, which code for the AR NTD as well as the DBD. These three exons appear to form the minimum requirement for a transcriptionally active ARV [50]. However, ARVs differ in their utilization of exons 4-8, with most ARVs incorporating one of the seven currently identified cryptic exons coded for by the AR locus [41]. Problematically, multiple naming systems have been proposed to refer to the various ARVs. For example, the ARV encoded by contiguously spliced exons 1, 2, 3, and 2b has been alternately named AR-V4 [47], AR5 [46],

and ARV6 [48]. Therefore, for the purposes of this review, we will refer to the variants by their exon composition, e.g. AR 1/2/3/2b, to alleviate confusion. To date, only three ARV transcripts have been mechanistically investigated in cell lines, xenografts, or clinical samples: AR 1/2/3/CE3, AR 1/2/3/2b, and AR 1/2/3/4/8.

The most studied and currently best characterized ARV is coded for by AR exons 1/2/3/CE3, alternatively termed AR-V7 and AR3 [46,47]. AR 1/2/3/CE3 has been shown to be expressed at the mRNA and protein level in normal and cancerous prostate tissue, multiple commonly used PCa cell lines, and human tumor xenografts. Expression of this isoform was also demonstrated to be increased in locally recurrent and metastatic castration resistant PCa tissue compared to prostatectomy specimens from hormone naïve men [46]. A separate study found that 1/2/3/CE3 mRNA expression levels in prostatectomy specimens could predict the likelihood of biochemical recurrence after surgery [47]. Biochemically, 1/2/3/CE3 was shown to function as a constitutively active transcription factor independent of androgen ligand [46]. However, the exact transcriptional program mediated by this variant may differ slightly from full-length AR. In one study, transient transfection of LNCaP cells with an AR 1/2/3/CE3 expression vector was shown to effect a strikingly similar transcriptional program compared with ligand-activated full length AR [47]. On the other hand, a second study using targeted siRNA knockdown of endogenous full length AR versus 1/2/3/CE3 demonstrated that the CE3 isoform activated Akt expression, whereas full-length AR did not [47]. More recently, Hu and colleagues [51] have reported

a unique role for AR 1/2/3/CE3 in the activation of M-phase specific cell cycle genes. For example, whereas full-length AR target genes appeared to be largely associated with pathways important for biosynthesis and metabolism, the 1/2/3/CE3 variant was able to activate transcription of pro-mitotic cell cycle regulators such as UBE2C, CDCA5, ZWINT, TPX2, and CDC25C. Taken together, these data strongly support a role for the AR 1/2/3/CE3 splice variant as a constitutively active AR isoform with significant clinical implications for biology and treatment of castration resistant PCa tumors.

The AR 1/2/2b and AR 1/2/3/2b mRNA variants were initially identified by 5' RACE experiments in the 22Rv1 cell line [45]. Specific knockdown of these ARVs using an exon 2b-targeted siRNA resulted in an expected reduction in the truncated 75-80 kDa AR species, suggesting that one or both of the 1/2/2b and 1/2/3/2b mRNAs were translated. However, our laboratory recently developed an antibody specific to the COOH-terminal extension encoded by AR exon 2b, which revealed that only the AR 1/2/3/2b variant is productively translated to functional protein in 22Rv1 cells [50]. Importantly, siRNA knockdown of AR 1/2/3/2b significantly reduced the ability of 22Rv1 cells to proliferate in the absence of androgen, but had no effect on androgen dependent proliferation, supporting a role for this ARV as a driver of castration resistance in 22Rv1 cells [45].

Finally, AR 1/2/3/4/8 was shown to arise through the skipping of exons 5-7 in the mRNA transcript [49]. This exon skipping event places exon 8 out-of-frame, resulting in formation of a premature translation termination codon in exon 8. This variant, originally named AR^{v567es}, is expressed at the mRNA level in a

wide range of normal and cancerous prostate tissues, although protein expression has not yet been confirmed using variant-specific antibodies. Sun and colleagues also demonstrated that AR 1/2/3/4/8 mRNA is expressed endogenously in the LuCaP 86.2 and 136 xenografts, and inferred that this protein was expressed endogenously due to its molecular weight. Interestingly, upon castration, mRNA levels of AR 1/2/3/4/8 increased in these xenografts compared with intact hosts. When expressed ectopically in LNCaP cells, AR 1/2/3/4/8 displayed constitutive transcriptional activity and could interact directly with full length AR, resulting in enhanced ligand dependent and -independent activity of the full length receptor in these cells. A later study by Hu and colleagues demonstrated that a novel ninth exon, located downstream of AR exon 8, was incorporated into the mRNA transcript of this AR 1/2/3/4/8 variant in VCaP cells [51]. However, because incorporation of exon 9 does not affect the premature translation stop codon in exon 8, this exon simply alters the 3' untranslated region of this mRNA. Therefore, AR 1/2/3/4/8/9 mRNA codes for exactly the same protein as AR 1/2/3/4/8 mRNA, and thus it is not surprising that this variant displayed constitutive, ligand independent activity in promoter-reporter assays. Interestingly, in this study, the strength of AR 1/2/3/4/8/9 transcriptional activity appeared to depend on which cell line it was tested in, with higher activity apparent in PC-3 vs. LNCaP PCa cell lines.

Although all active gain of function ARVs identified to date consist of the AR NTD and DBD, they harbor unique COOH-terminal extensions encoded by the various exons that can be spliced into the 3' mRNA termini of AR variant

transcripts. This has been proposed to bear significant implications for ARV biochemistry because the bipartite nuclear localization signal (NLS), $RKx_{10}RKLKK$, spans the exon 3-4 junction in wild type AR [52]. Therefore, since most of the ARV mRNAs identified to date do not harbor exon 4, the bipartite NLS would be disrupted in these variants. However, recent work has demonstrated that the AR NTD/DBD core displays a high level of constitutive nuclear localization in the absence of ligand that is independent of both HSP90 and the nuclear import adapter protein importin-β, resulting in transcriptional activation of endogenous AR targets [50]. Moreover, this study demonstrated that differences in ARV transcriptional activity that have been observed are promoter-dependent phenomena as opposed to arising from differential rates of nuclear access.

GENOMIC REARRANGEMENTS PROMOTE DISEASE PROGRESSION AT MULTIPLE STAGES OF PROSTATE CANCER DEVELOPMENT

Gene Rearrangements Prior to ADT: From PIN to PCa and Beyond

Beginning with the discovery of recurrent Ets-family gene rearrangements in 2005 [53], it has become increasingly clear that structural alterations are frequent events in the PCa genome and underpin many aspects of tumor biology and disease progression. These events include the highly prevalent TMPRSS2-Ets family of gene fusions [53] as well as fusions involving Raf family members [54]. A number of other rearrangements have also been identified in primary

prostate tumors, which may represent novel mechanisms for driving tumor invasiveness, proliferation/survival, and anchorage-independent growth in PCa [55,56]. These gene rearrangements have been reviewed in detail elsewhere [57]. More recently, chromosomal alterations involving the PTEN locus have been shown to cooperate with allelic loss to drive PCa progression [[58]. Interestingly, this mechanism of PTEN inactivation, as well as the rearrangements reported by Pflueger *et al.* [56], was highly correlated with underlying TMPRSS2-ERG chromosomal rearrangement, supporting a role for Ets family rearrangements as a genome-destabilizing event early in prostate tumorigenesis. This may also explain the observation that patients with fusion-positive PCa experience more aggressive and lethal disease compared with fusion-negative cases [59,60], though a number of studies have reported that TMPRSS2:Ets rearrangement may alternatively correlate with low Gleason grade [61], favorable prognosis [62], or may not be predictive of disease outcome at all [63]. Regardless, clinical samples from men with metastatic castration-recurrent PCa exhibit a wide range of mutations, deletions, and rearrangements as determined by exome sequencing [64]. Overall, these genomic rearrangements have been shown to be associated with and predictive of PCa genesis and/or progression, such that molecular subtyping of based on these criteria may result in improvements in patient management and/or clinical trial designs [57].

Rearrangements of the AR Locus: a New Paradigm for ARV Expression and Activity Following ADT?

These recent whole genome studies have also supported the long-held fundamental concept that the AR signaling axis is a critical master regulator in PCa. Foremost, this axis has been shown to be the most frequently-altered pathway in hormone-naïve PCa, and 100% of castration-resistant PCa metastases display genomic and/or mRNA expression alterations in this pathway, most frequently in the AR gene itself [66]. The observation that AR exon 2b is incorporated into the 1/2/3/2b transcript downstream of exon 3 in 22Rv1 cells, despite the fact that 2b is located 5' of exon 3 in the normal reference genome [45,47] (Figure 1.2), raised an intriguing question: what is the molecular basis for this splicing pattern? One clue came from the observation that the full-length AR in 22Rv1 cells is slightly larger due to an extra zinc finger in the DBD encoded by tandem duplication of AR exon 3. Interestingly, in addition to these unanticipated splicing patterns, it was demonstrated that the 22Rv1 cell line exhibits significantly increased mRNA expression of the AR 1/2/3/CE3 variant [65]. In the same study, the androgen-dependent CWR22Pc cell line, which was derived from the same original CWR22 xenograft model as 22Rv1, was found by quantitative RT-PCR analysis to express extremely low but detectable transcript expression of these ARVs. These observations suggested that the observed splicing patterns may not be true “alternative splicing” events in 22Rv1 cells, but may instead be due to an underlying alteration in AR gene structure. Indeed, interrogation of AR gene structure demonstrated that the region harboring exon 2b, 3, and CE1-3 was present in the genome at two-fold higher copy number in castration-recurrent 22Rv1 cells, but not CWR22Pc, suggesting the presence of

a tandem duplication [65]. More detailed analysis confirmed that a ~35kb segment, comprised of exon 3 and its flanking cryptic exons, was involved in a tandem duplication event within 22Rv1 cells (Figure 1.2). Importantly, long term culture of the lineage-related CWR22Pc cell line in the absence of androgen resulted in the outgrowth of a castration resistant population of cells that harbored the exact same break fusion junction and repair signature as 22Rv1, and displayed increased expression of truncated ARVs mRNAs and proteins

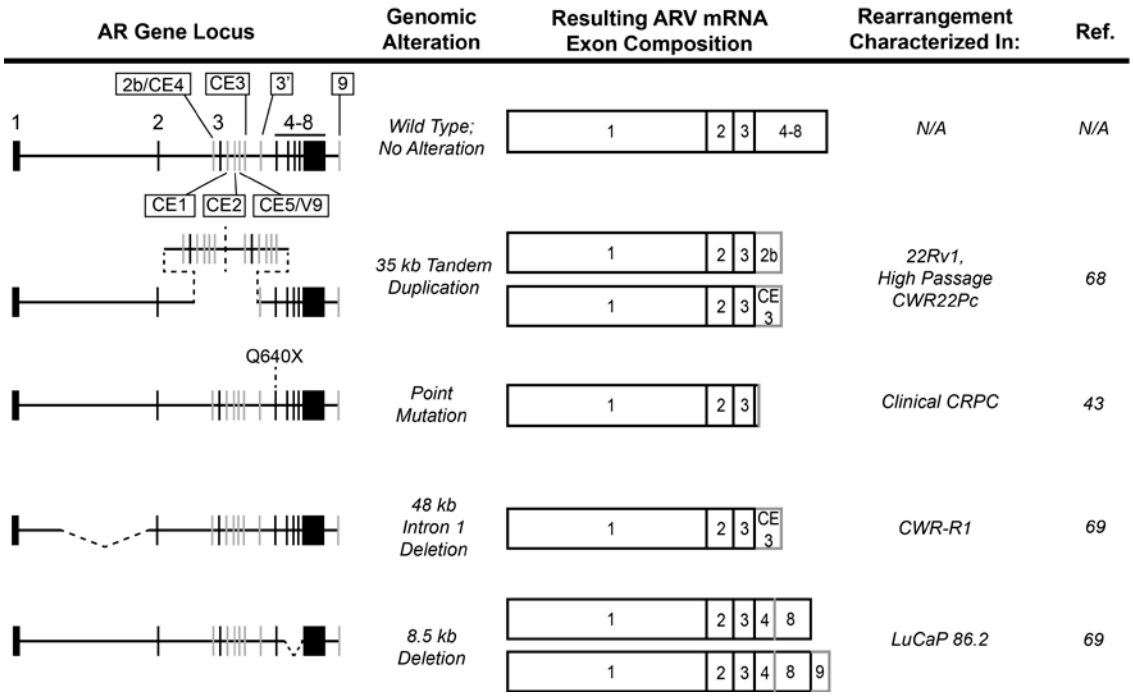

Figure 1.2: AR Genomic Alterations and Altered Splicing Patterns Leading to ARV Expression. The 180 kb androgen receptor gene locus harbors eight canonical exons (black vertical hashes) that code for the wild type AR mRNA and protein (black boxes). Seven alternative, or cryptic, exons have also been identified (gray vertical hashes) that can be incorporated into the AR transcript upon activation of alternative splicing pathways (gray borders/boxes). Four discrete AR gene rearrangements or mutations, depicted as dashed black lines, have been shown to disrupt AR splicing and favor the expression of AR variants in PCa cell lines and xenografts.

including 1/2/3/2b and 1/2/3/CE3. These data indicate that a subset of cells within the original CWR22 tumor harbor this rearrangement and are driven by constitutive, ligand-independent ARV activity prior to androgen deprivation. In this cell line, ADT simply results in selective outgrowth of these ARV-driven cells harboring the 35kb tandem duplication. Importantly, complex patterns of AR gene copy imbalance were also observed in metastatic CRPC samples, but not in hormone-naïve primary tumors [65], suggesting that generation of constitutively active ARV through genomic rearrangements may be a recurring theme in human disease progression.

Interestingly, ARV have also been described in the mouse PCa cell line Myc-CaP [66], in which the AR is amplified through genomic copy number gain. Mouse AR (mAR)-V2 was shown to result from splicing of exons 1-3 together with a novel cryptic exon located ~250 kb downstream of the AR gene locus. Perhaps even more compelling, a second ARV termed mAR-V4 was generated by splicing of exons 1-4 and a novel cryptic exon located nearly 1 Mb upstream of the AR transcriptional start site. Whereas mAR-V2 showed little activity in functional assays, mAR-V4 was constitutively active and localized to the nucleus, similar to ARVs identified in human cell lines and tissues. Though the molecular basis for splicing of mAR-V4 was not addressed in this study, it is likely contingent upon the known amplification of the AR gene in Myc-CaP cells. Following this rearrangement of the AR gene, the V4 cryptic exon could be situated downstream of the AR open reading frame, thus accounting for the incorporation of the V4 exon at the 3' terminus of the transcript.

Further investigation of genomic copy number imbalance in additional models of CRPC progression has confirmed AR gene rearrangements as an important mechanism involved in the generation of constitutively active ARVs [67]. Multiplex ligation dependent probe assays (MLPA) were employed to query the copy number of AR exons in a variety of PCa cell lines and tissues. Interestingly, LuCaP 86.2 cells displayed reduced copy number of AR exons 5-7, which was shown subsequently to result from an 8.5kb intragenic deletion of this genomic segment (Figure 1.2). Clearly, deletion of AR exons 5-7 provides an attractive mechanistic explanation for synthesis of the AR 1/2/3/4/8 variant in this xenograft model [49]. Interestingly, deletion of exons 5-7 prevents synthesis of full-length AR, indicating that this CRPC tumor would no longer be driven by androgen/AR signaling, but rather depends exclusively on the AR 1/2/3/4/8 variant for ongoing growth and survival.

An additional model of CRPC that has been shown to express high levels of truncated ARVs is the CWR-R1 cell line. To determine the basis for the splicing alterations in this model, Illumina paired-end massively parallel sequencing was employed to determine the sequence and structure of the AR locus [67]. This approach detected copy number loss spanning a 48 kb region of AR intron 1 (Figure 1.2), which was supported by MLPA data querying copy number throughout AR intronic sequences. Interestingly, this deletion was initially observed only within a subpopulation of CWR-R1 cells. However, long term culture of CWR-R1 cells in androgen-depleted growth medium resulted in the outgrowth of the deletion-positive population. Importantly, the outgrowth of

this subpopulation was accompanied by a corresponding increase in the protein expression of the constitutively active AR 1/2/3/CE3 variant. This finding supports the possibility that within at least some prostate tumors, subpopulations of ARV-driven cells with underlying rearrangements in the AR gene may exist prior to administration of AR-targeted therapies and, by virtue of constitutively active ARV expression, be able to overcome any drug in the current arsenal of AR-based therapies to repopulate the tumor. Based on the finding that ARV expression is an important feature of CRPC progression [46,47,49,68,69] and these recent data demonstrating AR gene rearrangements as a mechanism for altered AR splicing [65,67], it is possible that AR gene rearrangements may represent a new class of genomic markers with predictive and/or prognostic value in CRPC.

STRUCTURE AND FUNCTION OF THE AR NTD

The role of ARVs in clinical PCa and castration resistance highlights the need for a greater understanding of NTD structure and function to aid in the design of AR-targeted therapeutics that do not require an intact AR LBD. The principal role of the NTD is to serve as a docking site for AR transcriptional co-regulators [70], and it is well established that the NTD is the predominant transcriptional activation domain of the AR [2,19,71]. This stands in contrast to other steroid hormone receptors, in which the CTD harbors the primary transcriptional activation domain [19]. The NTD is divided into two primary

transcriptional activation units (TAUs) termed TAU-1 and TAU-5, which have been shown to have distinct roles in AR-mediated transcription [2,72] (Figure 1.1). The TAU-5 domain maps to amino acids 361-490 of the AR NTD, and has been shown to promote AR activity specifically under conditions of low/no androgens [72,73]. Deletion of TAU-5 causes near-complete loss of AR function in the absence of DHT in both androgen dependent LNCaP [72] and castration resistant C4-2 cells [73]. Further work mapped TAU-5 activity to a conserved Trp-His-Thr-Leu-Phe (WHTLF) motif, and deletion or mutation of the hydrophobic W/L/F residues to alanine significantly inhibited androgen independent AR activity [71]. Interestingly, however, a recurring W435L mutation found in metastatic PCa tissue from patients relapsing after ADT was shown to increase ligand-dependent AR transcriptional activity, possibly through stabilization of an N/C intramolecular interaction between this domain and the AF-2 region [31].

The other major domain within the NTD, TAU-1, maps to amino acids 101-360 and houses two smaller subdomains, known as activation function (AF)-1a (amino acids 101-211) and AF-1b (amino acids 252-360). Deletion of either of the AF-1 sub domains causes complete loss of AR transcriptional activity in both androgen dependent LNCaP cells as well as castration resistant C4-2 cells, whereas deletion of the internal spacer region between AF-1a and -1b actually enhances AR transcription [73]. The transcriptional activity of TAU1 has traditionally been ascribed to an LxxLL-like motif, LKDIL, located within AF-1a [69]. Deletion or mutation of this sequence causes significant loss of AR activity, similar to deletion of the entire AF-1a fragment [70]. Intriguingly, the LKDIL motif

overlaps an Lx_7LL motif described by Zhu and colleagues [74], which is critical for mediating interaction with the transcriptional co-repressor NCoR and its binding partner TAB2. When TAB2 was phosphorylated by MEKK1, the NCoR/TAB2 complex was released, resulting in AR de-repression. However, no transcriptional co-activators have yet been identified that specifically bind to the LKDIL motif following co-repressor dissociation [75]. Furthermore, attributing TAU-1 activity exclusively to LKDIL does not account for the transcriptional loss observed upon deletion of AF-1b, suggesting that other elements within the TAU-1 domain may be important to the activity of this region [73].

Therapeutic Targeting of the AR NTD

The AR represents a nearly ideal drug target, in that pharmacologic targeting of the AR signaling axis produces profound results on prostate tumor biology with relatively minimal toxic side effects. While therapies that require an intact AR LBD have proven effective in treating PCa, mounting evidence suggests that the CTD may be ultimately dispensable for AR function in the context of CRPC. Observations of CTD-truncated ARVs, which function as potent, constitutively active transcription factors independent of the CTD, suggest that the NTD itself could be an alternative target for inhibition of AR transcriptional activity. Despite significant progress in defining the structural and functional composition of the AR NTD with the goal of therapeutic targeting, one principal challenge is the inherent flexibility and lack of tertiary structure throughout the NTD [76]. These structural characteristics are likely to be of

fundamental importance to the transcriptional activity of the AR, but they have also proven to be a major obstacle to crystallographic analysis of AR structure and subsequent intelligent drug design. Nonetheless, two promising classes of drugs have recently been identified that seem to interact specifically with the NTD to mediate its inhibition. EPI-001 is a chlorinated bisphenol A diglycidyl ether (BADGE) identified in a high-throughput screen for compounds that could inhibit AR NTD activity. EPI-001 was demonstrated to function by preventing binding of the CBP/p300 histone acetyltransferase to the AR NTD, thereby preventing AR activity at target gene enhancers and preventing outgrowth of castration recurrent tumors in a xenograft model [77,78]. A similar drug screen for compounds isolated from the marine sponge *Niphates digitalis* identified a class of drugs termed Niphatenones [79], which were shown by click chemistry to covalently bind to an unknown portion of the AR NTD. This binding was shown to rely on a glycerol ether substructure and an extended saturated alkyl chain flanking the central ketone of Niphatenone B, which was shown to mediate growth inhibition in AR-expressing LNCaP cells but not AR-negative PC3 cells. These data suggest that the effect is AR specific, though no studies were performed to rule out effects on other steroid hormone receptors. Importantly, these compounds have not yet been tested against cell or xenograft models bearing truncated ARV, a critical experiment that will likely determine their impact and usefulness in the long-term maintenance of PCa. Taken together, however, the recent identification of these AR NTD inhibitors provides strong proof of principle that the NTD remains a vital and viable therapeutic target, and may be a

key to containing the progression of late-stage PCa.

SUMMARY AND FUTURE DIRECTIONS

The discovery and characterization of ARVs has indicated that tumors driven by these species may represent a clinically relevant molecular subtype of CRPC that may require different therapeutic intervention than tumors only harboring full length AR. Whereas Ets family gene rearrangements have been proposed as a specific biomarker of PCa, high levels of ARV expression may serve as a marker of true androgen independence: ARV-positive tumors are highly unlikely to respond to any currently available antiandrogens or ADT strategies. Even next-generation AR targeted therapies, including the potent antiandrogen enzalutamide and induction of a super-castrate state with the CYP17 inhibitor abiraterone, fail to provide clinical benefit in a significant fraction of patients. It is tempting to hypothesize that these patients might progress due to AR gene rearrangements and/or expression of ARVs that lack the domain targeted by these new drugs. Used in conjunction with the classification schema suggested by Rubin and colleagues [57], ARV status could serve as an additional biomarker to inform the optimal use of current and next-generation ADT, as well as non-AR based therapies, in the treatment of PCa.

AUTHOR'S NOTE

This chapter was reproduced from a review published in *Current Drug Targets*

[80] and is © Bentham Science Publishers, 2013. Reprinted by permission of Eureka Science, Ltd.

CHAPTER 2

EPI-001 IS A SELECTIVE PEROXISOME PROLIFERATOR-ACTIVATED RECEPTOR-GAMMA MODULATOR WITH INHIBITORY EFFECTS ON AR EXPRESSION AND ACTIVITY IN PROSTATE CANCER

OVERVIEW

The androgen receptor (AR) is a driver of prostate cancer (PCa) cell growth and disease progression. Therapies for advanced PCa exploit AR dependence by blocking the production or action of androgens, but these interventions inevitably fail via multiple mechanisms including mutation or deletion of the AR ligand binding domain (LBD). Thus, the development of new inhibitors which act through non-LBD interfaces is an unmet clinical need. EPI-001 is a bisphenol A-derived compound shown to bind covalently and inhibit the AR NH_2-terminal domain (NTD). Here, we demonstrate that EPI-001 has general thiol alkylating activity, resulting in multilevel inhibitory effects on AR in PCa cell lines and tissues. At least one secondary mechanism of action associated with AR inhibition was found to be selective modulation of peroxisome proliferator activated receptor-gamma (PPARγ). These multi-level effects of EPI-001 resulted in inhibition of transcriptional activation units (TAUs) 1 and 5 of the AR NTD, and reduced AR expression. EPI-001 inhibited growth of AR-positive and AR-negative PCa cell lines, with the highest sensitivity observed in LNCaP cells. Overall, this

study provides new mechanistic insights to the chemical biology of EPI-001, and raises key issues regarding the use of covalent inhibitors of the intrinsically unstructured AR NTD.

INTRODUCTION

Prostate cancer (PCa) is the most commonly diagnosed male cancer in the US with approximately 233,000 new cases and 30,000 deaths predicted in 2014 [29]. Normal and cancerous prostate tissues are dependent on activation of the androgen receptor (AR) to support cell proliferation and survival [81,82]. Thus, inhibiting AR activation serves as the basis for treating metastatic disease [83]. However, these therapies ultimately fail via a variety of molecular mechanisms [84]. Importantly, these castration-resistant PCa (CRPC) tumors remain AR-dependent, as evidenced by the increased overall survival of patients treated with second-generation androgen deprivation therapies enzalutamide [39,85,86] and abiraterone [87]. Despite these advances, resistance to enzalutamide and abiraterone is frequent and several AR re-activation mechanisms have been reported as likely drivers [88-92]. Therefore, development of novel AR-targeted therapeutics that are active in CRPC remains an important area of investigation [93].

The AR is a modular steroid hormone receptor transcription factor with the primary transcriptional activation function mapping to Transcriptional Activation

Units (TAU)1 and TAU5 in the intrinsically unstructured AR NH_2-terminal domain (NTD) [2,94]. The functional importance of these domains is evidenced by the expression of AR splice variant proteins in CRPC, which are constitutively active AR species composed of the AR NTD and central DNA binding domain (DBD), but lacking the regulatory LBD [80,95]. This highlights the clinical need for new therapeutics that exert action through non-LBD interfaces on the AR protein [80,95]. The Bisphenol A Diglicydyl Ether (BADGE) derivative, EPI-001, was identified as a specific inhibitor of the AR that bound covalently to an undetermined structural motif in the AR NTD and inhibited the growth of androgen sensitive PCa and CRPC cells *in vitro* and *in vivo* [77,78]. Here, we interrogated the mechanism by which EPI-001 inhibits the AR NTD. We show that EPI-001 is a general thiol modifier with myriad effects on AR expression and activity, as well as selective modulation of the peroxisome proliferator-activated receptor-gamma (PPARγ). Overall, this study provides novel insights to EPI-001 chemical biology that will be critical for ongoing development of AR NTD inhibitors.

RESULTS

EPI-001 Inhibits Transcriptional Activity of Both AR TAU1 and TAU5

LNCaP cells were treated with a range of EPI-001 concentrations to identify doses that effectively inhibited AR-responsive luciferase reporters.

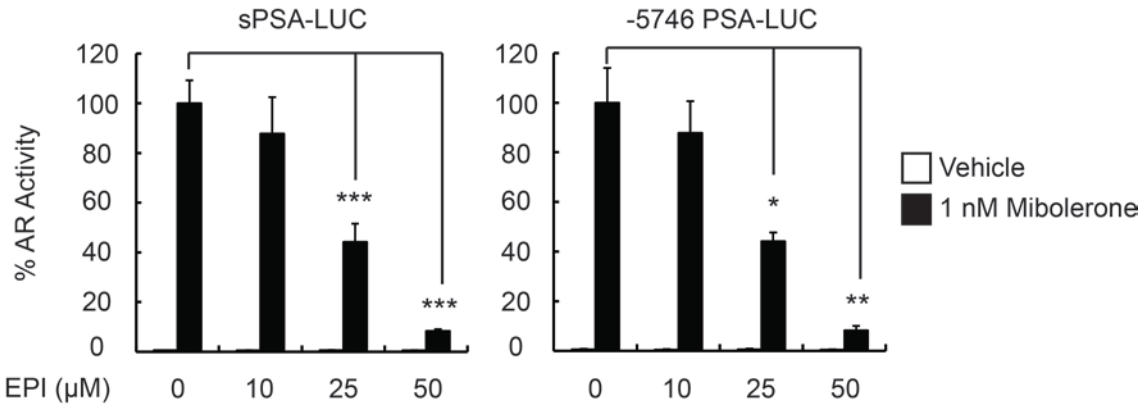

Figure 2.1: LNCaP cells were transfected with the indicated reporter constructs and cultured for 24 h in androgen-depleted medium. Cells were then transferred to serum-free medium supplemented with 1 nM Mibolerone or vehicle control, and treated 24 h with increasing concentrations of EPI-001 as indicated. Bars represent mean +/- SE for n = 6 samples from two biological replicates.

Contrary to previous reports showing that 10 μM EPI-001 achieved robust AR inhibition [77], we observed that a 50 μM dose of EPI-001 was required to inhibit AR activation by the synthetic androgen mibolerone (Figure 2.1). To identify the specific AR TAU through which 50 μM EPI-001 inhibited AR activity, we performed promoter tethering assays with an AR^{Gal4} hybrid wherein the AR DBD had been replaced with the yeast Gal4 DBD (Figure 2.2A, construct 2). As a negative control, we used bisphenol A bis[2,3-dihydroxypropyl] ether (BABDHE), as it is structurally similar to EPI-001 but contains a diol instead of a reactive chlorohydrin (Figure 2.2B) [78]. EPI-001 inhibited ligand-dependent AR^{Gal4} transcriptional activity in LNCaP cells (Figures 2.3A and 2.3B), as well as aberrant, ligand-independent AR-Gal4 transcriptional activity in the CRPC C4-2 cell line (Figure 2.3B). Deletion of TAU5 from AR^{Gal4} increased androgen-dependent AR^{Gal4} activity and decreased androgen-independent AR^{Gal4} activity, consistent with previous reports [73], but this deletion did not affect

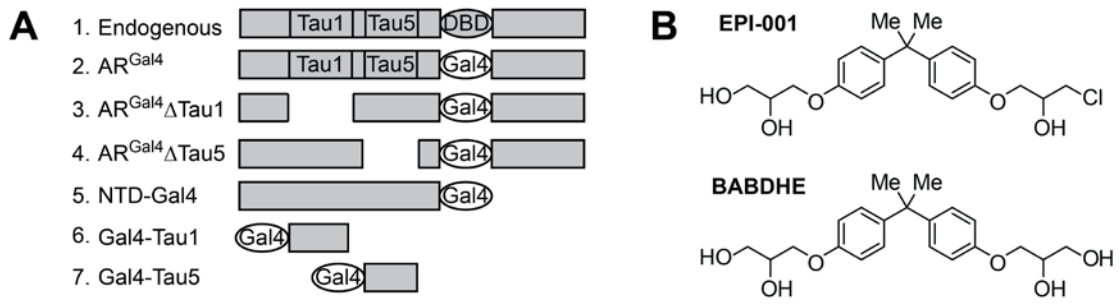

Figure 2.2: (*A*) Schematic of Gal4-based AR expression constructs. (*B*) Chemical structures of EPI-001 and BABDHE.

responsiveness to EPI-001 (Figure 2.3B). Conversely, deletion of TAU1 decreased androgen-dependent and -independent modes of AR^{Gal4} transcriptional activity in LNCaP and C4-2 cells (Figure 2.3B). This precluded evaluation of EPI-001 effects on TAU1 in LNCaP, but residual androgen-independent AR^{Gal4} transcriptional activity in C4-2 cells remained responsive to EPI-001 (Figure 2.3B). To test the responsiveness of discrete AR TAUs to EPI-001 directly, we tethered the entire AR NTD, or TAU1 or TAU5 fragments to the

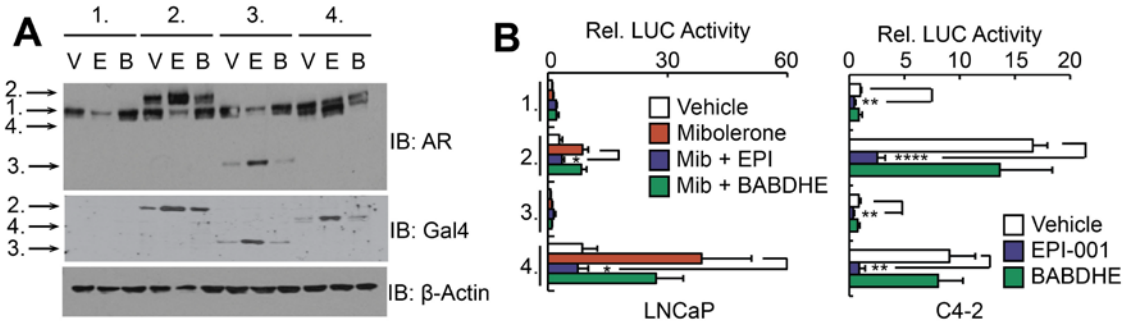

Figure 2.3: LNCaP and C4-2 cells were transfected with constructs shown in panel *A* along with $sPSA^{Gal4}$-luciferase and treated as indicated (V: Vehicle control; E: EPI-001 50 μM; B: BABDHE 50 μM). (*A*) LNCaP lysates treated in the absence of serum and androgen were subjected to western blot. (*B*) LNCaP and C4-2 protein lysates were subjected to luciferase assay. Bars depict mean +/- standard error (C4-2: n = 4 from 2 independent duplicate experiments; LNCaP: n=5 from 2 independent duplicate/triplicate experiments). * = $p < 0.05$, ** = $p < 0.01$, *** = $p < 0.001$, **** = $p < 0.0001$.

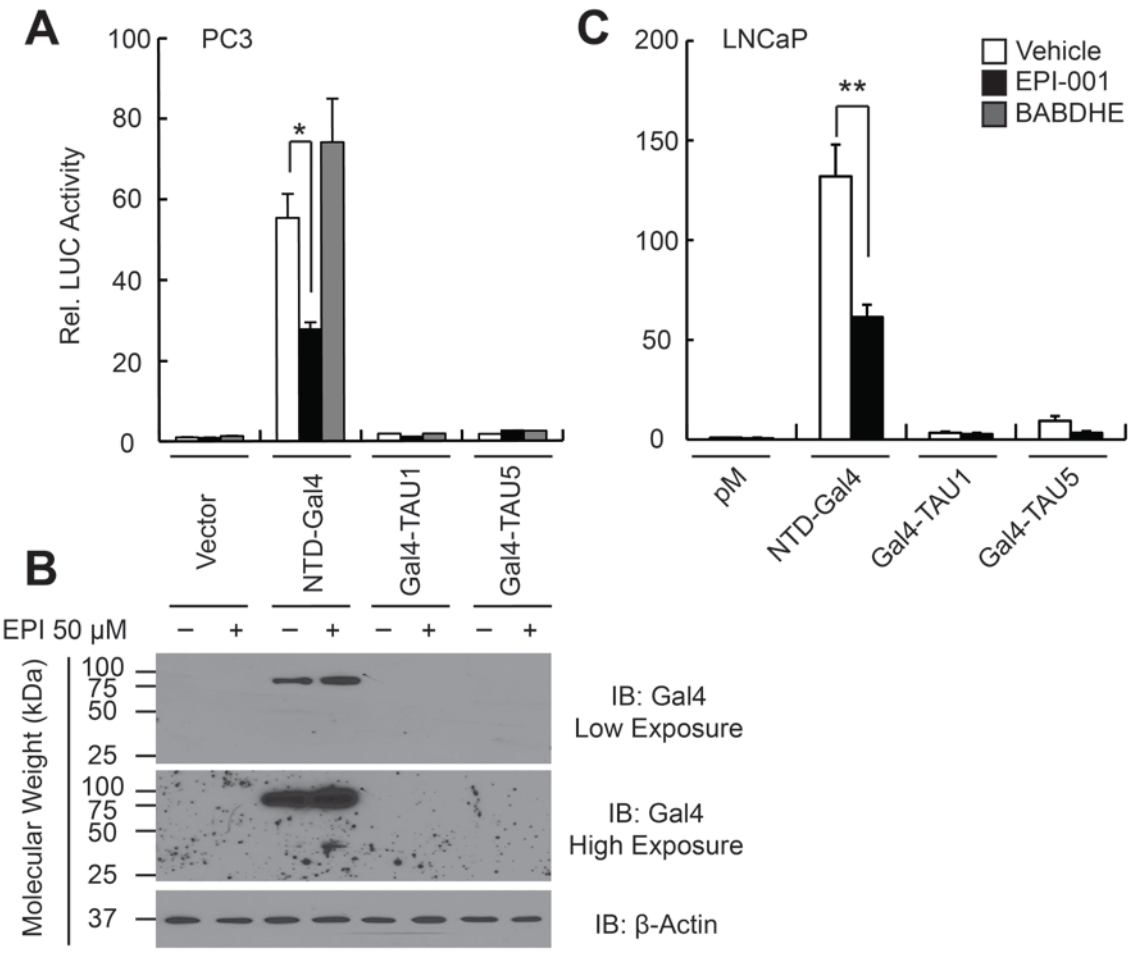

Figure 2.4: (*A*) PC-3 and (*B*) LNCaP cells were transfected with the indicated NTD domains tethered to Gal4 DBD (see Fig. 1A for schematic) and the Gal4-responsive pG5-Luciferase reporter, then treated overnight with 50 μM EPI-001, 50 μM BABDHE, or vehicle control. (*C*) PC-3 cells were transfected with the indicated constructs corresponding to panel (*A*) and treated overnight with 50 μM EPI-001 or vehicle control. Lysates were subjected to western blot. Bars represent mean +/- SE for n = 6 samples from two separate experiments.

Gal4 DBD (Figure 2.2A, constructs 5-7). In all cell lines tested, EPI-001 inhibited transcriptional activity of the NTD-Gal4 hybrid (Figures 2.4 and 2.5). The Gal4-TAU1 and Gal4-TAU5 fusion proteins displayed cell line-specific transcriptional activity, due to inefficient expression in PCa cell lines (Figures 2.4 and 2.5). In

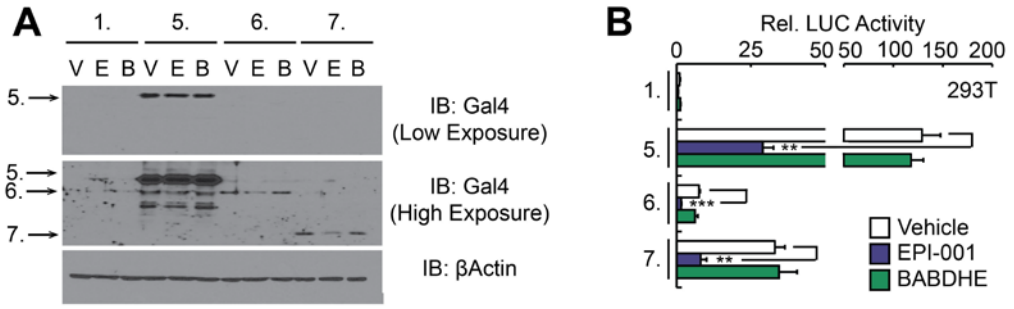

Figure 2.5: 293T cells were transfected with the constructs shown in panel *A* along with pG5-luciferase and treated with the indicated drugs. Protein lysates were subjected to (*A*) western blot or (*B*) luciferase assay. Bars depict mean +/- standard error (n=6 from 2 independent triplicate experiments). * = $p < 0.05$, ** = $p < 0.01$, *** = $p < 0.001$, **** = $p < 0.0001$.

293T fibroblasts, transcriptional activity of the Gal4-TAU1 and –TAU5 constructs was potently inhibited by EPI-001 (Figure 2.5). These data agree with previous reports of direct AR inhibition by EPI-001, but extend this knowledge by demonstrating the effects could not be mapped to a discrete AR TAU. This indicates two possible scenarios: 1) EPI-001 binds specifically to both TAU1 and TAU5, or 2) EPI-001 has a more general effect on transcriptional activities of TAU1 and TAU5.

EPI-001 inhibits endogenous AR mRNA and protein expression.

Interestingly, we observed that endogenous AR protein levels were consistently repressed in PCa cell lines treated with EPI-001 (Figure 2.3). To explore this phenomenon, we tested the effect of EPI-001 on AR protein levels in a panel of androgen sensitive PCa (Figure 2.6A) and CRPC (Figure 2.6B) cell lines. In all cell lines, EPI-001 treatment decreased expression of full-length AR protein to varying degrees (Figures 2.6A and B). AR protein loss occurred

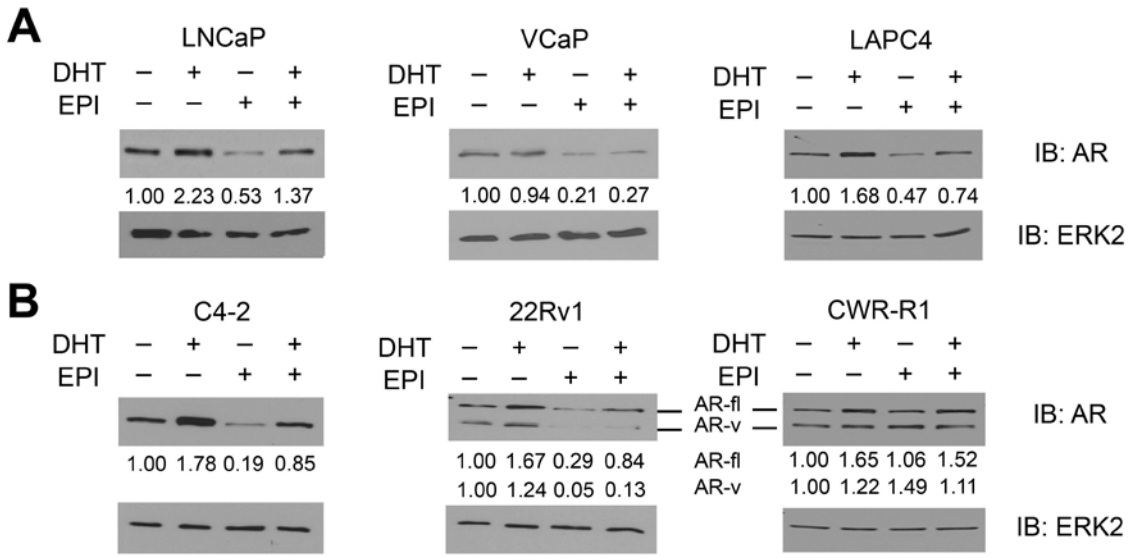

Figure 2.6: (*A*) Androgen sensitive PCa and (*B*) CRPC cell lines were treated overnight in serum-free medium with 1 nM DHT and/or 50 μM EPI-001 as indicated, and analyzed by western blot. Densitometry data for both full length (AR-fl) and truncated variant (AR-v) isoforms are provided.

between 8 and 16 hours of treatment and was independent of the proteasome (Figure 2.7). In line with this, AR mRNA expression in LNCaP and C4-2 cells was reduced in response to EPI-001 at time points preceding the observed decreases in AR protein expression (Figure 2.8). EPI-001 also inhibited the mRNA expression of AR and the AR target gene PSA in LAPC4 cells (Figure 2.9A). EPI-001 treatment also decreased expression of truncated AR variant (AR-v) proteins expressed in the CRPC 22Rv1 cell line (Figure 2.6B). Interestingly, AR mRNA and protein expression in CWR-R1 cells did not respond to EPI-001, nor did EPI-001 inhibit the expression of the AR target gene FKBP5 (Figure 2.9B).

To test if the effects of EPI-001 on AR expression were due to decreased AR mRNA stability, we treated LNCaP with Actinomycin D alone or in combination with EPI-001. Treatment with EPI-001 did not accelerate AR mRNA decay

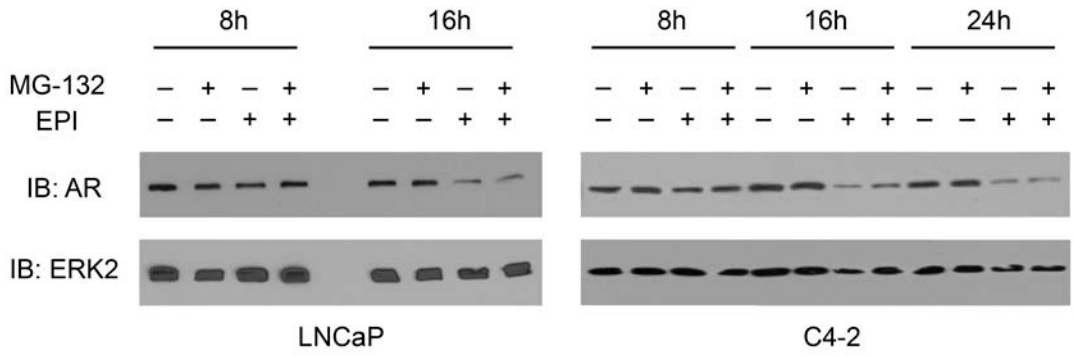

Figure 2.7: LNCaP (left) and C4-2 (Right) were serum starved overnight, then treated with 50 μM EPI-001 and/or 10 μM MG-132 as indicated. EPI-001-mediated AR protein loss occurred between 8 and 16 hours and was not reversed by proteasome inhibitor treatment.

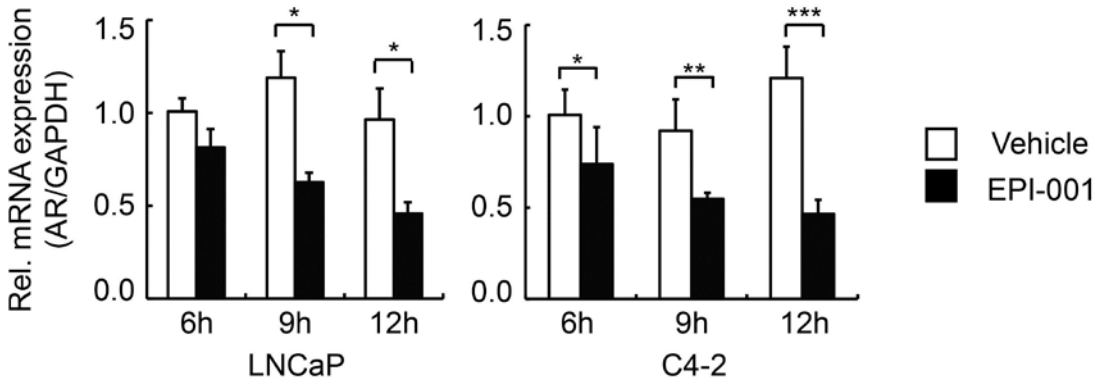

Figure 2.8: AR mRNA expression was analyzed by qRT-PCR at indicated time-points in LNCaP (*left*) and C4-2 (*right*) cells treated with 50 μM EPI-001. n = 3 from a triplicate experiment representative of two biological replicates. * = P < 0.05; ** = P < 0.01; *** = P < 0.001.

following transcriptional blockade with Actinomycin D (Figure 2.10). Consistent with this, we found that 50 μM EPI-001 reduced the rate of nascent AR mRNA synthesis in LNCaP cells (Figure 2.11). Collectively, these data demonstrate that EPI-001 inhibits transcription of the AR gene.

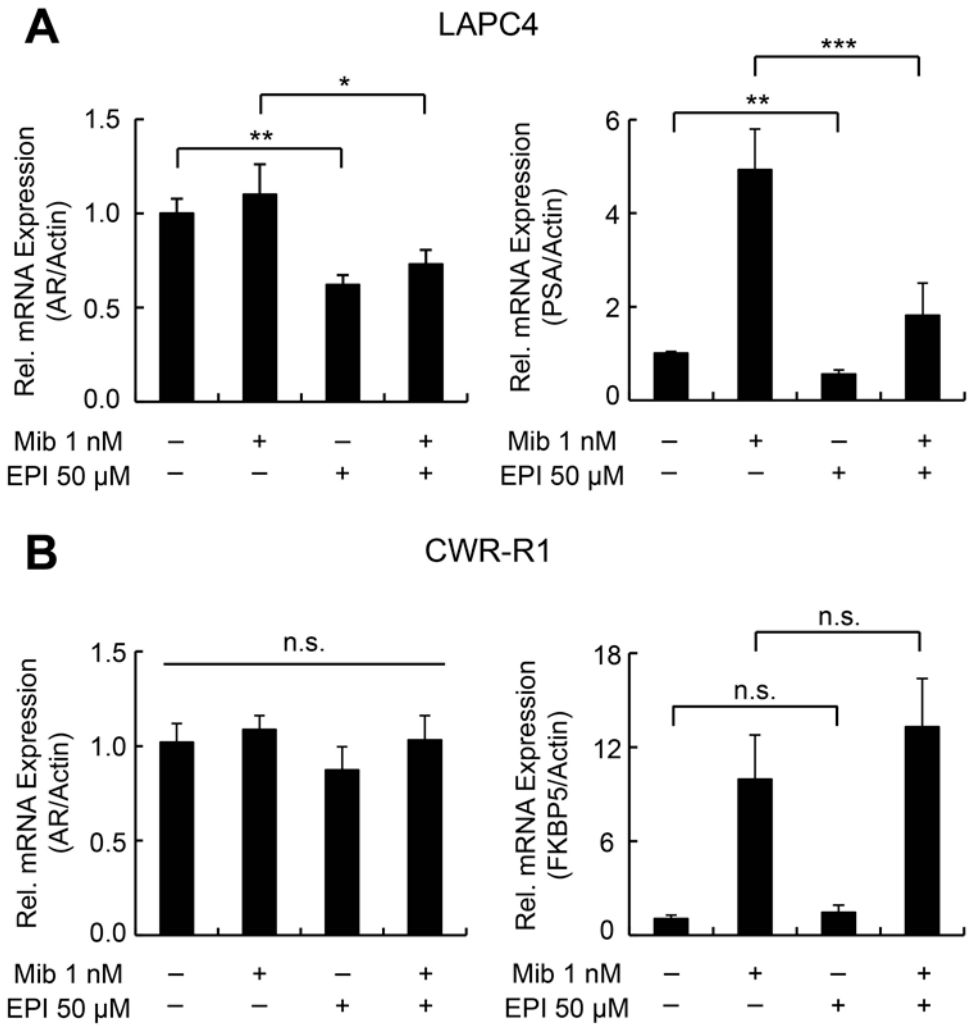

Figure 2.9 LAPC4 (A) and CWR-R1 (B) cells were cultured in androgen-depleted medium for 48 hours, then treated 24 hours in serum-free medium with Mibolerone and/or EPI-001 or vehicle control as indicated. RNA extracts were prepared and subjected to qRT-PCR for total AR (left panels) and AR targets (right panels).

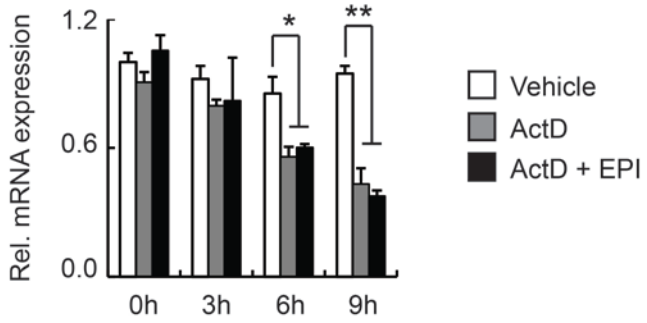

Figure 2.10: LNCaP cells were serum-starved overnight, then treated with 10 µg/mL Actinomycin D +/- 50 µM EPI-001 for the indicated times. qRT-PCR analysis of AR mRNA expression relative to GAPDH was performed. Treatment with EPI-001 did not affect the rate of mRNA decay relative to Actinomycin D alone. Bars represent mean +/- SD of a triplicate experiment (n = 3), which was validated in a repeat triplicate experiment.

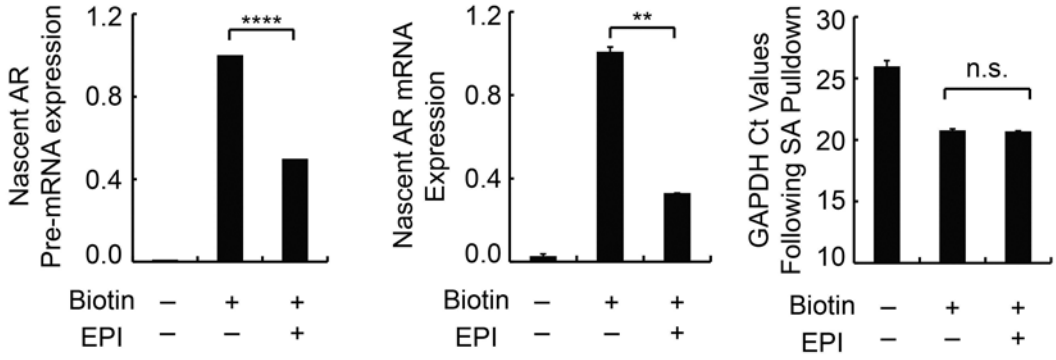

Figure 2.11: LNCaP cells were treated with 50 µM EPI-001 or vehicle control for 8 h in serum free medium. Nascent transcripts were isolated and subjected to qRT-PCR using primers for AR pre-mRNA (Exon 1 FW & Intron 1 RV) or spliced mRNA (Exon 1 FW & Exon 2 RV). Bars depict mean +/- standard deviation of n = 6 from two biological replicates performed in triplicate). ** = P < 0.01; **** = P < 0.0001.

Inhibition of AR expression correlates with reduced cell growth in PCa and CRPC cell lines.

Based on these findings, we reasoned that inhibition of AR synthesis could

be an important component of the EPI-001 anti-AR mechanism. EPI-001 inhibited growth of LNCaP cells at low concentrations, but in all other PCa cell lines, the concentrations at which EPI-001 inhibited growth (Figure 2.12A) were the same concentrations that inhibited expression of AR or AR-V protein levels (Figure 2.12B). BABDHE also inhibited PCa and CRPC growth and AR expression, although higher doses were required than for EPI-001 (Figure 2.13),

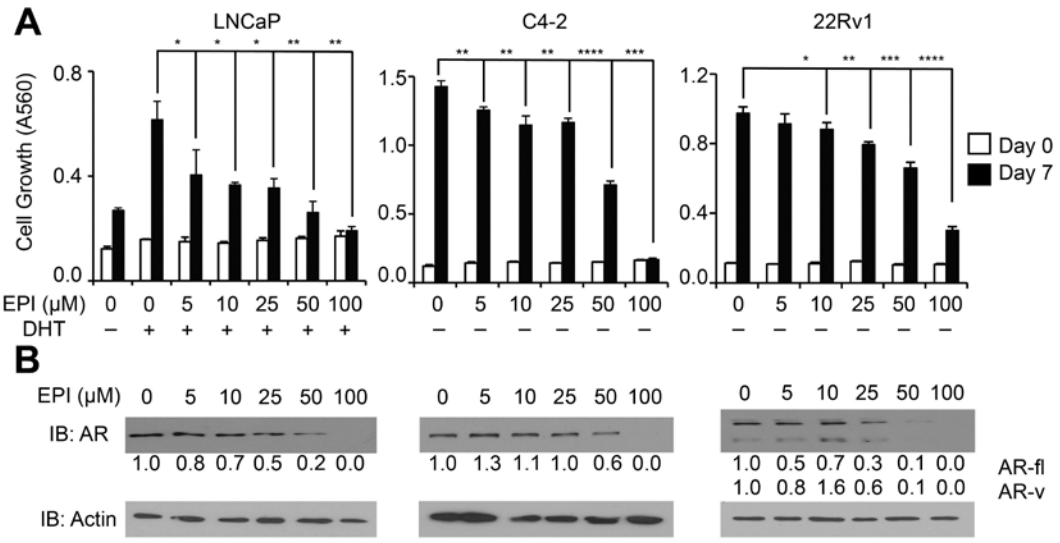

Figure 2.12: (*A*) LNCaP, C4-2, and 22Rv1 cells were treated for 7 days in steroid-depleted medium containing 1 nM DHT and/or EPI-001 as indicated. Growth was monitored by crystal violet staining. Bars depict mean +/- standard deviation (n = 3 from a triplicate experiment representative of two biological replicates). (*B*) LNCaP, C4-2, and 22Rv1 cells were treated for 24 hours in serum free medium as in (*A*) and subjected to western blot. Densitometry data are provided. Bars depict mean +/- standard deviation (n = 3 from a triplicate experiment representative of two biological replicates). * = P < 0.05; ** = P < 0.01, *** = P < 0.001, **** = P < 0.0001.

indicating the EPI-001 chlorohydrin moiety is important for inhibition of AR expression. Surprisingly, EPI-001 also inhibited growth of AR-negative PC-3 and DU 145 cell lines (Figure 2.14), as well as the T47D breast carcinoma cell line

(Figure 2.15A and B). In T47D, reduced expression of AR as well as estrogen and progesterone receptors (ER and PR) was observed (Figure 2.15C). These data signify AR-independent effects of EPI-001 in multiple cell types.

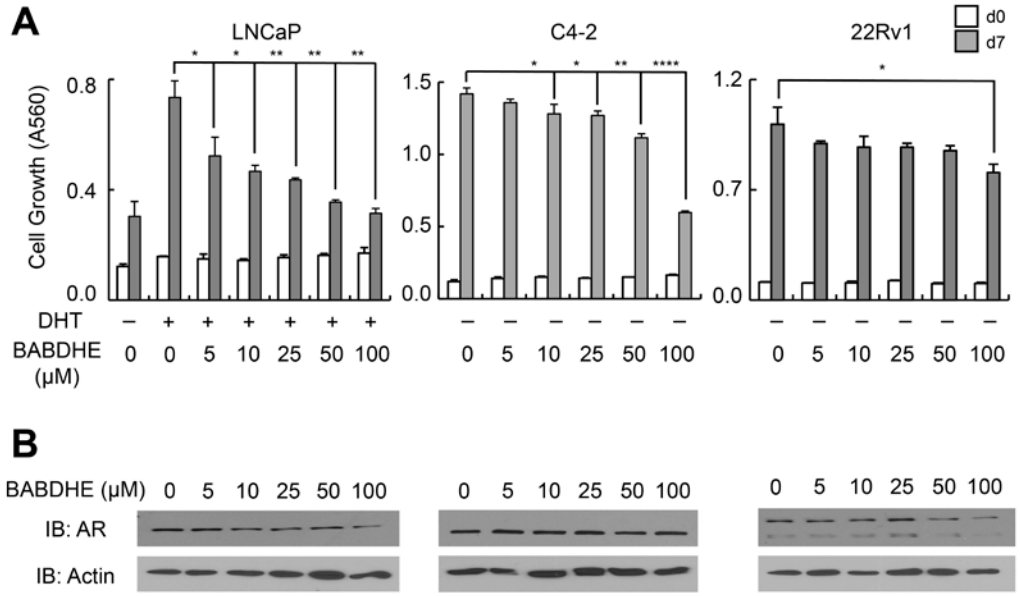

Figure 2.13: LNCaP, C4-2, and 22Rv1 cells were seeded as in Figure 2.12 and treated with 1 nM dihydrotestosterone +/- BABDHE at indicated concentrations, then subjected to crystal violet growth assays (*A*) or western blots (*B*). Bars represent mean +/- SD for a triplicate experiment (n = 3), which was validated in a repeat triplicate experiment. * = P < 0.05; ** = P < 0.01, **** = P < 0.0001.

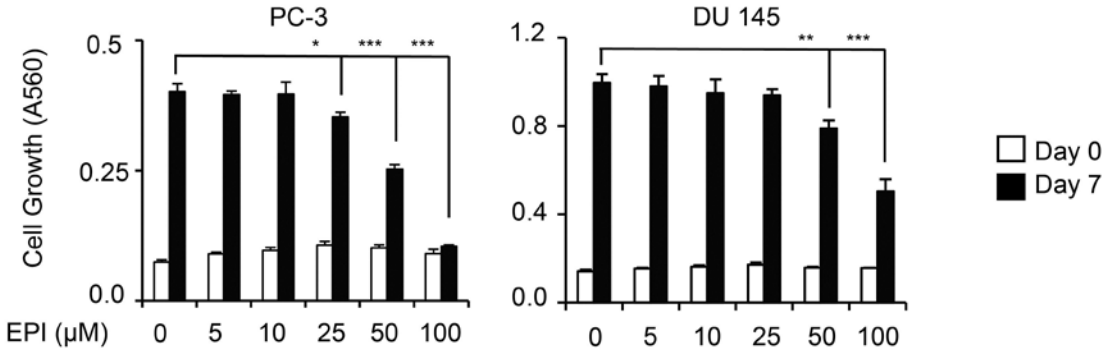

Figure 2.14: AR-negative PC-3 and DU 145 cells were treated with EPI-001 and analyzed for growth exactly as in Figure 2.12A. Bars depict mean +/- standard deviation (n = 3 from a triplicate experiment representative of two biological replicates). * = P < 0.05; ** = P < 0.01, *** = P < 0.001

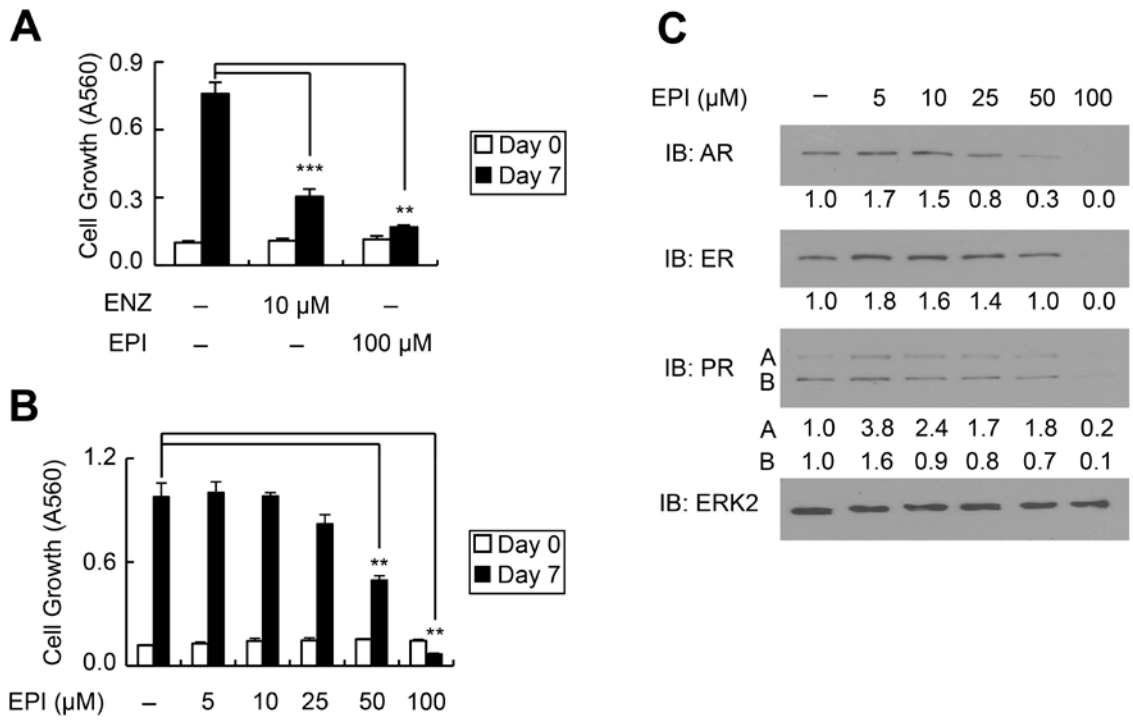

Figure 2.15: (A) T47D cells were seeded in MEM +5% FBS and treated with EPI-001 or enzalutamide as indicated for 7 days, then stained with crystal violet. (B) Cells were seeded as in (A) and treated with increasing doses of EPI-001 for 7 days, then stained with crystal violet. (C) Western blot of T47D lysates treated overnight with EPI-001 in serum-free MEM as indicated. Denitometry measurements are included below their corresponding bands. Bars represent mean +/- SD from a triplicate experiment (n = 3), which was validated in an independent triplicate experiment. ** = $P < 0.01$, *** = $P < 0.001$.

EPI-001 action in PCa cells is similar to the PPARγ agonist, troglitazone.

Bisphenol A Diglycidyl Ether (BADGE), which is related structurally to EPI-001 but contains a bis-epoxide, has been shown to act as a selective PPARγ modulator (SPPARM) with diverse effects in different cell types [96-98]. Given that PPARγ has also been shown to play a role in prostate development and maintenance [99], and PPARγ agonists such as troglitazone have been demonstrated to inhibit AR expression and PCa cell growth in vitro and in vivo

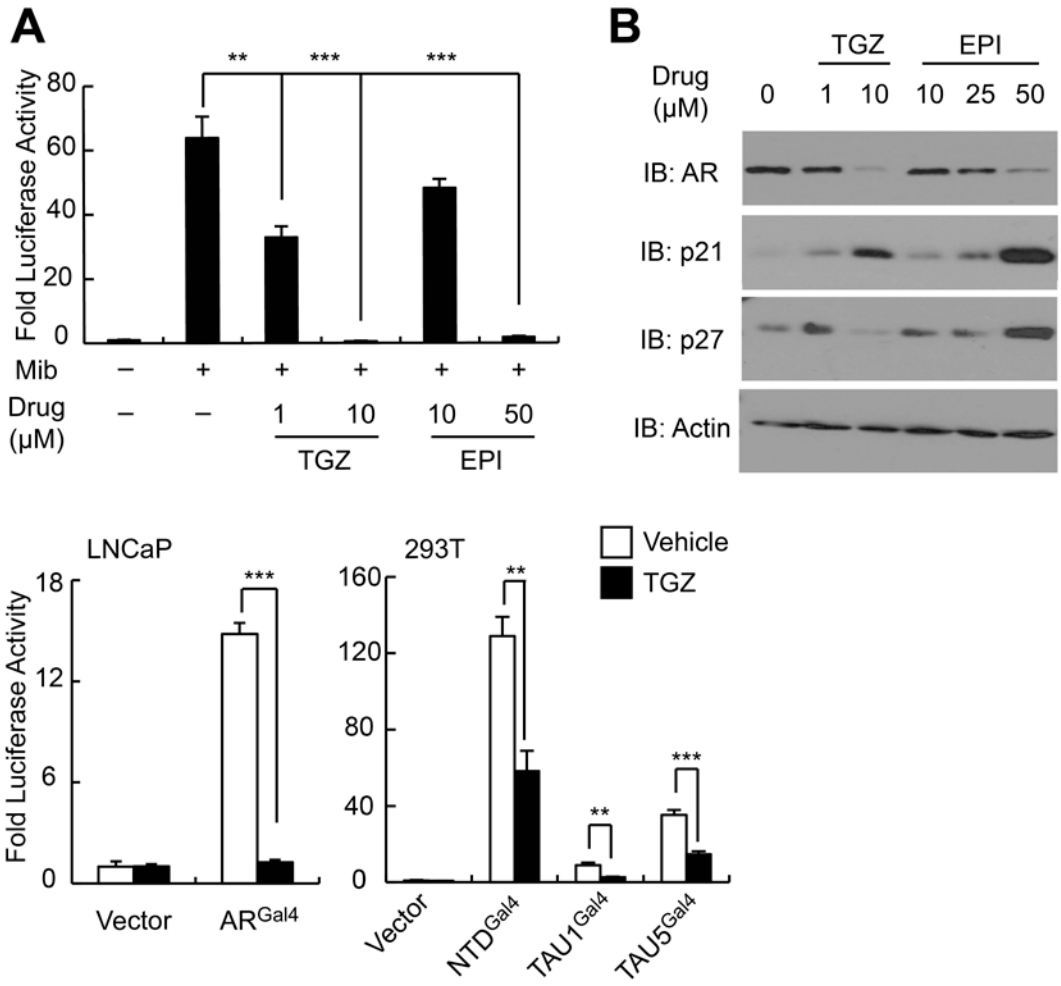

Figure 2.16: (*A)* LNCaP cells were transfected with sPSA-Luciferase, treated with troglitazone (TGZ) or EPI-001 as indicated, and subjected to luciferase assay. (*B*) LNCaP cells were treated with troglitazone (TGZ) or EPI-001 as indicated and subjected to western blot. (*C*) LNCaP and 293T were transfected with the indicated Gal4-tethered AR constructs and either $sPSA^{Gal4}$-Luciferase or pG5-Luciferase, respectively, and treated with 10 μM troglitazone or vehicle control as indicated. Bars represent mean +/- standard error (n=6 samples from two independent triplicate experiments). * = P < 0.05; ** = P < 0.01, *** = P < 0.001.

[100-102], we reasoned that PPARγ modulation may be an unanticipated activity of EPI-001 in PCa cells. Indeed, troglitazone or EPI-001 caused inhibition of AR transcriptional activity in promoter reporter assays in LNCaP cells (Figure 2.16A) at doses that correlated with inhibition of AR protein expression (Figure 2.16B).

Furthermore, treatment of LNCaP cells with troglitazone or EPI-001 resulted in dose-dependent reduction of AR protein levels as well as induction of p21 and p27 (Figure 2.16B). Troglitazone inhibited AR expression at lower doses than observed in prior studies [101,103], which may be due to the absence of serum in the cell culture medium during drug treatment in our study. Finally, troglitazone treatment also inhibited the activity of AR^{Gal4}, as well as the Gal4-tethered AR NTD, TAU1, and TAU5 (Figure 2.16C), analogous to the effect of EPI-001 in these models (Figures 2.3 and 2.5).

To expand these observations to clinical disease, we treated fresh human PCa tissue maintained as explants [104-106] with troglitazone and EPI-001 (Figure 2.17A). The doses of EPI-001 and troglitazone used in this model were increased 2- to 4-fold relative to *in vitro* experiments to reflect the higher doses of drug that have been used for *in vivo* [78] or *ex vivo* [107] experimentation. Importantly, both EPI-001 and troglitazone effected decreases in AR protein, AR mRNA, and AR target gene expression in PCa explants (Figure 2.17B and C).

EPI-001 is a selective modulator of PPARγ in PCa cells.

We next tested for SPPARM activity of EPI-001 in PCa cells. Similar to troglitazone, EPI-001 activated a PPARγ-response element (PPRE)-regulated luciferase reporter in LNCaP cells (Figure 2.18A). This SPPARM activity was AR-independent, as troglitazone and EPI-001 both induced mRNA expression of the PPARγ targets CIDEC [108], TXNIP [103], and PDK4 [99] in the AR-null PC-3 cell line [100] (Figure 2.18B). However, in 3T3-L1 cells that had been differentiated to

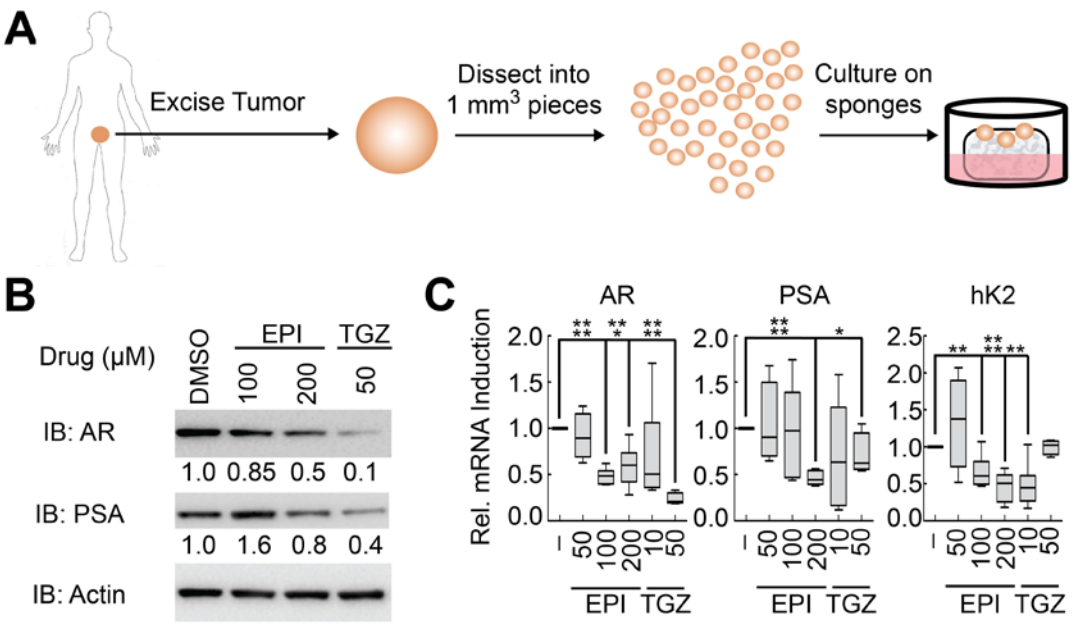

Figure 2.17: (*A*) Schematic of explant model for culturing fresh prostate cancer tissue. (*B* and *C*) PCa tissue explants were treated with EPI-001 or troglitazone (TGZ) as indicated for 48 h, then subjected to (*B*) western blot or (*C*) qRT-PCR. Box plots represent mean and range of two replicates from three patients each per treatment condition (n = 6). * = P < 0.05; ** = P < 0.01, *** = P < 0.001, **** = P < 0.0001.

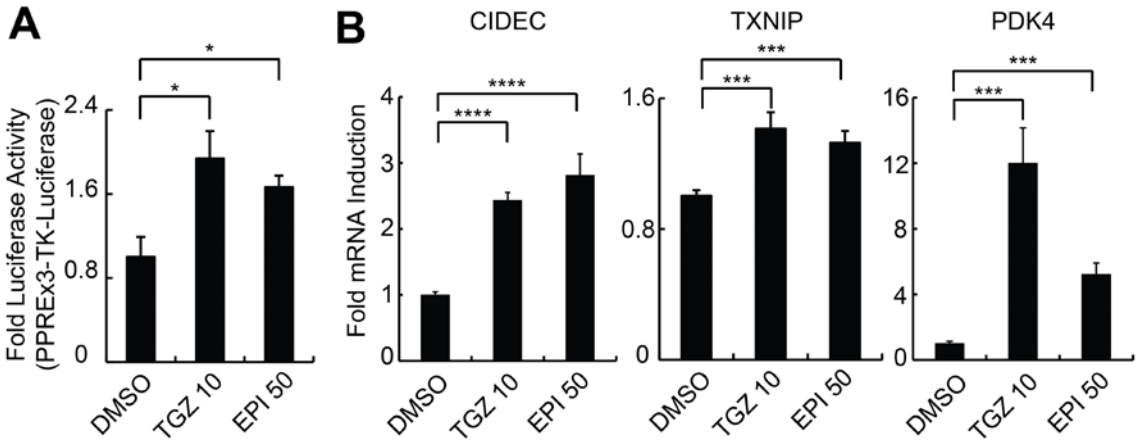

Figure 2.18: (*A*) LNCaP cells were transfected with PPREx3-TK-Luciferase, treated as indicated for 8 h, and subjected to luciferase assay. (*B*) PC-3 cells were treated with EPI-001 overnight and RNA was isolated for analysis of PPARγ target gene expression by qRT-PCR. Bars represent mean +/- standard error (n=6 from two independent triplicate experiments). * = P < 0.05; ** = P < 0.01, *** = P < 0.001, **** = P < 0.0001.

PPARγ-positive adipocytes, EPI-001 repressed expression of classical PPARγ target genes aP2 and LPL (Figure 2.19A) and inhibited lipid droplet formation (Figure 2.19B). These effects are consistent with previous reports of BADGE-mediated repression of PPARγ activity in 3T3-L1 adipocytes at micromolar concentrations [96]. Taken together, these cell type-specific PPARγ agonist/antagonist effects support a SPPARM function for EPI-001, with

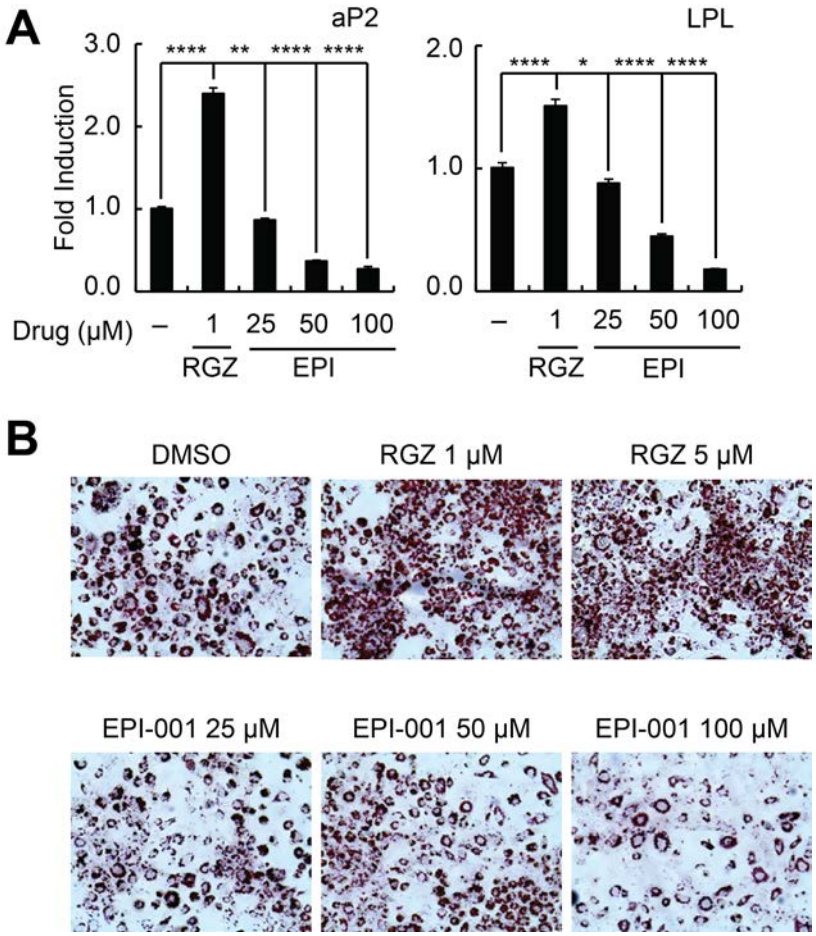

Figure 2.19: 3T3-L1 fibroblasts were grown to confluence and differentiated into mature adipocytes in the presence of rosiglitazone or EPI-001 as indicated. Cells were then lysed and subjected to qRT-PCR for PPARγ target genes (*A*) or stained with Oil Red O to measure lipid droplet accumulation (*B*). Bars represent mean +/- SE of n = 6 samples from two independent biological replicates. * = P < 0.05; ** = P < 0.01, **** = P < 0.0001 relative to untreated control.

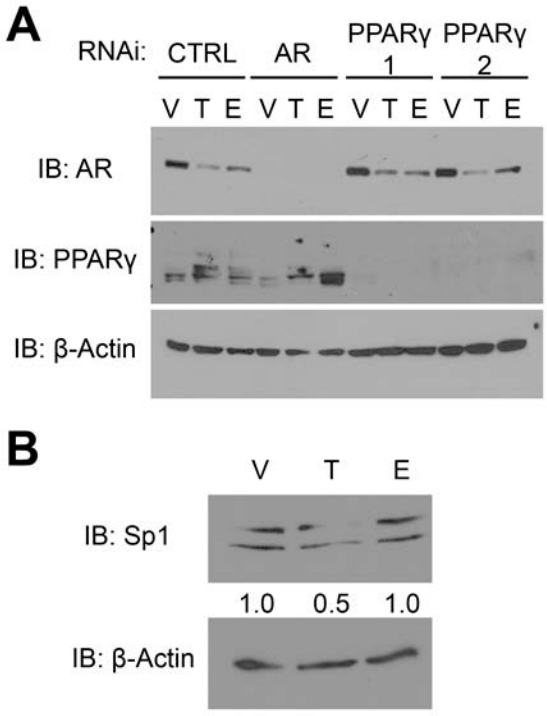

Figure 2.20: (*A*) LNCaP cells were transfected with 300 pmol siRNA against AR, PPARγ, or nontargeting control and cultured in RPMI +10% CSS for 48 hours, then treated as indicated overnight in serum-free RPMI prior to lysis for western blot for AR, PPARγ, and β-Actin (loading control). (*B*) LNCaP were seeded in RPMI +10%CSS, then treated overnight as indicated prior to lysis for western blot for Sp1 or β-Actin (loading control). V = vehicle, T = 10 μM troglitazone, E = 50 μM EPI-001.

thiazolidinedione-like effects on PPARγ activity in PCa cells.

To investigate the relationship between EPI-001-mediated PPARγ activation and AR inhibition, we knocked down PPARγ with siRNA in LNCaP cells. Despite effective silencing of PPARγ expression, both troglitazone and EPI-001 maintained robust inhibition of AR protein expression (Figure 2.20A). This finding is consistent with a previous study showing that troglitazone-mediated inhibition of AR expression is due to PPARγ-independent degradation of the

transcription factor Sp1 [101]. However, EPI-001 had no effect on Sp1 levels (Figure 2.20B). Conversely, siRNA-mediated knock down of PPARγ partially rescued the inhibition of AR transcriptional activity effected by EPI-001, but not troglitazone (Figure 2.21), demonstrating that PPARγ participates in EPI-001-mediated inhibition of AR transcriptional activity, but not inhibition of AR expression.

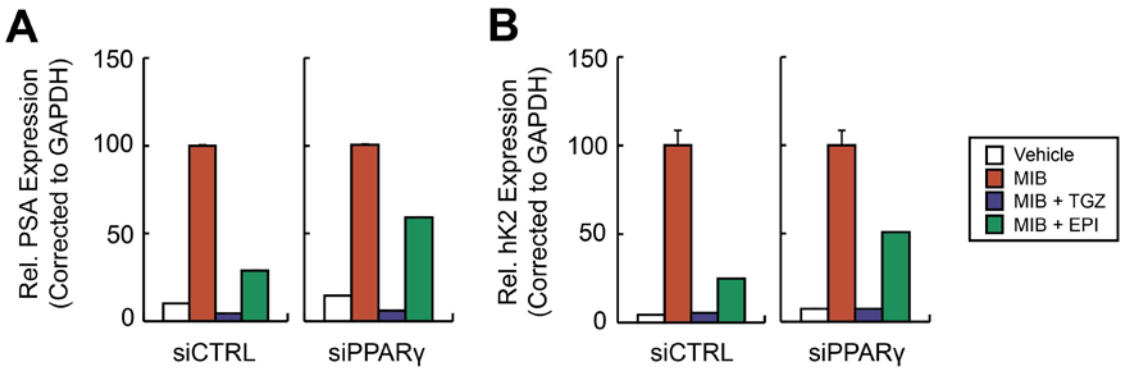

Figure 2.21: LNCaP cells were transfected with siRNAs targeting AR or PPARγ and treated with mibolerone (Mib), troglitazone (TGZ) or EPI-001 as indicated. Expression of AR target genes PSA (*A*) and hK2 (*B*) was analyzed by qRT-PCR. Bars represent mean +/- standard deviation (n = 2 from a duplicate experiment representative of 3 biological replicates).

EPI-001 forms covalent adducts with thiols in vitro*.*

Because SPPARM activity did not fully account for the multi-level anti-AR effects of EPI-001, we considered the fact that Bisphenol A (BPA) and BADGE are endocrine disruptors used in the production of polycarbonate plastics and epoxy resins [109,110]. The epoxide rings in BADGE and related compounds readily

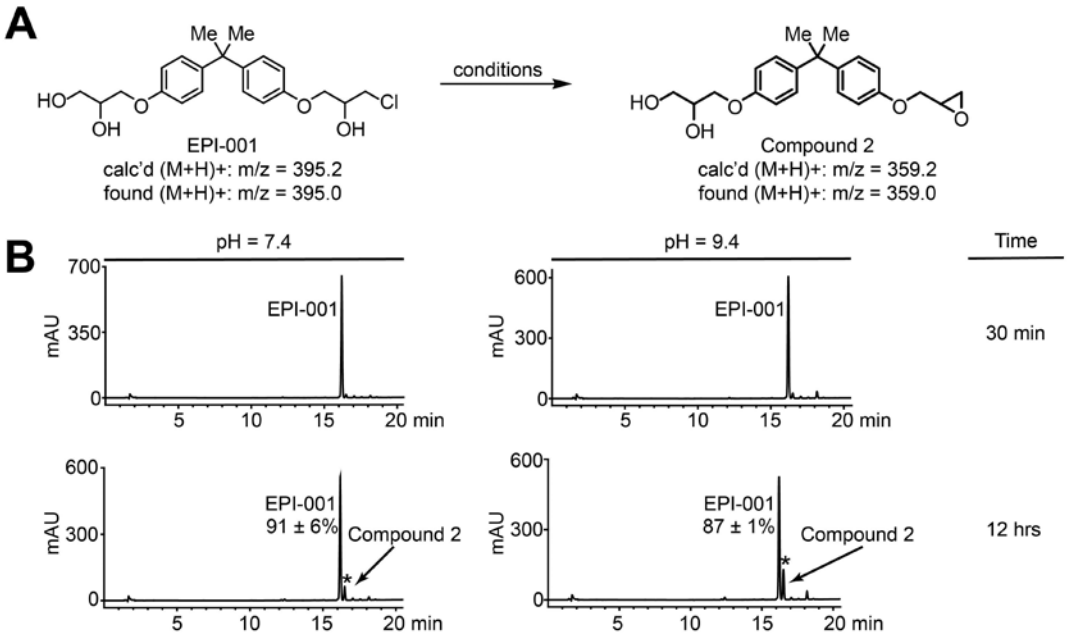

Figure 2.22: (*A*) Reaction scheme for conversion of EPI-001 to compound 2. EPI-001 was shaken at 37 ^{o}C in PBS/DMSO at pH 2.4, 7.4, and 9.4. (*B*) HPLC chromatograms for conversion of EPI-001 to compound. Reaction mixtures were analyzed by LC-MS to confirm the presence of epoxide; *m/z* $[M+H]^+$ 359.2 (calc'd); 359.0 (found). New peaks that arose during the course of the reaction and are distinct from background signals (Supplementary Fig. 20A) are denoted with an asterisk. Percent remaining was calculated by dividing the amount of measured EPI-001 remaining at t = 12 h by the amount remaining at t ~ 30 min and multiplying by 100%. Experiments were performed in triplicate and values shown are mean +/- standard deviation. EPI-001:thiol adducts were characterized by LC-MS.

undergo hydrolysis and hydrochlorination reactions with substrates in aqueous solution [111], resulting in hydroxylated and halogenated derivatives, of which EPI-001 (BADGE.HCl.H_2O) is one example [112]. Chlorohydrin moieties also have the potential to spontaneously interconvert to epoxides in aqueous solution [113]. Therefore, we used HPLC to interrogate whether EPI-001 can convert to a BADGE-like mono-epoxide in solution (Compound 2, Figure 2.22A). Indeed, the epoxide was observed after 12h incubation at neutral and basic pH (Figure 2.22B), but not under acidic conditions (Figure 2.23). The identity of compound 2

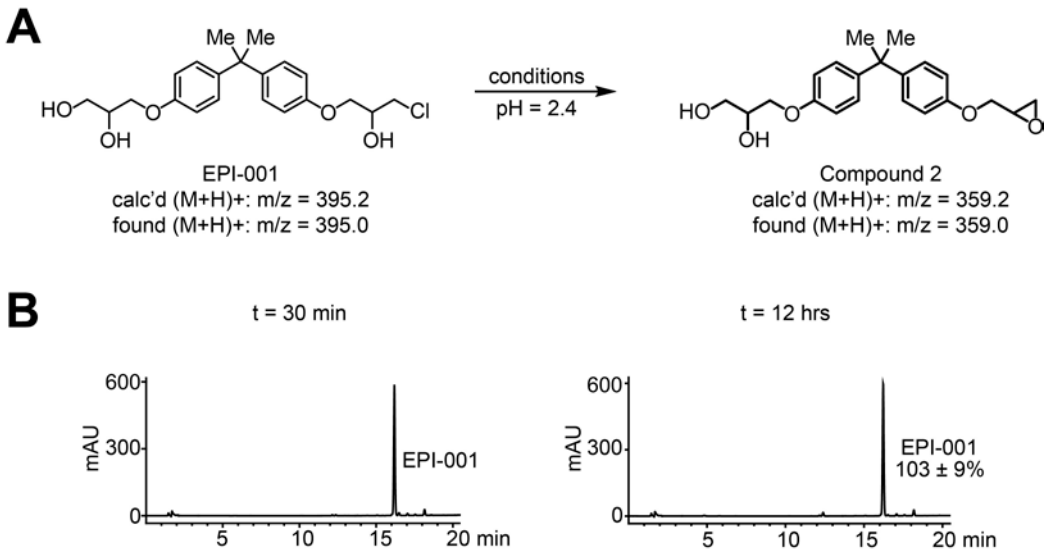

Figure 2.23: (*A*) Spontaneous conversion of the EPI-001 chlorohydrin to a reactive epoxide. EPI-001 was shaken at 37 ^{o}C in aq. PBS / DMSO (~10:1) at pH 2.4. The reactions were analysed by reverse-phase HPLC at t ~30 min and t = 12 h for the appearance of epoxide. (*B*) The reaction mixtures were analyzed by LC-MS confirming the absence of epoxide.

was confirmed by co-injection with an authentic standard and LC-MS analysis (Figure 2.24). BADGE has been shown to react with nucleophilic side chains of food proteins in plastic-lined cans [114], which is the same reaction proposed for the specific AR-binding mechanism of EPI-001 [78]. In a previous study, non-specific reactivity of EPI-001 with nucleophilic thiols was not observed [78]. However, given our observation that EPI-001 spontaneously converts to the epoxide at neutral and basic pH, and that BADGE is reactive to nucleophiles, we queried reactivity of EPI-001 with the nucleophilic thiols glutathione, 2-mercaptoethanol, and cysteamine at various pH conditions (Figure 2.25A). Reaction of EPI-001 with glutathione resulted in a trace amount of thiol adduct

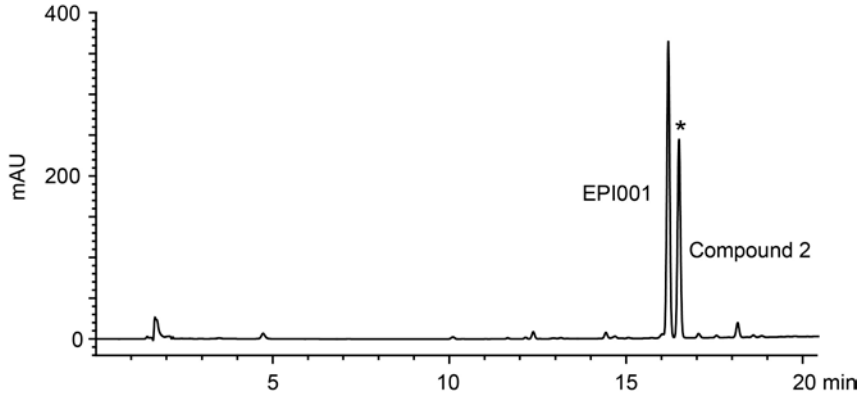

Figure 2.24: A solution of EPI-001 in aq. PBS / DMSO incubated 12 h at pH = 9.4 was spiked with 12 uL of 8.5 mM Compound 2 in DMSO. The EPI-001 degradation product and the co-injected standard eluted from the column in tandem (marked with an asterisk).

formation at pH 7.4, and nearly complete conversion to the glutathione adduct at pH 9.4 after 12 hours (Figure 2.25B). No EPI-001:thiol adducts were formed under acidic conditions (Figures 2.26 and 2.27). Similarly, 2-mercaptoethanol displayed limited adduct formation at neutral pH, but underwent complete conversion to the EPI-001:thiol adduct at basic pH (Figure 2.25B). Finally, EPI-001 did not react with cysteamine at pH 7.4, but displayed nearly complete adduct formation at pH 9.4 (Figure 2.25B). All EPI-001-thiol adducts were confirmed by mass spectrometry (Figure 2.28). Additionally, the monoepoxide, compound 2, formed adducts with all thiols examined and displayed an enhanced reactivity profile overall (Figure 2.29). Collectively, these data indicate that EPI-001 spontaneously converts to the more reactive epoxide in solution at neutral and basic pH. Furthermore, EPI-001 extensively alkylates thiols under basic conditions with appreciable amounts of EPI-001:thiol adducts observed at

neutral (7.4) pH. Our results suggest that EPI-001 is a reactive electrophile which may display some selectivity in modulation of proteins by virtue of local pH influence.

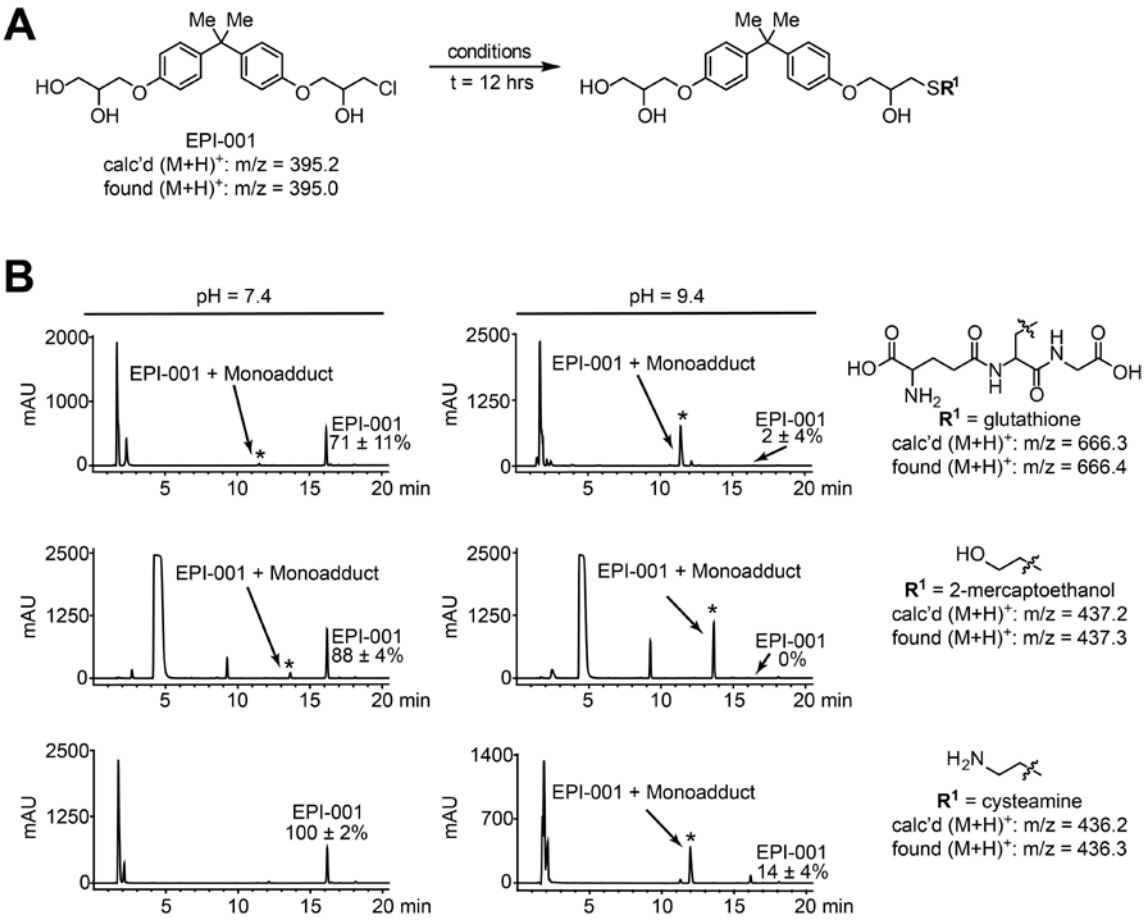

Figure 2.25: (*A*) Scheme for covalent modification of EPI-001 by reactive thiols. Solutions of EPI-001 and thiols in PBS/DMSO at pH 2.4, 7.4, and 9.4, respectively, were shaken at 37 ^{o}C. (*B*) HPLC chromatograms for covalent adduct formation between EPI-001 and thiols (t = 12 h). New peaks that arose during the course of the reaction and are distinct from background signals (Supplementary Fig. 20A) are denoted with an asterisk. Percent remaining was calculated by dividing the amount of measured EPI-001 remaining at t = 12 h by the amount remaining at t ~ 30 min and multiplying by 100%. Experiments were performed in triplicate and values shown are mean +/- standard deviation. EPI-001:thiol adducts were characterized by LC-MS.

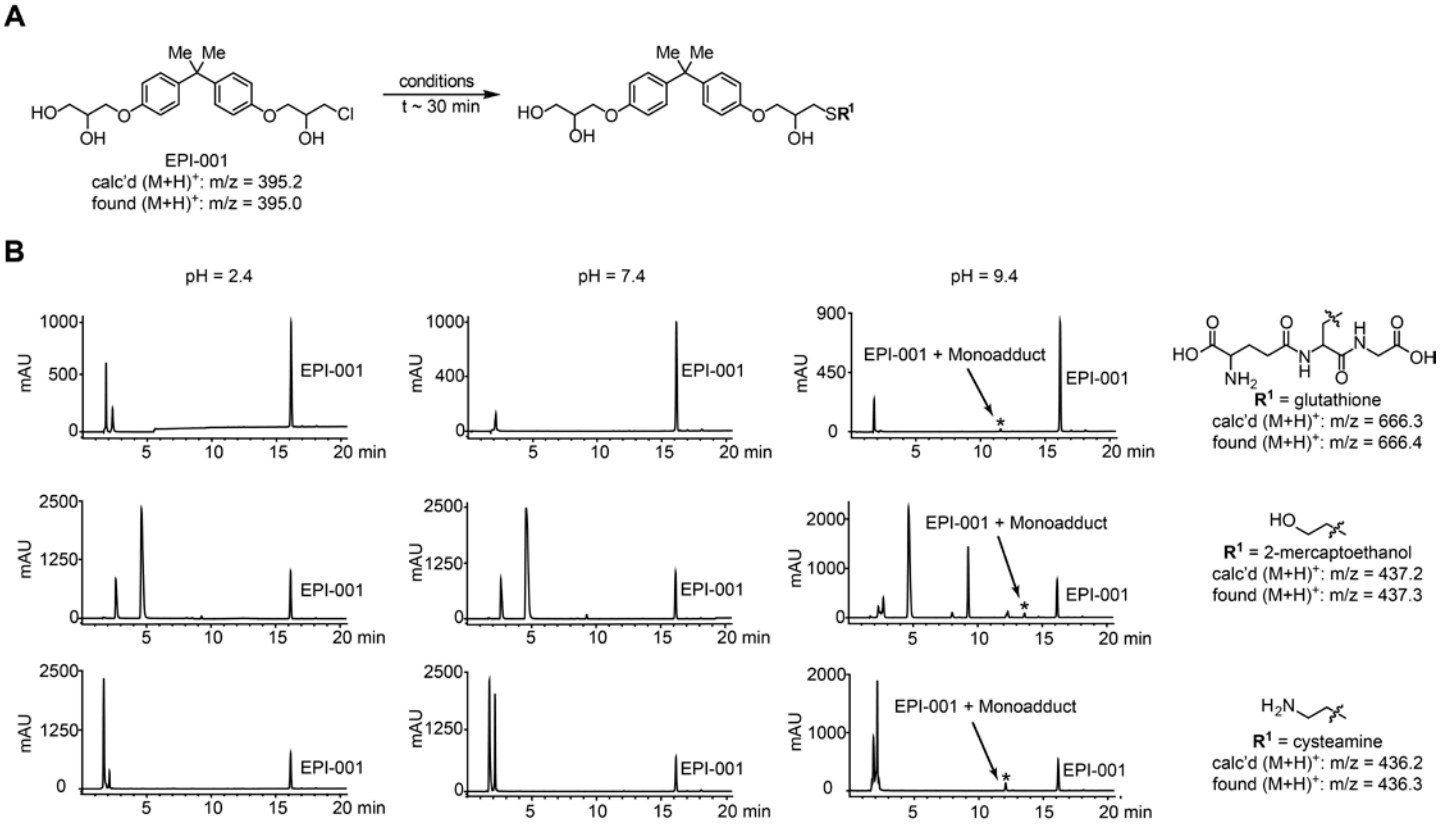

Figure 2.26: (A) Solutions of EPI-001 and thiol in aq. PBS / DMSO (~10:1) at pH 2.4, 7.4, and 9.4, respectively, were shaken at 37 ^{o}C. The reactivity of the following thiols with EPI-001 was investigated: reduced L-glutathione, 2-mercaptoethanol, and cysteamine. The reactions were analyzed by reverse-phase HPLC at t ~30 min for the appearance of thiol adducts. (B) At t ~ 30 min, EPI-001 adducts were only observed under strongly basic conditions (pH=9.4). Under such conditions, EPI-001 exhibits reactivity with each of the three thiols. New products formed during the course EPI-001-thiol incubation are marked with an asterisk. Background signals collected in the absence of EPI-001 are shown in Supplementary Figure S20A. Experiments were performed in triplicate, and the identities of the monoadducts were confirmed by LC-MS.

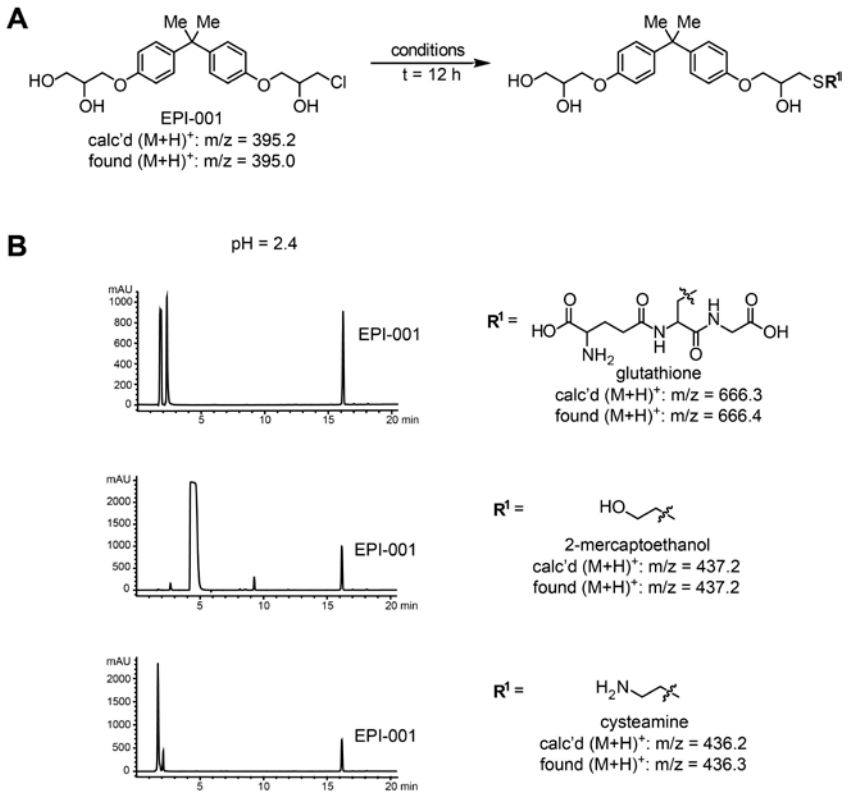

Figure 2.27: (*A*) Reaction schematic demonstrating covalent modification of reactive thiols by EPI-001. Solutions of EPI-001 and thiol in aq. PBS / DMSO (~10:1) at pH 2.4 were shaken at 37 ^{o}C. The reactivity of the following thiols with EPI-001 was investigated: reduced L-glutathione, 2-mercaptoethanol, and cysteamine. The reactions were analyzed by reverse-phase HPLC at t = 12 h for the appearance of thiol adducts. (*B*) At t = 12 h, no new peaks were observed under acidic conditions.

DISCUSSION

In this study, we describe unanticipated multi-level effects of EPI-001 on the AR and PPARγ pathways, leading to inhibition of cell growth. In previous reports, EPI-001 was shown to bind specifically to the AR NTD through a nucleophilic substitution reaction with the EPI-001 chlorohydrin group [78], thereby inhibiting AR activity via occlusion of an unidentified CBP binding domain [77]. We were

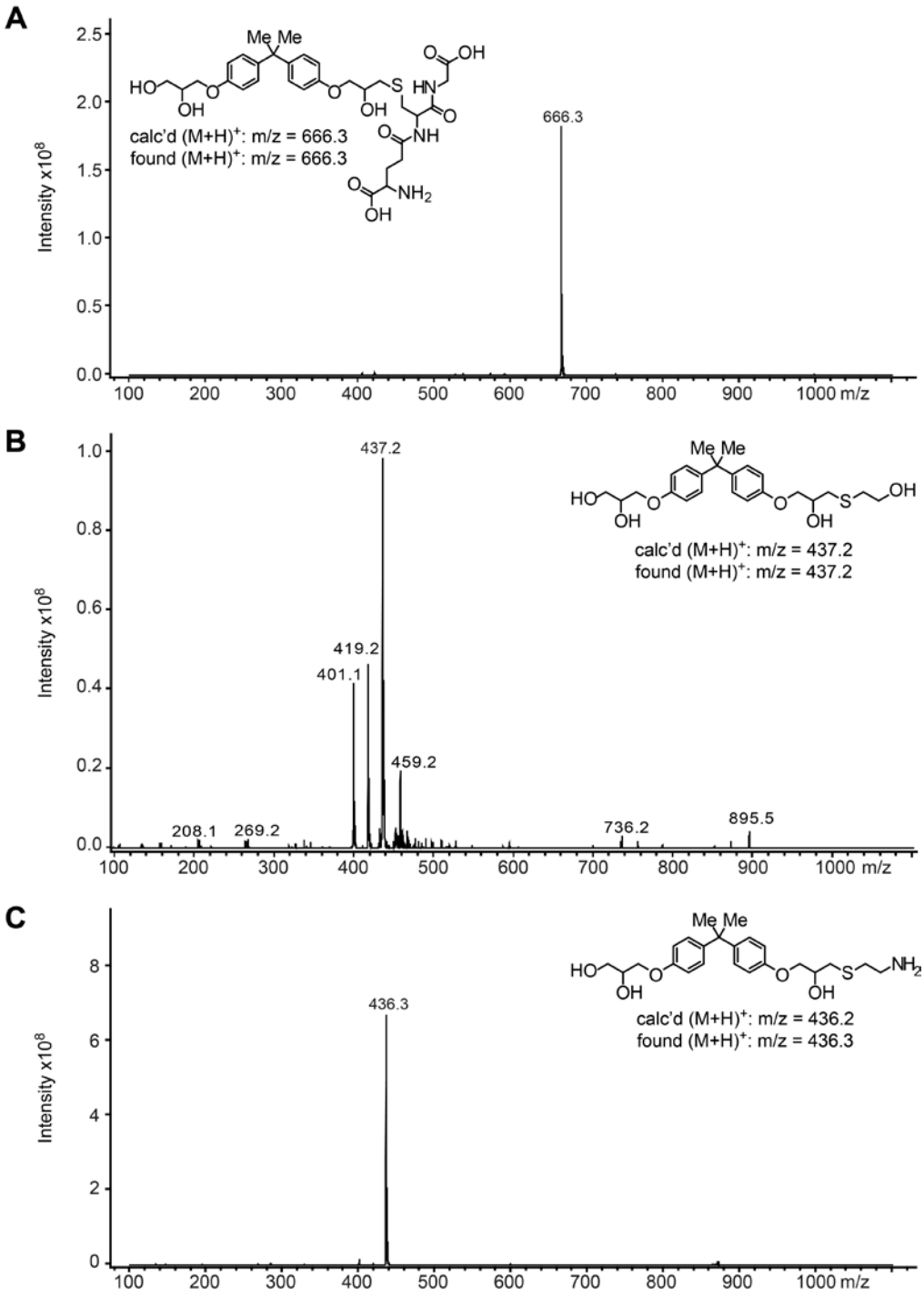

Figure 2.28: (*A*) Mass spectrum of the monoadduct of glutathione and EPI-001; *m/*z [M+H$^+$] 666.3 (calc'd); 666.3 (found). (*B*) Mass spectrum of the monoadduct of 2-mercaptoethanol and EPI-001; *m/*z [M+H$^+$] 437.2 (calc'd); 437.2 (found). (*C*) Mass spectrum of the monoadduct of cysteamine and EPI-001; *m/*z [M+H$^+$] 436.2 (calc'd); 436.3 (found)

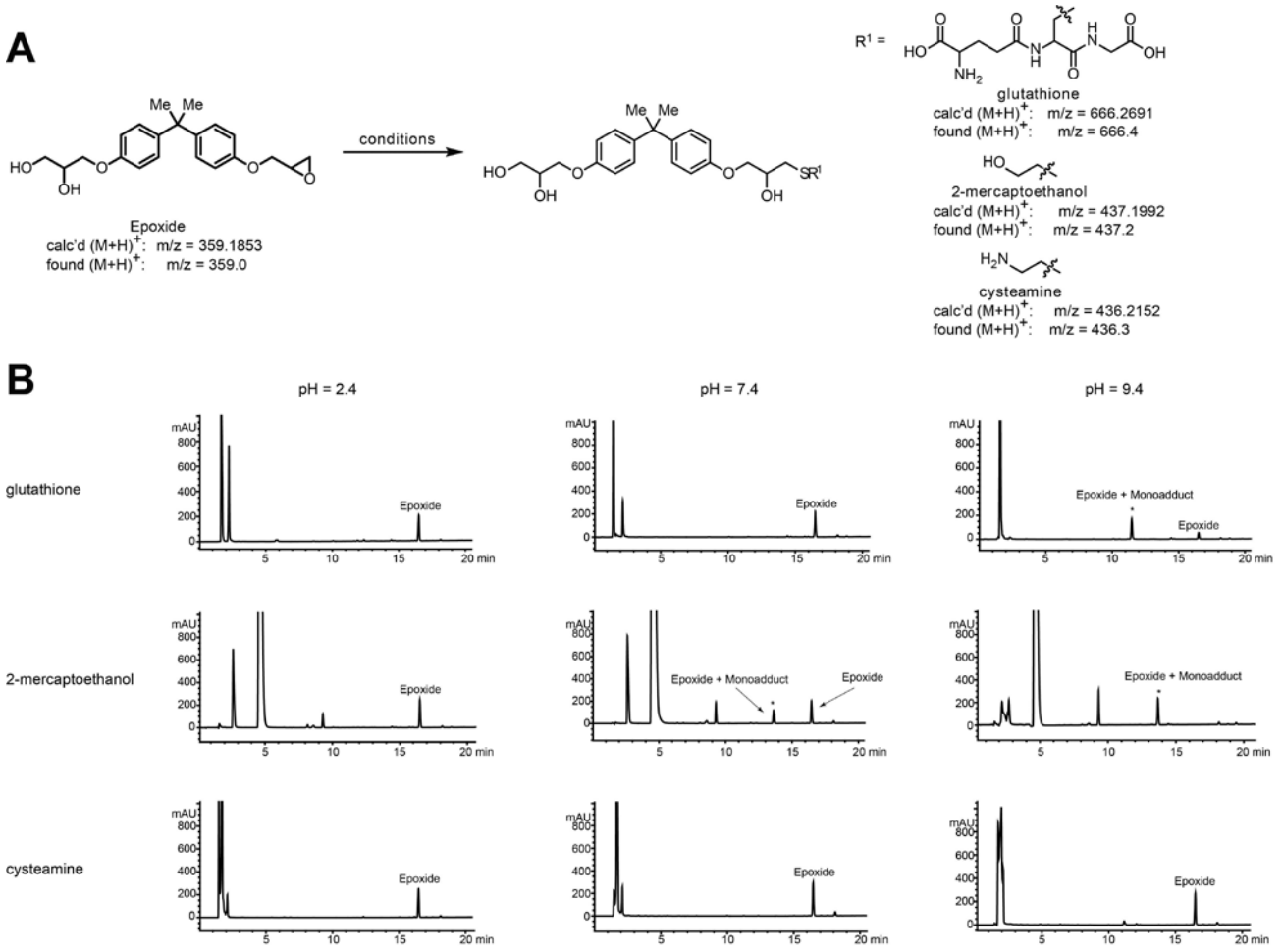

Figure 2.29 (cont'd next page)

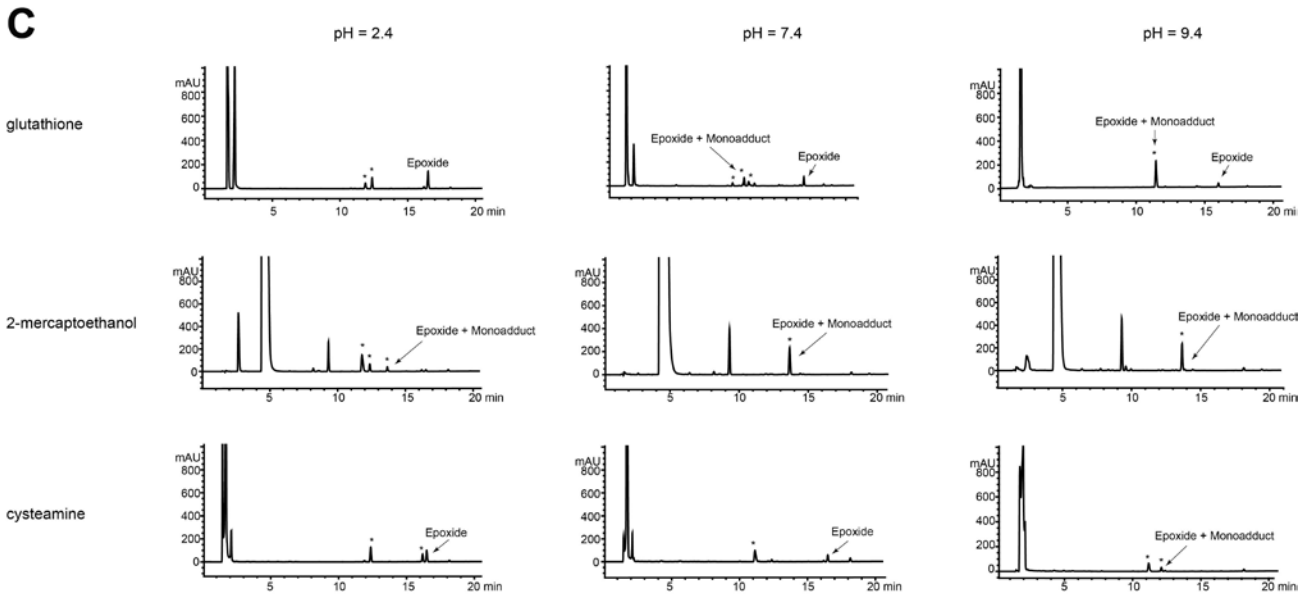

(Cont'd) Figure 2.29: (*A*) Solutions of epoxide and thiol in aq. PBS / DMSO (~10:1) at pH 2.4, 7.4, and 9.4, respectively, were shaken at 37 ^{o}C. The reactivity of the following thiols with epoxide was investigated: reduced L-glutathione, 2-mercaptoethanol, and cysteamine. The reactions were analyzed by reverse-phase HPLC at t ~30 min and t = 12 h for the appearance of thiol adducts. (*B*) At t ~ 30 min, a GSH/epoxide monoadduct was observed under basic conditions (pH = 9.4) as the primary component of the reaction mixture. At pH = 7.4, a 2-mercaptoethanol monoadduct was observed. At pH = 9.4, no evidence of the epoxide remained and only the monoadduct was present. (*C*) At t = 12 h, a multitude of new peaks (many are thiol adducts) were observed following incubation of Compound 2 with each thiol. New products formed during the course Compound 2-thiol incubation are marked with an asterisk. Background signals collected in the absence of Compound 2 are shown in Supplementary Figure S20A. Experiments were performed in triplicate, and the identities of the explicitly assigned monoadducts were confirmed by LC-MS.

unable to nominate a discrete AR NTD motif that could account for a specific mechanism of EPI-001-mediated AR transcriptional repression in this study. Conversely, we found that EPI-001 inhibited synthesis of AR in PCa cell lines and clinical tissues at doses that corresponded with the inhibition of AR target genes and PCa cell growth. The LNCaP cell line was an exception to this general dose relationship between AR expression inhibition and cell growth inhibition, displaying the highest sensitivity to EPI-001- and BABDHE-mediated growth inhibition. This is important, as the majority of pre-clinical data supporting the efficacy and specificity of EPI-001 for AR has been generated using the LNCaP model [77,78]. Moreover, we found that EPI-001 inhibited the growth of AR-negative PC-3 and DU 145 cells. These data conflict with a previous report [77], but we propose that this discrepancy is due to two key differences in experimental design. First, our study incorporated longer-term (i.e. 7 day) growth assays as opposed to early time point (i.e. 3 day) BrdU incorporation readouts. Secondly, previous reports used 10 μM EPI-001 to treat PC-3 and DU 145, a dose which was not inhibitory to the growth of PC-3 and DU 145 in our study, but inhibitory LNCaP cells. These data highlight the cell line-specific responses to EPI-001, which supported earlier conclusions of AR specificity.

Our data indicate that PPARγ activation represents at least one AR-independent activity of EPI-001 in PCa cells. However, EPI-001 displayed PPARγ inhibitory activity in a classical 3T3-L1 adipocyte differentiation model, indicating SPPARM activity as opposed to pure agonist activity. SPPARM activity for EPI-001 is consistent with studies demonstrating that the structurally-related

compound, BADGE, is a SPPARM that binds to the PPARγ LBD [96] and exhibits distinct molecular effects in PCa and 3T3-L1 cells when compared with synthetic thiazolidinedione PPARγ agonists [96-98] including troglitazone [109-111]. Furthermore, our data from thiol reactivity assays demonstrate that small molecule thiolates (e.g., glutathione, 2-mercaptoethanol, cysteamine) are readily alkylated by EPI-001 and this reactivity is attenuated at acid and neutral pH conditions. Consequently, our data suggest that any protein bearing an accessible nucleophilic residue within a suitably basic binding pocket may be a target for covalent modification by EPI-001. This is further supported by the established reactivity of BADGE *in vitro* [114], and our data that EPI-001 is converted to an analogous epoxide (compound 2) in solution at physiological pH. Collectively, these data suggest EPI-001 and BADGE bear substantial proteome reactivity features in addition to their reported interactions with AR and PPARγ. These new data indicate that structural changes to the core bisphenol of EPI-001 as well as the covalent warhead may be required to mitigate the AR-independent effects reported in this study and in the toxicology literature [109-111,114,115]. However, this task is complicated because no 3-dimensional structure has been reported for the intrinsically disordered AR NTD [116,117], which impedes the rational design of improved inhibitors. Nevertheless, EPI-002, the (2*R*, 20*S*) isomer of racemic EPI-001, has been shown to display stronger AR interactions and reduced toxicity in mice [78], indicating this direction may be feasible. Our findings that EPI-001-mediated inhibition of AR activity is associated with inhibition of AR expression and activation of PPARγ in PCa, coupled with the

finding that EPI-001 can capture nucleophilic thiols, will be important for ongoing pre-clinical development of EPI-001 and other anti-AR compounds that target functional domains independent of the AR LBD.

MATERIALS AND METHODS

Cell Culture and Growth Assays

LNCaP, C4-2, DU 145, VCaP, 22Rv1, 293T, and PC-3 cell lines were obtained from ATCC. The ATCC validates the authenticity of these cell lines via short tandem repeat (STR) analysis. CWR-R1 prostate cancer cells were the generous gift of Dr. Elizabeth Wilson (University of North Carolina at Chapel Hill, Chapel Hill, NC). CWR-R1 cells were authenticated by sequence-based validation of two characteristic AR mutations: a H874Y mutation in the LBD, and a 50 kb deletion in AR intron 1 [67]. VCaP and 293T were maintained in Dulbecco's Modified Eagle's Medium (DMEM) with 10% FBS. All other cell lines were maintained in RPMI 1640 medium with 10% FBS, and all cell lines were maintained in 100 Units/mL Penicillin + 0.1 mg/mL Streptomycin. Cells were cultured in a 37^{o} C incubator with 5% CO_2 for no longer than 15 passages after resuscitation of frozen stocks. Cell growth was assessed by crystal violet staining as previously described [65]. T47D breast cancer cells were the generous gift of Dr. Carol Lange (University of Minnesota, Minneapolis, MN). Cells were maintained in Minimal Essential Medium (MEM) supplemented with 5% Fetal Bovine Serum (FBS), 5 mg/mL insulin, 2 mM L-glutamine, 100 Units/mL

Penicillin, and 0.1 mg/mL Streptomycin. 3T3-L1 cells (kindly provided by Dr. David Bernlohr from the Department of Biochemistry, Molecular Biology and Biophysics, University of Minnesota) were cultured in DMEM with 10% bovine calf serum (Sigma Aldrich, Saint Louis, MO) and 100 IU/ml penicillin/streptomycin (Invitrogen, Carlsbad, CA) until confluence. Two days after confluence, cells were subjected to two-day incubation in the adipocyte differentiation cocktail containing 10% fetal bovine serum (JRH Biosciences, Inc., Lenexa, KS), 115 mg/ml methylisobutylxanthine (Sigma Aldrich, Saint Louis, MO), 1mg/ml insulin (Sigma Aldrich, Saint Louis, MO), and 390 ng/ml dexamethasone (Sigma Aldrich, Saint Louis, MO). During the following 6 days, cells were maintained in DMEM containing 10% fetal bovine serum, 100 IU/ml penicillin/streptomycin and 1mg/ml insulin until fully differentiated with robust accumulation of lipid droplets. In the treated groups, Rosiglitazone at the concentration of 1 μM or EPI at various concentrations was added to the cultures during the entire 8-day differentiation period. On day 8, cells were stained with Oil-red O or harvested for RNA extraction.

Reagents

Dihydrotestosterone (DHT), mibolerone (MIB), and BABDHE (Bisphenol A bis[2,3-dihydroxypropyl] ether) were purchased from Sigma. Enzalutamide (ENZ) was purchased from Selleck Chemicals. Troglitazone was purchased from Cayman Chemical. EPI-001 (Bisphenol A [3-chloro-2-hydroxypropyl][2,3-dihydroxypropyl] ether) was synthesized (See Appendix) or purchased from

commercial sources (Santa Cruz Biotechnology or Sigma-Aldrich). EPI-001 was analyzed for purity via HPLC and NMR (Appendix, Figures A1 and A2). EPI-001 was dissolved in DMSO was used for all experiments (Appendix, Figure A3). All other drugs were suspended in DMSO with the exception of DHT, MIB, and ENZ, which were prepared in absolute ethanol. Final DMSO or ethanol concentrations did not exceed 0.1% (v/v) in culture medium.

Table 2.1: Mutagenic Primer Sequences

Amplicon	Direction	Cut site	Sequence (5' → 3')
TAU1	F	EcoR1	CGGAATTCCGTAGAGGCCCCACAGGCTACC
TAU1	R	BamH1	CGGGATCCTCACTGGTACGCAGCTGCCTCGTCC
TAU5	F	EcoR1	CGGAATTCAGTCGCGACTACTACAACTTTCCACT
TAU5	R	BamH1	CGGGATCCTCACAGCCCCTGAGGGGGCCGAGT

Plasmids

Plasmids encoding human AR (p5HBhAR-A), AR^{Gal4}, NTD-Gal4, $AR^{Gal4}\Delta$TAU1, $AR^{Gal4}\Delta$TAU5, sPSA-Luciferase (also referred to as PSAenh(ARE)-LUC), and $sPSA^{Gal4}$-Luciferase (also referred to as PSAenh(GAL4)-LUC) have been described [73]. SV40-Renilla, CMV-Renilla, and pG5-Luciferase were purchased from Promega. PPREx3-TK-Luciferase has been described [118], and was obtained from Addgene. The Gal4 DBD expression plasmid (pM) was purchased from Clontech. Gal4 tethering of AR TAU1 (amino acids 101-360) and TAU5 (amino acids 361-490) was achieved by PCR amplification of TAU1 or TAU5 from p5HBhAR-A using primers listed in Table 2.1. Primers were designed to introduce in-frame recognition sites for EcoRI and BamHI, which were used to ligate the

insert with EcoRI/BamHI-digested pM.

Western Blot

Western blotting with antibodies listed in Table 2.1 was performed as previously described [65].

Table 2.2: Primary and Secondary Antibodies

Target	Epitope	Type	Vendor	Catalog #
AR	N-20	Rabbit Polyclonal	Santa Cruz	sc-816
ERK2	D-2	Mouse Monoclonal	Santa Cruz	sc-1647
Gal4	DBD	Rabbit Polyclonal	Santa Cruz	sc-577
Lamin A/C	4C11	Mouse Monoclonal	Cell Signaling	4777
PPAR-gamma	81B8	Rabbit Monoclonal	Cell Signaling	2443
beta-Actin	AC-15	Mouse Monoclonal	Sigma	A1978
HRP-Conjugated Secondary Ab	Mouse IgG	Goat	Santa Cruz	sc-2005
HRP-Conjugated Secondary Ab	Rabbit IgG	Goat	Santa Cruz	sc-2004

Cell Transfection

LNCaP cells were transfected via single-pulse electroporation as previously described [45]. C4-2 cells were transfected with Superfect reagent (Qiagen) according to manufacturer specifications. 293T cells were transfected with Lipofectamine 2000 (Life Technologies) according to manufacturer specifications. Treatment of transfected cells with androgen and/or drug was performed for 8 hours or overnight in serum-free medium as indicated.

Dual Luciferase Assays

Transfected cells were lysed in 1X Passive Lysis Buffer (Promega) and subjected to dual luciferase assays using a Dual Luciferase Assay Kit (Promega) as previously described [45].

Proteasome Inhibition

LNCaP and C4-2 were seeded in RPMI +10% CSS. Cells were then serum-starved overnight and co-treated with 10 μM MG-132 (Sigma) and/or 50 μM EPI-001 and harvested at the indicated time points for western blot.

Nascent RNA Labeling and Isolation

Nascent transcripts were labeled with biotin and subjected to streptavidin pull-down using the Click-iT Nascent RNA Capture Kit (Life Technologies) according to manufacturer specifications. Briefly, LNCaP cells were serum-starved overnight, then treated with 50 μM EPI-001 or vehicle control. After 7 hours incubation, cells were pulsed with 5-ethynyl Uridine (5EU) for an additional hour in the presence of EPI-001 or vehicle to label nascent transcripts, then harvested in Trizol (Life Technologies). Total RNA was then subjected to a Click chemistry reaction which attached a biotin molecule to 5EU-labeled nascent transcripts. RNA was re-precipitated, then bound to streptavidin-conjugated magnetic beads and washed 10X to remove unlabeled transcripts, leaving only biotin-5EU-labeled nascent RNA attached to the beads. First-strand cDNA synthesis was

performed directly on RNA:bead conjugates using the SuperScript VILO cDNA synthesis kit (Life Technologies) according to manufacturer specifications, then subjected to qRT-PCR.

Quantitative RT-PCR

RNA isolation and quantitative RT-PCR analysis were performed as described [[65]] using primers listed in Supplementary Table 3.

Table 2.3: qPCR Primer Sequences

Gene	Species	Direction	Sequence (5' → 3')
AR Exon1	Human	F	TGG ATG GAT AGC TAC TCC GG
AR Intron 1	Human	R	TTT ACC CTG CTG AGC TCT CC
AR Exon2	Human	R	CCC AGA AGC TTC ATC TCC AC
PSA	Human	F	AGG CCT TCC CTG TAC ACC AA
PSA	Human	R	GTC TTG GCC TGG TCA TTT CC
hK2	Human	F	CTG TCA GAG CCT GCC AAG AT
hK2	Human	R	GCA AGA ACT CCT CTG GTT CG
TMPRSS2	Human	F	CTG CCA AGG TGC TTC TCA TT
TMPRSS2	Human	R	CTG TCA CCC TGG CAA GAA TC
FKBP5	Human	F	AGG AGG GAA GAG TCC CAG TG
FKBP5	Human	R	TGG GAA GCT ACT GGT TTT GC
CIDEC	Human	F	ATT GAT GTG GCC CGT GTA ACG
CIDEC	Human	R	CAG CAG TGC AGA TCA TAG GAA A
PDK4	Human	F	AGA GGT GGA GCA TTT CTC GC
PDK4	Human	R	ATG TTG GCG AGT CTC ACA GG
Actin	Human	F	ATG CAG AAA GAG ATC ACC GC
Actin	Human	R	ACA TCTGCT GGA AGG TGG AC
GAPDH	Human	F	GAA GGT GAA GGT CGG AGT C
GAPDH	Human	R	GAG GAT GGT GAT GGG ATT TC
TBP	Mouse	F	GAA GAA CAA TCC AGA CTA GCA GCA
TBP	Mouse	R	CCT TAT AGG GAA CTT CAC ATC ACA G
aP2 (FABP4)	Mouse	F	GAT GAA ATC ACC GCA GAC GAC A
aP2 (FABP4)	Mouse	R	ATT GTG GTC GAC TTT CCA TCC C
LPL	Mouse	F	TGA GAA AGG GCT CTG CCT GA
LPL	Mouse	R	GGG CAT CTG AGA GCG AGT CTT

Prostate Cancer Explants

Patient tissues were obtained from the University of Texas Southwestern Medical Center tissue core under UTSW IRB STU 112013-056 and explant studies were performed as previously described [104,105]. Briefly, cancerous prostates were excised from patients with high-risk (GG8-10) high volume (>2 positive cores) prostate cancers via robotic laparoscopic prostatectomy. Pathology-validated cancer tissue was dissected into 1 mm^3 cubes, and cultured on Surgifoam oral gelatin sponges (Ethicon) for 24 hours in RPMI + 10% FBS supplemented with insulin and hydrocortisone at 10 mg/L each. Explants were then washed 3 x 1 hr in RPMI + 10% CSS supplemented +/- 1 nM Mibolerone alone or in combination with Troglitazone (10 or 50 μM) or EPI-001 (50, 100, or 200 μM) as indicated. Tissue explants were then cultured in RPMI + 10% CSS supplemented with 1 nM Mibolerone alone or in combination with Troglitazone or EPI-001 for 48 hrs at 37^o C. Explants were then removed from the sponges and lysed for western blot or qRT-PCR analysis using a tissue grinder in the appropriate lysis buffer.

Oil Red O Staining

Oil-red O staining was performed on 3T3-L1 cell cultures as previously described [119]. Briefly, cells were fixed in Baker's Formalin for 30 min at room temperature, followed by staining in a 60% (w/v) solution of Oil-red O (Sigma-Aldrich, Milwaukee, WI) in isopropyl alcohol for 10 min.

pH Stability Studies of EPI-001 and Thiol Reactivity Assays

2-Mercaptoethanol, cysteamine, and rose bengal were purchased from Sigma-Aldrich, and reduced glutathione and tris(2-carboxyethyl)phosphine hydrochloride salt (TCEP•HCl) were purchased from Alfa Aesar. All chemicals were used without additional purification unless noted. A solution of thiol (10 equiv.) and TCEP•HCl (100 µL of a 0.5 M DMSO stock soln.) in 1x aqueous PBS (5 mL) was adjusted to the desired pH (2.4, 7.4, or 9.4) using either aqueous HCl (6 M) or aqueous NaOH (6 M) as determined by a pH meter (Thermo Scientific Orion 3 Star). Reduced l-glutathione, 2-mercaptoethanol, and cysteamine [120], were used as thiols in this assay. To a solution of the appropriate individual thiol (170 µL) was added either EPI-001 or compound 2 (1 equiv.; both compounds were solubilized as 50 mM DMSO stock solutions). The total composition of DMSO did not exceed 7.5% in any experiment and the ratio of thiol to EPI-001/compound 2 was 10:1. Note: This order of addition is key to achieving the appropriate pH environment for the reaction as the addition of reduced l-glutathione and TCEP acidify neutral solutions and cysteamine basifies neutral solutions. Aliquots of reactions were analyzed immediately (t ~30 min) following initial mixing by reverse phase HPLC and LC-MS. Reactions were gently shaken at 37 ^{o}C for 12 h, then analyzed again using HPLC and LC-MS. Reactions were conducted in 2 mL clear screw cap glass vials (Agilent Technologies). Note: Thirty minutes was the earliest time point that could be collected after adding EPI-001, mixing, and injecting an aliquot onto the HPLC. The HPLC analytical method (Zorbax SB-C18 4.6 x 150 mm, 3.5 µm column, Agilent Technologies; flow rate = 1.0 mL/min)

involved isocratic 10% CH_3CN in 0.1% (v/v) aqueous CF_3CO_2H (0 to 2 min), followed by linear gradients of 10-85% CH_3CN (2-24 min) and 85%-95% CH_3CN (24-26 min). LC-MS analyses were performed on an Agilent 1100 series instrument equipped with an Agilent MSD SL Ion Trap mass spectrometer (positive-ion mode) and a Zorbax SB-C18 column (0.5 x 150 mm, 5 µm, Agilent Technologies). The analysis method (15 µL/min flow rate) involved isocratic 10% MeCN (containing 0.1% TFA) in ddH_2O (containing 0.1% HCO_2H; 0 to 2 mins) followed by a linear gradient of 10% to 90% MeCN (containing 0.1% TFA) in ddH_2O (containing 0.1% HCO_2H; 2 to 24 mins), and isocratic 90% MeCN (containing 0.1% TFA) in ddH_2O (containing 0.1% HCO_2H; 24-26 mins). The column was heated to 40 ^oC. Wavelength monitored = 254 nm for all experiments unless otherwise noted. LC-MS analysis was performed on crude reaction mixtures. To quantify the amount of parent compound remaining, the area under the curve (AUC) of the parent compound was divided by the AUC of an internal standard. Rose bengal (7.5 µM) was used as the internal standard and was added immediately before HPLC analysis Experiments were performed in triplicate and values shown are the mean ± standard deviation (calculated in Microsoft Excel). Calibration curves to normalize for injection variances during HPLC analysis were generated for each compound (Figure 2.30). For both compounds, $R^2 > 0.99$.

Data Analysis and Statistics

All statistical comparisons were made using the two-tailed Student's t-Test with a P value of 0.05 or less considered significant.

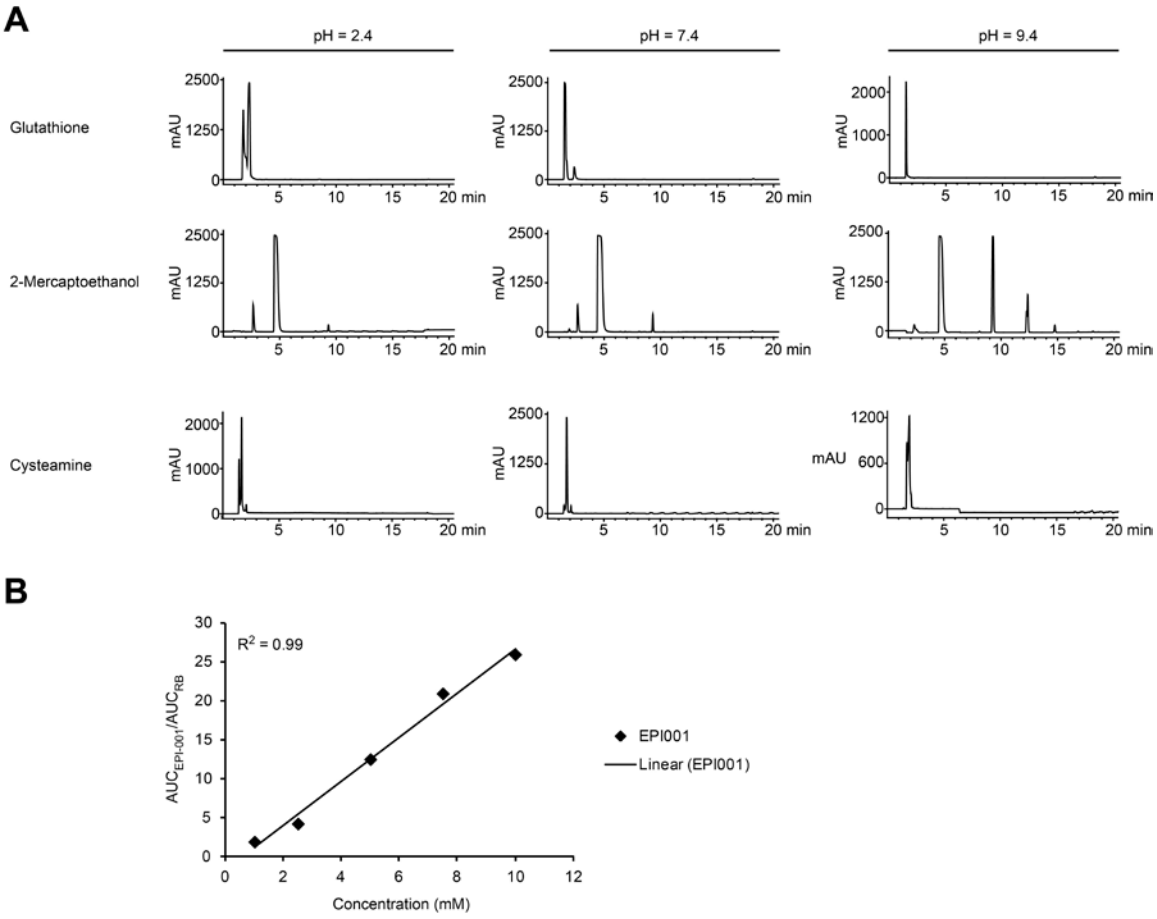

Figure 3.30: (*A*) Solutions of the three thiols (glutathione, 2-mercaptoethanol, cysteamine) in aq. PBS / DMSO (~10:1) at pH 2.4, 7.4, and 9.4, respectively, were shaken at 37 ^{o}C. The reactions were analyzed by reverse-phase HPLC at t = 12 h to establish background traces. (*B*) A calibration curve was generated to normalize for injection variances during HPLC analysis.

AUTHOR'S NOTE

This chapter was reproduced from a study published in *Oncotarget* [121]. Lucas

J. Brand and Scott M. Dehm were the lead authors of the study and wrote the manuscript. LJB and SMD were principally responsible for designing the experiments. LJB executed the experiments corresponding to figures 2.1 – 2.16, 2.18, 2.20, and 2.21. Figure 2.17 was generated by Preethi Ravindranathan and Ganesh V. Raj. Figure 2.19 was generated by Hong Guo and Xiaoli Chen. Margaret E. Olson and Daniel A. Harki designed and executed experiments to generate Figures 2.22 – 2.30. Technical assistance was provided by Aaron M. Kempema and Timothy E. Andrews.

CHAPTER 3

MOLECULAR CHARACTERIZATION OF ANDROGEN RECEPTOR NH2-TERMINAL TRANSCRIPTIONAL ACTIVATION DOMAINS

INTRODUCTION

The preceding chapters have discussed the impact of prostate cancer (PCa) on human health in the US [29], as well as the central role played by the androgen receptor (AR) in the development of the prostate and disease progression in PCa patients [82]. For patients whose cancer has spread outside of the prostate capsule or formed distal metastases, inhibiting AR activity is the current standard of care. This is achieved by preventing androgens from binding AR, either by blockade of androgen production or competitive inhibition of the ligand binding domain (LBD) of the AR [122,123]. While initially effective, these strategies ultimately fail through mutation or deletion of the LBD, or amplification of the AR gene [124]. These mechanisms render hormone-based therapy ineffective and trigger a transition to castration resistant prostate cancer (CRPC), for which no cure is currently available [84]. Due to the mutability of the LBD, there is an urgent clinical need for AR-targeted therapeutics that bind outside of the ligand binding pocket to exert their effect.

The AR NH2-terminal domain (NTD) contains the primary transcriptional activation functions of the AR (Figure 1.1), and therefore serves as an attractive

target for therapeutic intervention. The recent characterization of pathologic AR splice variants (ARV) (Figure 1.2) as a major driver of drug resistance in clinical specimens highlights the NH2-terminal domain as a target for AR-based PCa intervention [125-127]. However, little is known about the functional dynamics of the NTD in PCa cells due to a high degree of intrinsic disorder in this domain [76,117]. Previous studies have reported a central role for amphipathic helices in AR transcriptional activation, namely a ^{178}LKDIL^{182} motif resident in the AF1a region of the TAU1 domain [2,21] and a ^{435}WHTLF^{439} motif in the TAU5 domain [2,71,128] (Figure 1.1). Similar helices have been shown to act as anchors for coactivator recruitment and guides for proper folding of intrinsically disordered regions (IDR) of cellular proteins [129], but the precise role of LKDIL and WHTLF in mediating AR transcriptional activity has been elusive. Additionally, it is currently unknown whether the loss of the regulatory LBD influences the relative activity of TAU1 and TAU5 in pathologic ARV. Finally, characterization of IDR-containing proteins has demonstrated that the expression and functional role of IDRs can vary significantly between cell types due to factors such as alternative splicing, post-translational modification, and differential expression of binding partners [129-131]. Much of the initial biochemical characterization of the NTD was performed in non-prostate cell lines [19,70,72,75,128,132-134], raising concern that data derived from some early models may not accurately reflect the role of NTD functional domains in human PCa. Thus, while the AR NTD presents an attractive target for PCa intervention, the relevant structural and functional elements appropriate for targeting are yet to be clearly defined.

In this study, we performed biochemical assays to assess the functional dynamics of the constituent domains of the AR NTD in human prostate cancer cells. We showed that the TAU1 LKDIL motif is necessary, but not sufficient, for transcriptional activity of the broader TAU1 domain. To this end, we found that an additional domain within TAU1, termed AF1b (Figure 1.1), possessed intrinsic transactivation activity. Finally, we defined the relative input of TAU1, AF1a, AF1b, and TAU5 in AR-V7, an AR splice variant frequently expressed in CRPC. Overall, this study provides new insight into the functional dynamics of the AR NTD, and provides a framework for future translational studies of this domain.

RESULTS

The LKDIL motif does not recapitulate the full transcriptional activity of TAU1 in human AR.

Given the conclusions of previous studies that identified $AR^{178}LKDIL^{182}$ as the transcriptional core of TAU1 [2], we sought to test whether this mechanistic data holds true in the human PCa cells. In order to assess the activity of ectopic AR isoforms independently of the endogenous AR, we substituted the AR DNA binding domain with the yeast Gal4 DBD. These AR^{Gal4} constructs were then co-transfected along with the Gal4-responsive $sPSA^{Gal4}$-Luciferase reporter into LNCaP and C4-2 PCa cells (Figure 3.1). In androgen sensitive LNCaP cells, endogenous AR^{Gal4} activated the $sPSA^{Gal4}$-LUC reporter and this activity was further induced upon addition of the synthetic androgen mibolerone (Figure 3.1).

AR^{Gal4} also displayed constitutive androgen-independent activity in castration resistant C4-2 cells (Figure 3.1). Deletion of AF1a from AR^{Gal4} inhibited

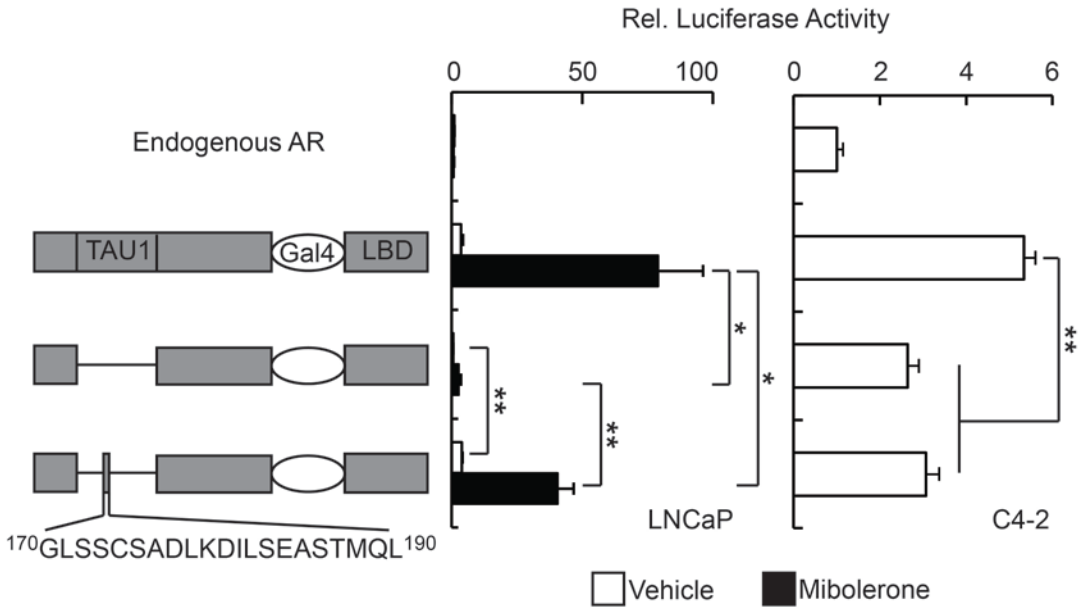

Figure 3.1: LNCaP and C4-2 cells were transfected with $sPSA^{Gal4}$-LUC and the indicated AR^{Gal4} constructs and treated 24 h with 1 nM Mibolerone or vehicle control, then subjected to luciferase assay. Bars represent mean +/- SD of n = 3 samples representative of two independent experiments. Please see the note in Materials and Methods regarding the representation of statistics in this chapter.

transcriptional activity in both cell lines. Restoration of a 21-amino acid peptide sequence including the ^{178}LKDIL^{182} motif (GLSSCSADLKDILSEASTMQL) rescued approximately 50% of androgen-induced AR^{Gal4} transcriptional activity in LNCaP cells, but did not affect androgen-independent AR^{Gal4} activity in either cell line.

Given the possibility that a small, 21-amino acid peptide may have omitted uncharacterized, LKDIL-proximal regulatory components, we tested whether re-introduction of larger peptide sequences might enhance transcriptional activity of LKDIL within TAU1-deleted AR^{Gal4}. Using the +21 peptide as a control, we tested three additional fragments of increased length (+25, +29, and +33), as well as a

putative “Core TAU1” sequence identified by Calleweart et al. [75] (Table 3.1). None of the expanded cassettes enhanced AR^{Gal4} transcriptional activity compared with the +21 control (Figure 3.2). Taken together, these data indicate an important role for the LKDIL motif in AR-mediated transcriptional activation. Furthermore, this work indicates that LKDIL may interact functionally with other TAU1 components to support full AR transcriptional activity in human PCa cells.

Table 3.1: Length and sequence of AF1a peptides

Peptide Size	*Sequence*
+21	170-GLSSCSADLKDILSEASTMQL-190
+25	168-FPGLSSCSADLKDILSEASTMQLLQ-192
+29	166-PTFPGLSSCSADLKDILSEASTMQLLQQQ-194
+33	164-LGPTFPGLSSCSADLKDILSEASTMQLLQQQQQ-196
Core TAU1 [134]	173-SCSADLKDILSEASTMQLLQQQQQ-196

AF1b has intrinsic transcriptional activity in human PCa cells and is required for full functionality of TAU1

We next tested whether small internal deletions within the AF1a domain could identify discrete regions that may contribute to LKDIL-mediated transcriptional activity in the human AR. A series of six tiling deletions that spanned the length of AF1a were prepared in the ARGal4 expression plasmid (Figure 3.3). Surprisingly, all AF1a deletions with the exception of Δ125-136

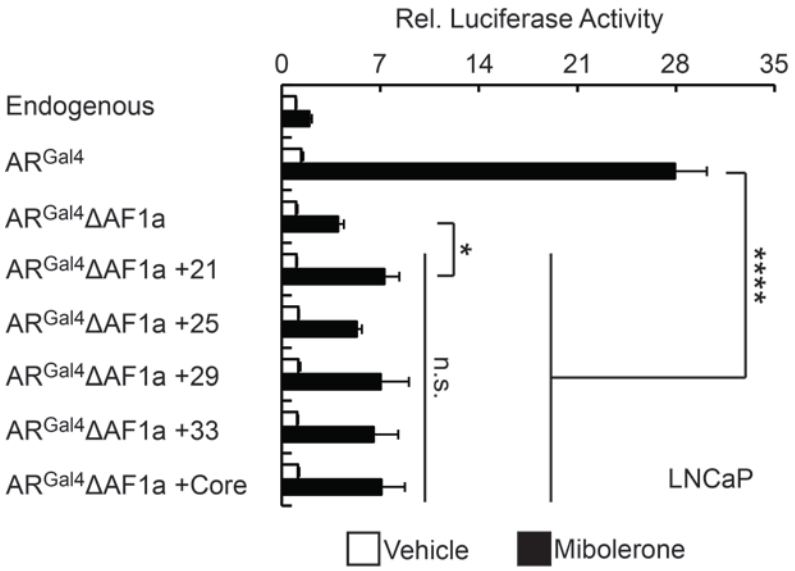

Figure 3.2: LNCaP cells were transfected with sPSA^{Gal4}-LUC and the indicated AR^{Gal4} constructs and treated overnight with 1 nM Mibolerone or vehicle control, then subjected to luciferase assay. Bars represent mean +/- SD for n = 3 samples representative of two independent experiments.

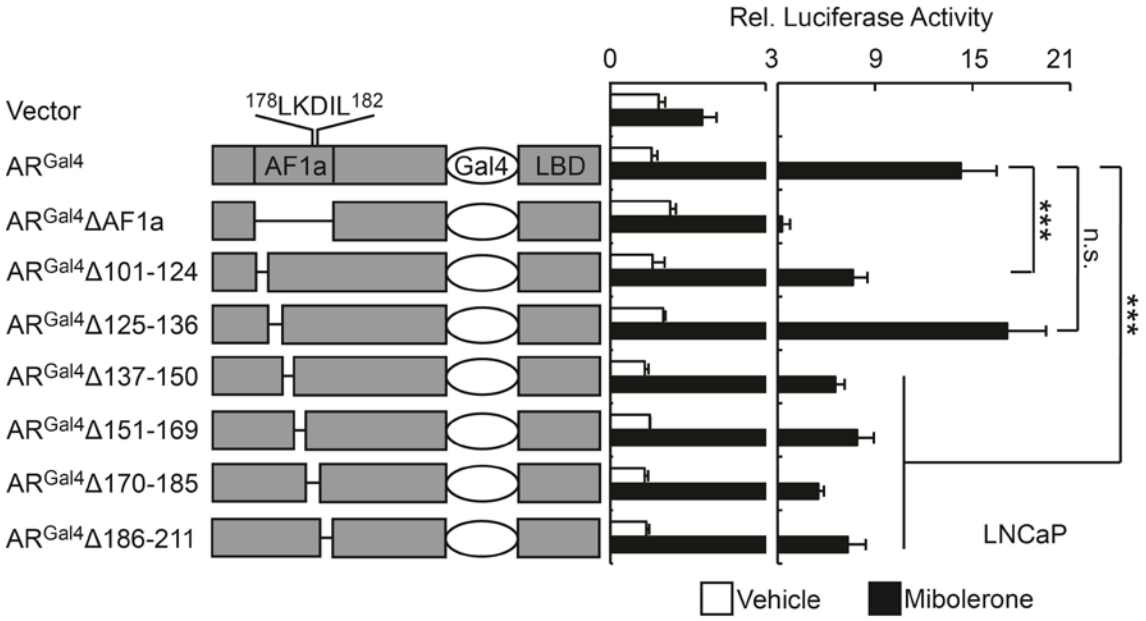

Figure 3.3: LNCaP cells were transfected with sPSA^{Gal4}-LUC and the indicated AR^{Gal4} constructs and treated overnight with 1 nM Mibolerone or vehicle control, then subjected to luciferase assay. Bars represent mean +/- SE for n = 6 samples from two independent experiments.

reduced androgen-dependent AR activity by approximately 50%, whereas Δ125-136 had no effect on AR activity (Figure 3.3, black bars). None of the deletions appeared to affect androgen-independent AR activity (Figure 3.3, white bars). Given that most of the deletions had a similar impact on AR activity in this model, we considered whether this approach may be disrupting unknown structural elements that could be critical for AR activity in LNCaP, e.g. recruitment of transcriptional co-regulators. To assess the transcriptional activity of these same

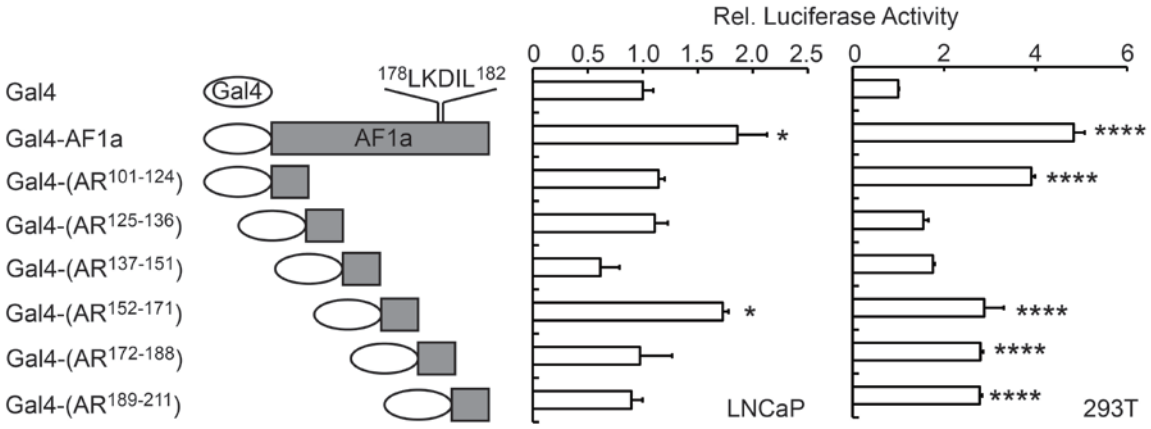

Figure 3.4: LNCaP and 293T cells were transfected with sPSA^{Gal4}-LUC or pG5-LUC, respectively, and the indicated AR^{Gal4} constructs. Superscripted numbers denote AR amino acid composition. Cells were incubated overnight in serum-free medium, then subjected to luciferase assay. Bars represent mean +/- SE for n = 6 samples from two biological replicates.

six AF1a sub-regions, we synthesized oligonucleotides coding for each of the corresponding regions deleted from AF1b in Figure 3.3 and cloned them into an expression vector in-frame with the Gal4 DBD. The resulting Gal4-AF1a fusions (Figure 3.4) were then co-expressed in LNCaP or 293T fibroblast cells with a Gal4-responsive luciferase reporter. In 293T cells, four of the six constructs exhibited intrinsic transcriptional activity (Figure 3.4). However, in LNCaP cells,

only the AR$^{152-171}$ fragment displayed transcriptional activity above the background (Figure 3.4). Paradoxically, this construct does not contain the ^{178}LKDIL^{182} motif or the Core TAU1 sequence previously shown to harbor intrinsic transactivation activities.

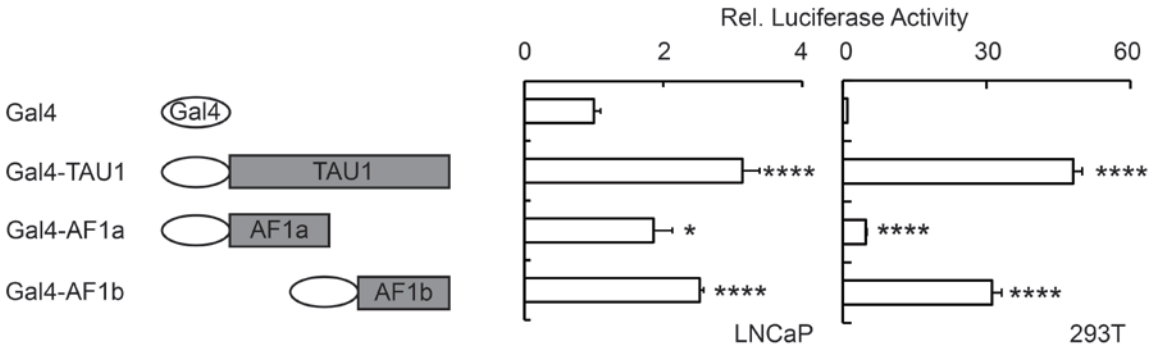

Figure 3.5: LNCaP and 293T cells were transfected with sPSA^{Gal4}-LUC or pG5-LUC, respectively, and the indicated AR^{Gal4} constructs. Cells were incubated overnight in serum-free medium, then subjected to luciferase assay. Bars represent mean +/- SE for n = 6 samples from two biological replicates.

Previous studies of the AR in non-prostate cell lines led to the conclusion that the AF1a domain, and the ^{178}LKDIL^{182} motif in particular, was the primary driver of TAU1-mediated AR transcriptional activity [2,70,75]. As demonstrated in Figure 3.4 and 3.5, however, ectopically expressed AR fragments may harbor different levels of transcriptional activity in prostate vs. non-prostate cells. We therefore tested the activity of Gal4-tethered AF1a relative to Gal4-tethered TAU1 in LNCaP and 293T cells (Figure 3.5). Surprisingly, Gal4-AF1b displayed higher transcriptional activity than Gal4-AF1a in both cell lines (Figure 3.5).

To further characterize the AF1b domain, we introduced tiling deletions

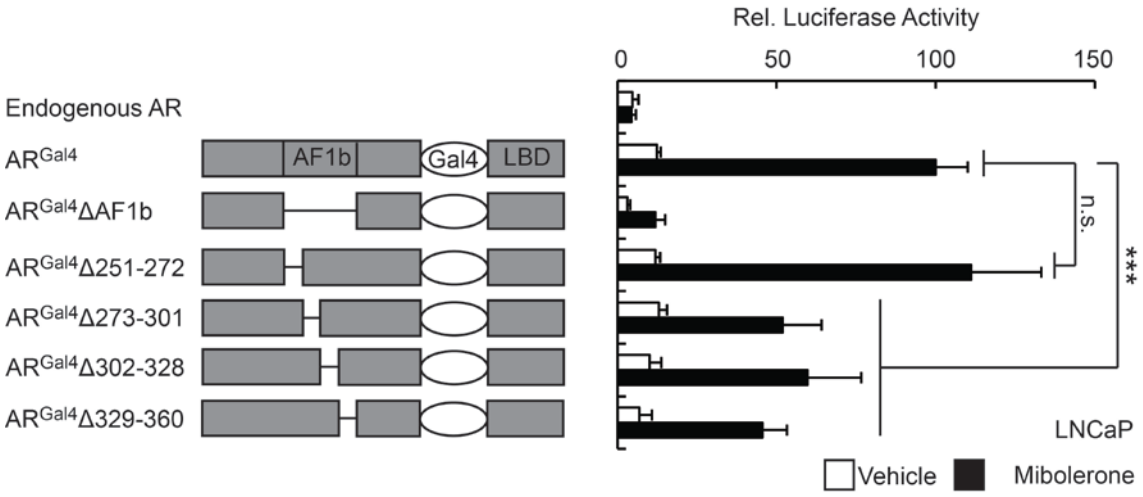

Figure 3.6: LNCaP and 293T cells were transfected with sPSA^{Gal4}-LUC or pG5-LUC, respectively, and the indicated AR^{Gal4} constructs. Cells were incubated overnight in serum-free medium, then subjected to luciferase assay. Bars represent mean +/- SE for n = 6 samples from two biological replicates.

within AF1b of AR^{Gal4} and assessed the impact on transcriptional activity (Figure 3.6). While deletion of the full AF1b domain reduced androgen-independent AR^{Gal4} activity, none of the tiling deletions appeared to have a significant impact in the absence of androgens. On the other hand, deletion of three independent segments between amino acids 273 and 360 inhibited androgen-dependent AR activity ~40-50%. Taken together, these data demonstrate that the AR AF1b domain harbors significant intrinsic transcriptional activity in prostate cancer cells and is required for full activity of the TAU1 domain.

Constitutively active AR splice variants differentially utilize NTD transactivation domains compared with full-length AR.

Given the emerging role of pathologic AR variants (ARV) in clinical prostate cancer [68,90,126], it is critical to develop a functional understanding of

the role of each of the known NH2-terminal transcriptional activation domains and how they differ in the context of full length versus truncated AR. Since the regulatory COOH-terminal domain is deleted in ARV [80,92,95], the dynamics and regulation of AR transcriptional activation are likely to be altered in cells expressing ARV. This raises the important question of whether AR TAU1 and -5 function equivalently in full-length AR compared with ARV. Previous studies of full-length AR in both androgen-dependent and CRPC cell lines revealed that TAU1 deletion completely inhibited AR transcriptional activity [73]. On the other hand, TAU5 deletion inhibited only androgen-independent AR activity, whereas AR activity was significantly enhanced in the presence of androgen [71,73]. To test the impact of TAU5 deletion on ARV activity in LNCaP and C4-2 cells, we ablated endogenous AR expression with siRNA and co-transfected with siRNA-resistant full-length AR, AR-V7 (also referred to as AR3 or 1/2/3/CE3), or AR-fl/AR-V7 in which TAU5 had been deleted (Figure 3.7). Expression of AR-V7 elicited strong, constitutive AR activity that was insensitive to androgen, whereas AR-fl was only active in the presence of mibolerone. Deletion of TAU5 in AR-V7 potently inhibited transcriptional activity under all conditions, whereas TAU5 was only required for AR-fl activity in the absence of ligand and enhanced AR-fl activity in the presence of androgen.

To further assess the utilization of NTD transcriptional activation domains by ARV, we generated AR-V7 isoforms in which TAU1, AF1a, AF1b, and TAU5 had been deleted (Figure 3.8). When expressed in DU 145 cells, deletion of

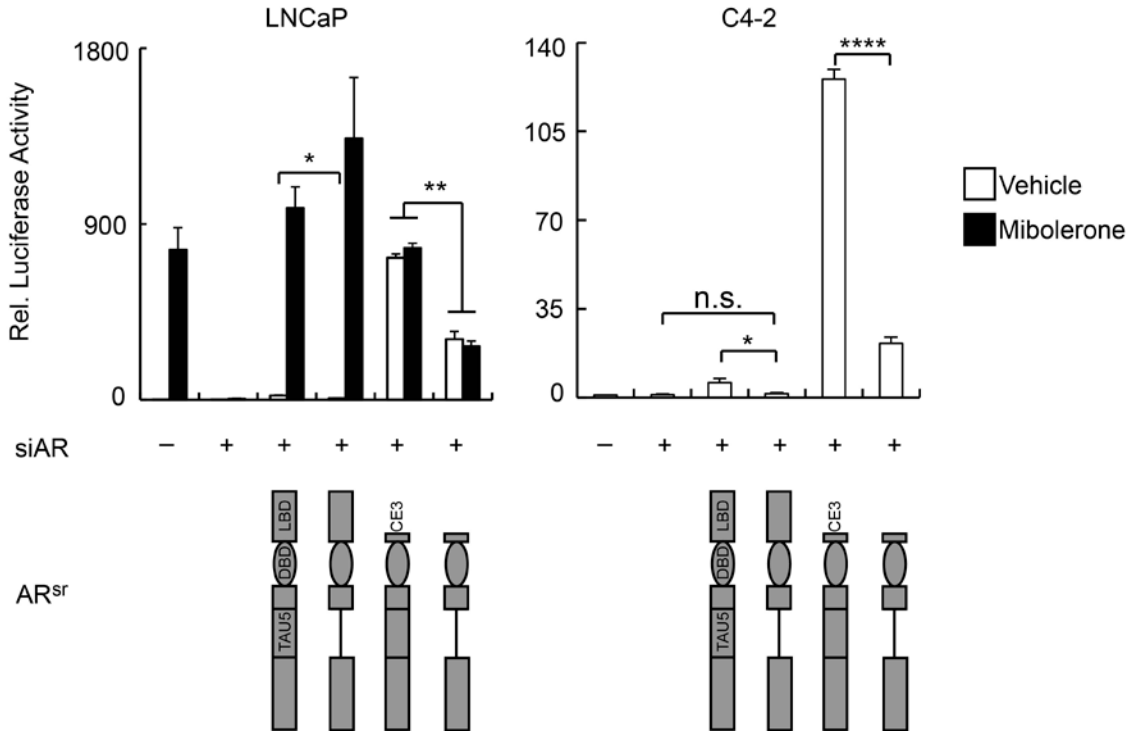

Figure 3.7: LNCaP and C4-2 cells were transfected with -5746 PSA-LUC and the indicated siRNA-resistant AR constructs, then treated overnight with 1 nM Mibolerone or vehicle control. Cells were then lysed and subjected to luciferase assay. Bars represent mean +/- SE of n = 6 samples pooled from two independent experiments.

TAU1 resulted in ~90% reduction in ARV transcriptional activity, similar to the effect of TAU1 deletion in previous studies [73]. Deletion of AF1a or AF1b inhibited AR-V7 activity by 45% and 60% respectively, again suggesting a critical role for AF1b in AR transcriptional activity. TAU5 deletion resulted in approximately 50% inhibition of AR-V7 activity. In LNCaP cells, deletion of AF1a, AF1b, and TAU5 inhibited AR-V7 activity on the order of 30% (AF1a) to 70% (AF1b and TAU5). Paradoxically, however, deletion of TAU1 doubled AR-V7 activity in this model. It has been previously suggested that ARV function by heterodimerizing with AR-fl and chaperoning it to the nucleus in the absence of

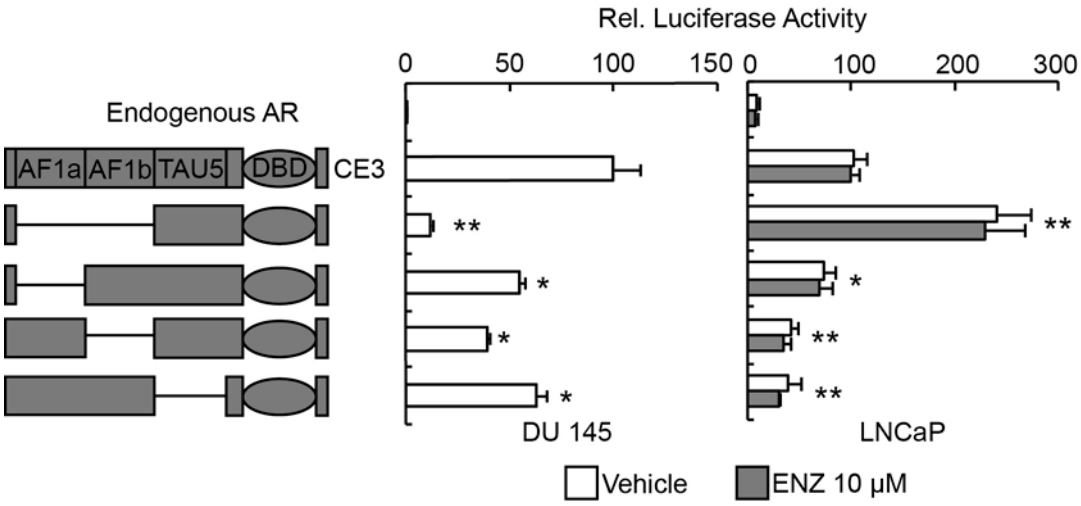

Figure 3.8: DU 145 and LNCaP cells were transfected with 4xARE-LUC or -5746 PSA-LUC, respectively, and the indicated siRNA-resistant AR constructs. Cells were treated overnight with 10 μM enzalutamide (ENZ) or vehicle control. Cells were then lysed and subjected to luciferase assay. Bars represent mean +/- SD of n = 3 samples representative of two independent experiments. * = $P < 0.05$, ** = $P < 0.01$ relative to CE3.

androgen, thus allowing for perpetuation of AR-fl signaling under castrate conditions [66]. To test if this might explain the effect of AR-V7ΔTAU1 in LNCaP cells, we treated LNCaP with enzalutamide, which inhibits AR-fl nuclear translocation and DNA binding [36]. Treatment with enzalutamide had no effect on the transcriptional activity of AR-V7 or any of the deletion mutants (Figure 3.8, gray bars), suggesting that AR-fl is not contributing to AR-V7 isoform activity in this experiment. Taken together, these data indicate differential utilization of AR NH2-terminal transcriptional activation domains by ARV compared to full-length AR, and that the presence or absence of androgen influences the function of these domains in AR-fl. Furthermore, the role of TAU1 in ARV transcriptional activity may be cell-line dependent, whereas TAU5 is a critical mediator of ARV activity in all cell lines tested. Finally, these data suggest that AF1b plays a

critical, previously under-appreciated functional role in both AR-fl and ARV transcriptional activity.

DISCUSSION

In this study, we performed biochemical assays to further define the activity and molecular dynamics of the AR TAU1 domain in human PCa cells using a Gal4-based reporter system. We demonstrated that, while the ^{178}LKDIL^{182} motif is required for full TAU1 activity, a peptide encompassing the LKDIL motif does not completely account for the transcriptional activity of AR TAU1 in LNCaP PCa cells. Our data also suggest a prominent role for AF1b in mediating AR transcriptional activity, which is supported by the observation of robust intrinsic transcriptional activity in LNCaP and 293T cells. However, we were not able to nominate discrete regions of AF1a or AF1b that could account for their respective transactivation functions. Rather, internal deletions produced seemingly equivalent intermediate effects, perhaps due to disruption of uncharacterized structural elements. Finally, we show that NTD transcriptional activation domains are differentially utilized by truncated ARV compared with full-length AR, suggesting that the presence or absence of the COOH-terminal domain may have an effect on the molecular dynamics of the NTD.

Short, amphipathic helices have been shown to play a critical role in AR NTD function [2,71,72,80,133]. Previous studies of TAU1 and its constituent domains concluded that the ^{178}LKDIL^{182} motif in AF1a was the primary driver of

TAU1 transcriptional activity. Our data support the role of the LKDIL motif as a major player in TAU1 transcriptional activity in human AR. However, in contrast to previous studies, our peptide rescue experiments indicated that the LKDIL motif only accounts for approximately half of AR TAU1 transcriptional activity. To this end, it should be noted that our study was conducted with an AR^{Gal4} hybrid in AR-positive human prostate cancer cells, whereas previous studies were modeled with ectopically-expressed AR in AR-null, non-prostate cell lines [19,70,72,75,128,132-134]. Furthermore, we demonstrated that AF1b harbors a high degree of intrinsic transcriptional activity in our AR^{Gal4} model, suggesting a more prominent role in AR transcriptional activity than previously appreciated. Problematically, standard approaches to biochemical dissection of the intrinsically disordered NTD, e.g. small internal deletions and promoter tethering experiments, does not appear to be an optimal approach to studying the dynamics of AR transcriptional activation. Intrinsically disordered proteins, of which the AR is an example, have been shown to rely on allosteric coupled binding and folding responses with transcriptional co-regulators in order to mediate their activity [135,136]. Internal deletions within protein interaction domains, therefore, may disrupt the biophysical properties of the domain as a whole rather than providing insight into the regulation of a specific region. Similarly, promoter tethering of small fragments of the NTD would likely not recapitulate the full allosteric binding elements. These challenges and their implications for future translational research on AR transcriptional activation domains will be discussed in more detail in the next chapter.

Previous studies have shown that the TAU5 domain of the AR NTD is differentially utilized in the presence or absence of androgens in full-length AR [71,73]. Whereas deletion of TAU5 in the full-length AR leads to increased activity in the presence of androgens, the same deletion is inhibitory when androgens are withdrawn. This raises the question of whether the absence of the regulatory CTD, such as in AR splice variants, may affect the transcriptional activation dynamics of the NTD. Our data demonstrate that deletion of TAU5 in AR-V7 mimics the latter scenario, suggesting that TAU5 is critical for full transcriptional activity of AR splice variants. On the other hand, TAU1 activity in AR-V7 appears to be more context-dependent. TAU1 deletion enhanced V7 activity in AR-expressing LNCaP cells, but is significantly inhibitory in AR-null DU145 cells. This may be due to 1) differences in AR co-regulator expression between the two cell lines, or 2) a promoter-dependent effect borne out by the use of a concatenated 4x-androgen response element-driven reporter in DU 145 vs. a PSA enhancer-driven reporter in LNCaP. Deletion of AF1a is inhibitory in both cell lines, though to a much lesser degree in LNCaP cells, particularly when contrasted to the effect of AF1a deletion in the full-length AR. Finally, deletion of AF1b was potently inhibitory in LNCaP cells, but less so in DU145. Taken together, these data demonstrate that AR variants differentially utilize NTD transcriptional activation domains, and that the activity of these domains may be context-dependent depending on the expression of transcriptional co-regulators or promoter/enhancer context. Future experiments should address these questions using stably transfected cell lines to characterize the binding partners associated

with each of these domains, and whether the co-regulatory cohort differs significantly in cells that express AR-fl, ARV, or are AR-null. We will discuss this strategy and its potential applications in Chapter 4.

In summary, we confirm that short, amphipathic helices are central to the transcriptional activity of the AR NTD, but that these helices are likely not responsible for the full level of AR NTD transcriptional activity. We also report robust intrinsic transcriptional activity of AF1b which is required for AR transcriptional activity, and that the utilization of the TAU1, AF1a, AF1b, and TAU5 domains differs between full-length AR and truncated AR variants. The utilization of these domains may also be context dependent, particularly with regard to the transcriptional coregulatory cohort expressed in the cell. Taken together, these data provide new insights into the regulation and activity of the AR NTD, which remains an attractive target for therapeutic intervention. Future translational inquiry into NTD dynamics should be informed by studies of other intrinsically disordered proteins, which will be discussed in the next chapter.

MATERIALS AND METHODS

Cell Culture

LNCaP, C4-2, DU 145, and 293T cell lines were obtained from ATCC and maintained in medium and serum as directed by ATCC protocols. The ATCC validates the authenticity of these cell lines via short tandem repeat (STR) analysis. Cells were cultured in a 37^{o} C incubator with 5% CO_2 for no longer than 15 passages after resuscitation of frozen stocks.

Reagents

Mibolerone (MIB) was purchased from Sigma. Enzalutamide (ENZ) was purchased from Selleck Chemicals. Superfect and Lipofectamine 2000 transfection reagents were purchased from Life Technology.

Plasmids

Plasmids encoding human AR (p5HBhAR-A), AR^{Gal4}, $AR^{Gal4}\Delta$TAU1, $AR^{Gal4}\Delta$TAU5, sPSA-Luciferase (also referred to as PSAenh(ARE)-LUC), and $sPSA^{Gal4}$-Luciferase (also referred to as PSAenh(GAL4)-LUC) have been described [45]. SV40-Renilla and pG5-Luciferase were purchased from Promega. The Gal4 DBD expression plasmid (pM) was purchased from Clontech. Gal4-TAU1 (AR a.a. 101-360) has been previously described [121].

Tiling deletions within AF1a (AR a.a. 101-211) and AF1b (AR a.a. 251-360), as well as deletions of the full AF1a and AF1b domains, were prepared by introducing in-frame BssHII recognition sites into the AR^{Gal4} expression vector using a Stratagene QuikChange site-directed mutagenesis kit (New England Biolabs) with custom mutagenic primers as listed in Table 3.2. Mutagenized plasmids were then digested with BssHII, ligated, and transformed into ultracompetent *E. coli*. Deletions were verified by restriction digest.
Gal4 tethering of AF1a and AF1b was performed by PCR amplification of the AF1a and AF1b domains with mutagenic primers that introduced in-frame 5' EcoRI and 3' HindIII recognition sites (AF1a EcoR1 Fwd:

GGTTCTCCCgAAttCCATCGTAGAGGCCCC; AF1a HindIII Rev: GGGAGCCCCGCAaGCtTCCCTCGCTCTCCC; AF1b EcoRI Fwd: GTGTCGGTGTCCATGGAATTCGGTGTGGAGGCG; AF1b HindIII Rev: CAGTGGAAGCTTGTAGTAGTC). Amplicons were digested with EcoR1 and HindIII, and then cloned into EcoRI/HindIII-digested pM. Insertions were verified by restriction digest.

Table 3.2: Mutagenic Primer Sequences for TAU1 Sub-domain Deletions

Amino Acid Position	*Forward/Reverse Mutagenic Primer Sequences (mutated residues noted in lowercase lettering)*
101/102	F: CAAGCCCATCGTAGAGcgCgCACAGGCTACCTGGTC R: GACCAGGTAGCCTGTGcGcgCTCTACGATGGGCTTG
124/125	F: CGGGACCTCACGGTGGcGCgCTCTCCAACGCAGGGTCTC R: GAGACCCTGCGTTGGAGAGcGCgCCACCGTGAGGTCCCG
136/137	F: CTCGGACGAGCCGCCGcGcgCGCCAGCAAGGGGCTG R: CAGCCCCTTGCTGGCGcgCgCGGCGGCTCGTCCGAG
150/151	F: CAGCTGCCAGCACCTgCgcgCGAGGATGACTCAGCTGCC R: GGCAGCTGAGTCATCCTCGcgcGcAGGTGCTGGCAGCTG
169/170	F: CTGGGCCCCACTTTCgCgcGCTTAAGCAGCTGCTCC R: GGAGCAGCTGCTTAAGCgcGcGAAAGTGGGGCCCAG
185/186	F: GACATCCTGAGCGAGGCgcGCACCATGCAACTCCTTCAG R: CTGAAGGAGTTGCATGGTGCgcGCCTCGCTCAGGATGTC
211/212	F: CAGCAGCAGCGGGAGAGCGcGcGAGGCCTCGGGGGCTC R: GAGCCCCCGAGGCCTCgCgCGCTCTCCCGCTGCTGCTG
251/252	F: GCAGTGTCGGTGTCCATGGcgCgcGGTGTGGAGGCGTTGGAG R: CTCCAACGCCTCCACACCgcGcgCCATGGACACCGACACTGC
272/273	F: GGGGATTGCATGTACGCgCgcCTTTTGGGAGTTCCACCC R: GGGTGGAACTCCCAAAAGgcGcGCGTACATGCAATCCCC
301/302	F: CTGCTAGACGACAGCGCgcGCAAGAGCACTGAAGATACTGC R: GCAGTATCTTCAGTGCTCTTGCgcGCGCTGTCGTCTAGCAG
328/329	F: GGCGAGAGCCTAGcgcGCTCTGGCAGCGCTGCAGCAGGG R: CCCTGCTGCAGCGCTGCCAGAGCgcgCTAGGCTCTCGCC
360/361	F: GCACTGGACGAGGCAGCTGCGcgCCAGAGTCGCGACTAC R: GTAGTCGCGACTCTGGcgCGCAGCTGCCTCGTCCAGTGC

Gal4 tethering of AF1a fragments was performed by synthesizing complementary oligonucleotides, which when annealed would form dsDNA cassettes encoding short peptide sequences (approximately 10-20 amino acids

Table 3.3: Synthetic AF1a Oligonucleotides

AF1a Region	*Oligo Sequences*	*Peptide Sequence*
100-125	Fwd: AATTC GGC CCC ACA GGC TAC CTG GTC CTG GAT GAG GAA CAG CAA CCT TCA CAG CCG CAG TCG GCC CTG GAG TGC CAC CCC GAG TAA A Rev: AGCTT TTA CTC GGG GTG GCA CTC CAG GGC CGA CTG CGG CTG TGA AGG TTG CTG TTC CTC ATC CAG GAC CAG GTA GCC TGT GGG GCC G	QF-GPTGYLVLDEEQQPSQPQSALECHPE-Stop
124-137	Fwd: AATTC CCC GAG AGA GGT TGC GTC CCA GAG CCT GGA GCC GCC GTG GCC TAA A Rev: AGCTT TTA GGC CAC GGC GGC TCC AGG CTC TGG GAC GCA ACC TCT CTC GGG G	QF-PERGCVPEPGAAVA-Stop
136-152	Fwd: AATTC GTG GCC GCC AGC AAG GGG CTG CCG CAG CAG CTG CCA GCA CCT CCG GAC TAA A Rev: AGCTT TTA GTC CGG AGG TGC TGG CAG CTG CTG CGG CAG CCC CTT GCT GGC GGC CAC G	QF-VAAASKGLPQQLPAPPD-Stop
151-171	Fwd: AATTC CCG GAC GAG GAT GAC TCA GCT GCC CCA TCC ACG TTG TCC CTG CTG GGC CCC ACT TTC CCC GGC TAA A Rev: AGCTT TTA GCC GGG GAA AGT GGG GCC CAG CAG GGA CAA CGT GGA TGG GGC AGC TGA GTC ATC CTC GTC CGG G	QF-PDEDDSAAPSTLSLLGPTFPG-Stop
170-187	Fwd: AATTC CCC GGC TTA AGC AGC TGC TCC GCT GAC CTT AAA GAC ATC CTG AGC GAG GCC AGC TAA A Rev: AGCTT TTA GCT GGC CTC GCT CAG GAT GTC TTT AAG GTC AGC GGA GCA GCT GCT TAA GCC GGG G	QF-PGLSSCSADLKDILSEAS-Stop
186-210	Fwd: AATTC GCC AGC ACC ATG CAA CTC CTT CAG CAA CAG CAG CAG GAA GCA GTA TCC GAA GGC AGC AGC AGC GGG AGA GCG AGG TAA A Rev: AGCTT TTA CCT CGC TCT CCC GCT GCT GCT GCC TTC GGA TAC TGC TTC CTG CTG CTG TTG CTG AAG GAG TTG CAT GGT GCT GGC G	QF-ASTMQLLQQQQQEAVSEGSSSGRAR-Stop

in length) within AF1a, with 5’ and 3’ sticky ends resembling DNA digested with EcoRI and HindIII, respectively (Table 3.3). An in-frame stop codon was included upstream of the 3’ HindIII end to restrict translation of the resulting peptide. dsDNA cassettes were cloned into EcoRI/HindIII-digested pM. Insertions were verified by restriction digest.

Cell Transfection

LNCaP cells were transfected via single-pulse electroporation as previously described [45]. C4-2 and DU 145 cells were transfected with Superfect reagent (Qiagen) according to manufacturer specifications. 293T cells were transfected with Lipofectamine 2000 (Life Technologies) according to manufacturer specifications. Treatment of transfected cells with androgen or enzalutamide was performed for 24 h in serum-free medium where indicated.

Dual Luciferase Assays

Transfected cells were lysed in 1X Passive Lysis Buffer (Promega) and subjected to dual luciferase assays using a Dual Luciferase Assay Kit (Promega) as previously described [45].

Western Blot

Western blotting was performed as previously described [65]. Antibodies used in this study were: anti-AR N-20 (Santa Cruz), anti-Gal4 DBD (Santa Cruz), anti-ERK2 D-2 (Santa Cruz), anti-β-Actin (Sigma), and HRP-conjugated

secondary antibodies for Mouse- or Rabbit IgG (Santa Cruz).

Data Analysis and Statistics

All statistical comparisons were made using the two-tailed Student's t-Test with a P value of 0.05 or less considered significant. Asterisks in figures denote levels of statistical significance, such that * = P < 0.05; ** = P < 0.01; *** = P < 0.001; **** = P < 0.0001; n.s. = not significant. Statistics are displayed relative to the vehicle/vector control unless otherwise noted by lines/bars showing specific comparisons in the figure.

CHAPTER 4

THERAPEUTIC TARGETING OF THE ANDROGEN RECEPTOR IN PROSTATE CANCER: PAST, PRESENT, AND FUTURE

OVERVIEW

Prostate cancer (PCa) is common in western men, and represents a significant clinical and financial burden in the US. The emergence of bilateral orchiectomy to induce a castrate level of testosterone in prostate cancer patients marked the advent of the first targeted cancer intervention, and led to the identification of the androgen receptor (AR) as the primary therapeutic target in PCa. Given the ongoing reliance of PCa on AR signaling, even after resistance to hormone-based therapy has developed, the AR continues to be an attractive therapeutic target. However, despite a long history of research, curative interventions for advanced prostate cancer have yet to be developed and drug resistance continues to pose a significant clinical problem. The mutability of the AR ligand binding domain, as well as the lack of structural data for the intrinsically disordered NH2-terminal transactivation domain (NTD), pose considerable challenges for the rational design of potent anti-AR therapies. Here, we discuss a brief history of AR targeting in PCa, as well as provide a perspective on possible future avenues of research that could lead to the development of new AR-targeted therapeutics.

ANDROGEN DEPRIVATION: THE CENTRAL THEME OF PCa THERAPY

Androgen signaling, and the inhibition thereof, has long been recognized as a critical component in the treatment of advanced and metastatic prostate cancer (PCa) [122,123]. Indeed, the critical role of testosterone in the progression of PCa was established in 1941 [137], well in advance of the advent of molecular medicine or even the discovery of the androgen receptor (AR) itself. By performing bilateral orchiectomy to remove the testes, and thus the source of most of the testosterone in the body, Huggins and Hodges noted dramatic reductions in serum phosphatases, which were known indicators of poor prognosis. Administration of estrogenic hormones caused reductions in the serum concentration of these same phosphatases, whereas administration of testosterone to patients caused their expression to increase. In effect, this discovery established androgen ablation as the first targeted cancer intervention, and laid the groundwork for decades of research into the role of androgens in the natural history of PCa. Today, this approach is known as androgen deprivation therapy (ADT), and it is the cornerstone on which therapeutic intervention for advanced and metastatic PCa is built [122,123].

Despite this early advance, PCa proved to be a tenacious disease. Nitrogen mustards and other cytotoxic chemotherapeutics which had shown promise in cancers such as leukemia and lymphoma were demonstrated to be ineffective treatments for prostate cancer [138]. This could potentially be attributed to the specialized metabolic state of prostate epithelial cells [81] as well

as the relatively slow growth rate of prostatic tumors compared to other cancers [139,140]. Microtubule inhibitors appear to be the exception, extending overall survival and enhancing quality of life in patients with CRPC [141]. Initially, the effectiveness of taxanes in CRPC was attributed inhibition of AR nuclear translocation along the microtubule network [142], though a recent study demonstrated that taxane action in PCa cells is independent of AR localization at pharmacologic doses [143]. Docetaxel has been shown to provide a modest, ~2 month survival benefit as a single agent therapy for metastatic CRPC [144]. More recently, a multi-center Phase III clinical trial concluded that the addition of docetaxel to ADT in hormone-naïve patients resulted in overall survival (~13.5 months) and time to progression (~6 months) benefits compared with ADT alone [145]. Cabazitaxel is a second-generation microtubule inhibitor with efficacy in patients who have progressed on docetaxel, extending overall survival by approximately 2 months [146]. Clinical trials assessing the functionality of cabazitaxel in the chemotherapy-naïve setting are currently under way. Nevertheless, even with the modest success of taxane-based chemotherapy, the general dearth of viable chemotherapeutic options that target pathways other than AR remains an ongoing problem in the management of clinical PCa.

Medical treatment of metastatic PCa via the AR, however, has persisted as an active area of research [123]. With the dawn of the molecular biology age in the late 1970's to the early 1980's and the concomitant expansion of our understanding of molecular signaling pathways, new avenues were opened to increase the therapeutic arsenal for targeting AR signaling. Gonadotropin-

releasing hormone agonists (GnRH-A), such as leuprolide and gosrelin, were shown to induce a castrate state without surgical removal of the testes [147]. These drugs function by stimulating a continuous release of luteinizing hormone from the pituitary, which stimulates testosterone synthesis by the testes. This surge in hormone secretion triggers a negative feedback loop, with cessation of testosterone production by the testes and nadir of circulating androgens as an endpoint [148]. This loop reduces serum testosterone to an equivalent level as orchiectomy over time, and medical castration was shown to be indistinguishable from surgical castration in terms of clinical outcome [149].

Anti-androgens, or AR antagonists, represented another critical step forward in AR-targeted therapy [83]. Rather than prevent the synthesis of androgens, drugs such as nilutamide [150], flutamide [151], and bicalutamide [152] were designed to bind competitively to the AR ligand binding domain (LBD) and inhibit the association of the AR with testosterone and dihydrotestosterone, thus preventing AR signaling. The ability to target both androgen production and the action of androgens on the AR led to the hypothesis that combined (or maximal) androgen blockade, i.e. treatment with both castration and an accompanying antiandrogen, might produce a stronger, more durable suppression of PCa growth and progression. Despite promising initial results, meta-analysis of randomized clinical trials demonstrated only minor differences in clinical outcome between patients receiving single-therapy ADT and those receiving combinatorial treatment [153]. Thus, while the arsenal of available intervention strategies has expanded significantly since Huggins and Hodges's

initial discovery, the principles of PCa therapy have changed little in the ensuing 75 years.

SECOND-GENERATION ADT AND THE CONTINUING CHALLENGE OF CASTRATION RESISTANCE

While both ADT and AR blockade have proven to be effective intervention strategies, hormone resistance poses a critical problem in the management of late-stage PCa [82,84,126]. After an initial response, patients receiving pharmacological treatment for PCa inevitably experience a transition from the initial, androgen-dependent tumor state to castration resistant (CRPC) disease [124]. Initially, CRPC was thought to be caused by the complete loss of androgen receptor expression or other AR bypass pathways. However, ongoing research has shown that loss of AR expression is a relatively rare event in the natural history of PCa. Current data support a continuing role for AR in PCa and CRPC progression as both a metabolic master regulator [81] as well as a pro-survival factor [82]. A multitude of molecular mechanisms have been identified that contribute to ongoing AR function in late-stage CRPC [1,127,154]. Chief among these is amplification of the AR gene locus leading to increased AR expression [155], which allows for hypersensitivity to castrate levels of androgen hormones. Further, bicalutamide has been shown to activate AR activity in the context of amplified AR [155], and several mutations of critical amino acid residues in the AR ligand binding pocket have been identified that allow for continuous AR

activation in the context of androgen deprivation or blockade [156-158]. Recently, alternate androgen synthesis pathways in the adrenal glands as well as in prostate cancer tissues have been shown to be up-regulated in CRPC, thus circumventing the effect of ADT by increasing local androgen concentration [91,154]. These mechanisms, as well as myriad alterations in the genetic landscape of advanced PCa [64], allow for the ongoing survival and proliferation of prostate tumors.

Given the propensity of PCa to develop into a castration resistant state with continued reliance on AR signaling for survival and proliferation, renewed emphasis was placed on developing compounds that could overcome the challenges posed by AR amplification, mutation, and peripheral androgen synthesis. These efforts have been successful, and recent studies have demonstrated a significant clinical benefit for the second-generation ADT therapeutics enzalutamide [36,39,85] and abiraterone [37,38,87,159]. Enzalutamide is a non-steroidal anti-androgen that was developed using bicalutamide as a molecular scaffold and which boasts a higher affinity for the AR LBD as well as an enhanced ability to inhibit AR transactivation. Enzalutamide produced a statistically significant survival benefit in men with CRPC, further emphasizing the ongoing role of AR in late-stage metastatic PCa. Abiraterone, on the other hand, functions to irreversibly inhibit the CYP17A1 aromatase enzyme responsible for conversion of adrenal hormones to testosterone precursors [159]. When combined with conventional ADT, abiraterone induces a so-called “super-castrate” state by further suppressing the levels of circulating androgens, as well

as preventing intratumoral androgen synthesis. Interestingly, due to its steroid hormone-like structure, abiraterone also directly binds and inhibits the AR LBD as an antagonist in vitro [160]. Abiraterone was recently shown to extend median time to progression in CRPC patients [37,38,87] and, along with enzalutamide, has been incorporated into the clinical repertoire. However, the onset of resistance to these interventions in men with previous exposure to hormone ablation is rapid, with a median time to progression of ~4-5 months [38,39]. Furthermore, a subset of patients in these studies harbored disease with de novo resistance to enzalutamide and abiraterone, and exhibited no response to treatment. Since enzalutamide and abiraterone target the same processes as front-line ADT (i.e., androgen production and AR binding), it is thought that prior exposure to hormone therapy may blunt the effect of these new, more effective interventions by priming PCa to tolerate lower levels of AR activity. Clinical trials are currently underway to determine the efficacy of enzalutamide and abiraterone in hormone-naïve patients, with the anticipation that more aggressive front-line therapy may produce more durable clinical responses.

AR splice variants (ARV) represent one possible mechanism by which CRPC could circumvent ADT and continue to progress in patients receiving hormone therapy [80,127]. As previously discussed, ARV lack the regulatory COOH-terminal ligand binding domain, and can be generated by alternative splicing of the AR mRNA, as well as by genomic rearrangements of the AR locus (see Chapter 1). Thus, ARVs are constitutively active transcription factors that are wholly insensitive to conventional ADT interventions. More recently, analysis

of ARV expression in clinical PCa samples revealed a higher incidence of expression in men treated with hormone therapy, with ARV expression detected in 39% of patients treated with enzalutamide and 19% of patients treated with abiraterone [126]. This finding suggests that ARV expression may be more intricately involved in PCa progression as opposed to tumorigenesis. Overall, these data highlight a critical unmet need in the clinic: a method by which AR transcriptional activity can be targeted and inhibited directly via the NH2-terminal transcriptional activation domains.

DISORDER IN THE AR NTD: THE NEXT FRONTIER

Given the critical role of the NTD in AR signaling, we are presented with the likely conclusion that durable inhibition of AR in PCa may only be feasible by inhibiting the NTD directly. This has proven to be a persistent challenge, as structural data for the domain has remained elusive due to its intrinsically disordered biophysical properties [76,116,117]. Intrinsically disordered regions (IDR) and intrinsically disordered proteins (IDP) are common in the human proteome, including well-known cell cycle and transcriptional regulators such as p53, p21, p27, CREB, and RELA [129]. These proteins use their IDR to mediate a broad range of functions that can be fine-tuned via amphipathic interactions or post-translational modifications, functioning as a molecular rheostat or signaling threshold detector within the cell. The lack of tertiary structure in IDR allows for easy access to clustered modifiable sites by kinases, phosphatases, and E3-

ligases [161], and many parallels can be drawn with the known biophysical and biochemical properties of the AR. For example, the AR NTD contains a multitude of post-translationally modified sites within the disordered NTD [162,163]. Thus, intrinsic disorder is central to the function of these proteins, allowing for rapid fine-tuning of target activity, stability, or protein-protein interactions.

However, the lack of structural specificity in IDR, as well as a high degree of motif conservation and repetition between different IDP, presents a major challenge to developing molecular interventions with a high degree of specificity for a particular IDP. EPI-001 is a quintessential example of the hazards of targeting IDR, particularly with covalent modifiers (Chapter 2). While local pH influence allows for some selectivity in the drug's ability to covalently modify proteins, the lack of specificity for the AR NTD leads to myriad off-target interactions within the cell. Without a highly nuanced understanding of the IDR in question, such an approach to IDR inhibition may not be feasible. Furthermore, conventional biochemical approaches to assessing the function of protein interaction domains may be ineffective for assessing the architecture and function of IDR, due to the inevitable disruption of unknown structural elements and allosteric binding interfaces (Chapter 3). Due to the nature of IDR, dissecting and separating individual components from the context of the IDR as a whole is not a viable strategy to characterize their activity. Rather, a more nuanced computational approach to this question may be required, as has been performed for the glucocorticoid receptor [164].

Regardless, deletion of AR TAU1, AF1a, AF1b, and TAU5 has revealed

critical roles for each domain under various conditions [2,71,73]. Thus, enumeration of the binding partners responsible for interacting with and imposing structure upon each of these domains, a process known as coupled folding and binding [135,136,165], will be a critical step in developing therapies that target the AR NTD directly. Determination of the differences in binding partner recruitment by the NTD in response to the presence or absence of androgens, and more importantly the presence or absence of the regulatory LBD itself, will also play a key role. Finally, in-depth characterization of AR NTD post-translational modifications and their effects, if any, on coactivator recruitment will be vital to this effort.

ACTIONABLE FEATURES OF THE AR NTD AS THERAPEUTIC TARGETS

Though many IDRs are expressed in a tissue-specific fashion via mechanisms such as alterative splicing [130,131], many retain common sequence elements and/or share binding partners with other IDP [129], and thus the discussion of how to therapeutically target the AR NTD should stem from its commonalities with other known IDP. For example, AR is well known to rely on interactions with CBP/p300 chromatin remodeling enzymes, as well as p160 nuclear receptor coactivators such as the SRC family [13]. CBP/p300 and p160 proteins have also been implicated in binding to other IDP such as CREB [166]. CBP binds via a molten globular KIX domain to the phosphorylated kinase-inducible domain (pKID) of CREB, an interaction in which both partners impose

structure upon one another through coupled folding and binding. CBP is then able to recruit p160 coactivators through its nuclear coactivator binding domain. These events work in concert to provide a ternary structure and scaffold upon which the transcriptional machinery assembles, and it is tempting to speculate that AR may interact with these binding partners in a similar fashion.

IDP are also characterized by an ability to interact with a wide variety of binding partners by virtue of transient, dynamic interactions through so-called “fuzzy” sites [167,168]. Fuzzy interactions are characterized by a lack of coupled folding and binding. Rather, these interactions are characterized by persistence of disorder throughout the interaction, and function to mediate interactions between multiple binding partners [169]. The AR has been shown to interact with numerous coregulatory proteins [13], and the ability to form low-affinity or allosteric interactions with a broad cohort of partners as well as higher-affinity coupled folding and binding responses may explain this property.

The presence of pre-formed helices in IDR is another mitigating factor in protein-protein interactions, though the precise role they play in regulation of transcription factor function is currently a matter of some debate. Some studies have indicated that these helices are required for recruitment of coactivators [170-172], whereas others have suggested that they are ultimately dispensable for IDR function or can even inhibit complex formation [173,174]. Regardless, the AR harbors a number of short, amphipathic helices that have garnered much interest as potential mediators of transcriptional activity, namely ^{23}FNQLF^{27}, ^{178}LKDIL^{182}, and ^{435}WHTLF^{439}. LKDIL is located in the TAU1 AF1a region and

appears to be required for full AR transcriptional activity (Chapter 3), and mutation to LKDNN significantly impairs AR transcriptional activity. WHTLF has been more thoroughly characterized, and is known to be required for TAU5-mediated activity [71]. FNQLF does not map to a known transcriptional activation domain, but has been implicated in intramolecular interactions between the AR NTD and AF-2 protein binding interface of the COOH-terminal domain [19]. The individual contribution of each of these helices in the function of the AR NTD as an IDR is currently unknown. However, amphipathic F/LxxLL/F, nuclear receptor box-type motifs [175,176] have been strongly implicated in interactions between p160 co-regulators and their binding partners [177], as well as a recently-characterized interaction between RelA and CBP/p300 [172]. In the latter study, mutation of the hydrophobic residues significantly attenuated the ability of RelA to interact with CBP, with concomitant inhibitory effects on NF-κB transcriptional activity. Taken together, these data imply that amphipathic helices in IDR have the potential to function as anchor points that enhance the fidelity of coupled folding and binding responses, and their interactions with co-regulatory binding partners should be considered putative targets for therapeutic intervention.

FUTURE DIRECTIONS

The AR NTD presents an intriguing challenge for translational PCa research. Decades of research into the mechanisms underlying AR transcriptional activity have identified many functional features within the NTD,

but how these features work in concert to fine-tune AR transcriptional output remains an elusive question. New findings on the role and regulation of IDR has the potential to shine a light into the inner workings of the NTD, but a number of critical questions are yet to be addressed with regard to the AR in particular. Perhaps the most pressing need from this standpoint is a comprehensive, mechanistic understanding of the specific function of each of the NH2-terminal transcriptional activation domains. Elucidation of the co-regulatory cohort associated with each functional domain in the NTD, as well as the conditions under which these associations exist, will significantly aid this effort. One possible avenue of exploration may include rapid immunoprecipitation and mass spectrometry of endogenous proteins (RIME) [178,179] performed on cells expressing wild-type and mutant versions of the AR, to match specific AR NTD mutations with loss of specific co-regulator associations. Single-molecule fluorescence resonance energy transfer (smFRET) could then be used in conjunction with RIME data and mutagenic scanning of the domains to identify proteins that interact directly with AR, as well as the structural features of the AR that mediate that interaction.

Direct AR-binding partners identified via the methods described above would serve as attractive targets for small-molecule peptidomimetic inhibitors that could be modeled after putative anchor regions, such as the amphipathic helices present in the AR NTD. Alternatively, peptidomimetics modeled after structural elements of AR binding partners that trigger a conformational or allosteric change in the AR NTD and render it incompetent for complex formation or transcriptional

activity may present another alternative. Efforts in rational drug design have met with success following both of these strategies in IDP [180,181], suggesting that such directions may be feasible for the design of AR NTD inhibitors as well. Recently, Ravindranathan and colleagues reported the development of an LXXLL-like peptidomimetic compound, D2, which effected potent anti-AR activity in prostate cancer models [182]. In this case, the drug is targeted against a protein-protein interaction with PELP-1 mediated by the COOH-terminal AF-2 protein binding interface. However, this interface, as well as the ability of D2 to inhibit AR activity, is lost with the generation of ARV. Thus, the design of NTD-targeted interventions of this type remains an unmet need.

Computational methods may also provide critical data on the binding and folding properties of IDR. Biophysical modeling of inter- and intra-molecular interactions between the AR and its binding partners could inform rational drug design efforts, particularly if used in concert with molecular and biochemical studies as discussed above. By determining likely binding partners and their biochemical interfaces with the IDR of the AR NTD, computational modeling could provide valuable insight into the biophysical properties of the domain in question. Determining the strength of binding to a given domain, e.g. whether the proteins engage in coupled folding and binding or in a “fuzzy” interface that may be less desirable for therapeutic targeting, will be critical to this effort. Viral proteins have been suggested as a possible starting point from which IDR-inhibiting therapeutics could be designed, due to their evolutionarily-selected properties that allow for interaction with a wide variety of proteins in order to

hijack host cellular machinery [129,183]. Finally, given the size of the AR IDR and the complexity of its multiple transcriptional activation domains, it may be necessary to target multiple domains at once. Computational models coupled with rational drug design have achieved success in this arena as well [184], and this strategy could be applied to prevent AR from engaging in coupled folding and binding processes along the length of the NTD.

SUMMARY

For almost 75 years, the androgen signaling axis has been the primary target for therapeutic intervention in advanced and metastatic prostate cancer. Though the clinical arsenal has expanded, the principles remain static and significant clinical burden stems from the problem of castration resistance. Therefore, new approaches to inhibiting AR activity are required to produce durable responses in patients with CRPC, particularly in light of the discovery of ARV that are insensitive to manipulation of the ligand binding domain. A promising target, therefore, lies in the intrinsically disordered but transcriptionally active AR NTD. Recent advances in the understanding of how IDRs function in human cells, as well as success in rational drug design targeting these regions, provides a strong basis for adopting similar strategies to target the AR and its transcriptional co-regulatory cohort. Looking ahead, new perspectives on lingering questions about NTD regulatory dynamics, coupled with innovative experimental approaches to drug design, have the potential to unlock new

avenues of translational research to strike a critical blow against prostate cancer.

REFERENCES

1. Heinlein CA, Chang C. Androgen receptor in prostate cancer. Endocrine reviews. 2004; 25: 276-308.
2. Claessens F, Denayer S, Van Tilborgh N, Kerkhofs S, Helsen C, Haelens A. Diverse roles of androgen receptor (AR) domains in AR-mediated signaling. Nuclear receptor signaling. 2008; 6: e008.
3. Shaffer PL, Jivan A, Dollins DE, Claessens F, Gewirth DT. Structural basis of androgen receptor binding to selective androgen response elements. Proc Natl Acad Sci U S A. 2004; 101: 4758-4763.
4. Wilson JD. The role of 5alpha-reduction in steroid hormone physiology. Reproduction, fertility, and development. 2001; 13: 673-678.
5. Tindall DJ, Rittmaster RS. The rationale for inhibiting 5alpha-reductase isoenzymes in the prevention and treatment of prostate cancer. The Journal of urology. 2008; 179: 1235-1242.
6. Pratt WB, Toft DO. Steroid receptor interactions with heat shock protein and immunophilin chaperones. Endocrine reviews. 1997; 18: 306-360.
7. Shang Y, Myers M, Brown M. Formation of the androgen receptor transcription complex. Mol Cell. 2002; 9: 601-610.
8. Wang Q, Carroll JS, Brown M. Spatial and temporal recruitment of androgen receptor and its coactivators involves chromosomal looping and polymerase tracking. Mol Cell. 2005; 19: 631-642.
9. Makkonen H, Kauhanen M, Paakinaho V, Jaaskelainen T, Palvimo JJ.

Long-range activation of FKBP51 transcription by the androgen receptor via distal intronic enhancers. Nucleic acids research. 2009; 37: 4135-4148.

10. Wu D, Zhang C, Shen Y, Nephew KP, Wang Q. Androgen receptor-driven chromatin looping in prostate cancer. Trends in endocrinology and metabolism: TEM. 2011; 22: 474-480.
11. Agoulnik IU, Weigel NL. Coactivator selective regulation of androgen receptor activity. Steroids. 2009; 74: 669-674.
12. Naar AM, Lemon BD, Tjian R. Transcriptional coactivator complexes. Annual review of biochemistry. 2001; 70: 475-501.
13. Heemers HV, Tindall DJ. Androgen receptor (AR) coregulators: a diversity of functions converging on and regulating the AR transcriptional complex. Endocrine reviews. 2007; 28: 778-808.
14. Pereira de Jesus-Tran K, Cote PL, Cantin L, Blanchet J, Labrie F, Breton R. Comparison of crystal structures of human androgen receptor ligand-binding domain complexed with various agonists reveals molecular determinants responsible for binding affinity. Protein science : a publication of the Protein Society. 2006; 15: 987-999.
15. Knudsen KE, Scher HI. Starving the addiction: new opportunities for durable suppression of AR signaling in prostate cancer. Clin Cancer Res. 2009; 15: 4792-4798.
16. Matias PM, Donner P, Coelho R, Thomaz M, Peixoto C, Macedo S, Otto N, Joschko S, Scholz P, Wegg A, Basler S, Schafer M, Egner U*, et al.*

Structural evidence for ligand specificity in the binding domain of the human androgen receptor. Implications for pathogenic gene mutations. J Biol Chem. 2000; 275: 26164-26171.

17. Sack JS, Kish KF, Wang C, Attar RM, Kiefer SE, An Y, Wu GY, Scheffler JE, Salvati ME, Krystek SR, Jr., Weinmann R, Einspahr HM. Crystallographic structures of the ligand-binding domains of the androgen receptor and its T877A mutant complexed with the natural agonist dihydrotestosterone. Proc Natl Acad Sci U S A. 2001; 98: 4904-4909.

18. Jasuja R, Ulloor J, Yengo CM, Choong K, Istomin AY, Livesay DR, Jacobs DJ, Swerdloff RS, Miksovska J, Larsen RW, Bhasin S. Kinetic and thermodynamic characterization of dihydrotestosterone-induced conformational perturbations in androgen receptor ligand-binding domain. Mol Endocrinol. 2009; 23: 1231-1241.

19. He B, Gampe RT, Jr., Kole AJ, Hnat AT, Stanley TB, An G, Stewart EL, Kalman RI, Minges JT, Wilson EM. Structural basis for androgen receptor interdomain and coactivator interactions suggests a transition in nuclear receptor activation function dominance. Mol Cell. 2004; 16: 425-438.

20. Watanabe C, Watanabe H, Tanaka S. An interpretation of positional displacement of the helix12 in nuclear receptors: preexistent swing-up motion triggered by ligand binding. Biochimica et biophysica acta. 2010; 1804: 1832-1840.

21. Dubbink HJ, Hersmus R, Verma CS, van der Korput HA, Berrevoets CA, van Tol J, Ziel-van der Made AC, Brinkmann AO, Pike AC, Trapman J.

Distinct recognition modes of FXXLF and LXXLL motifs by the androgen receptor. Mol Endocrinol. 2004; 18: 2132-2150.

22. Saporita AJ, Zhang Q, Navai N, Dincer Z, Hahn J, Cai X, Wang Z. Identification and characterization of a ligand-regulated nuclear export signal in androgen receptor. J Biol Chem. 2003; 278: 41998-42005.

23. Estebanez-Perpina E, Arnold LA, Nguyen P, Rodrigues ED, Mar E, Bateman R, Pallai P, Shokat KM, Baxter JD, Guy RK, Webb P, Fletterick RJ. A surface on the androgen receptor that allosterically regulates coactivator binding. Proc Natl Acad Sci U S A. 2007; 104: 16074-16079.

24. Grosdidier S, Carbo LR, Buzon V, Brooke G, Nguyen P, Baxter JD, Bevan C, Webb P, Estebanez-Perpina E, Fernandez-Recio J. Allosteric conversation in the androgen receptor ligand-binding domain surfaces. Mol Endocrinol. 2012; 26: 1078-1090.

25. Buzon V, Carbo LR, Estruch SB, Fletterick RJ, Estebanez-Perpina E. A conserved surface on the ligand binding domain of nuclear receptors for allosteric control. Molecular and cellular endocrinology. 2012; 348: 394-402.

26. De Leon JT, Iwai A, Feau C, Garcia Y, Balsiger HA, Storer CL, Suro RM, Garza KM, Lee S, Kim YS, Chen Y, Ning YM, Riggs DL*, et al.* Targeting the regulation of androgen receptor signaling by the heat shock protein 90 cochaperone FKBP52 in prostate cancer cells. Proc Natl Acad Sci U S A. 2011; 108: 11878-11883.

27. Joseph JD, Wittmann BM, Dwyer MA, Cui H, Dye DA, McDonnell DP,

Norris JD. Inhibition of prostate cancer cell growth by second-site androgen receptor antagonists. Proc Natl Acad Sci U S A. 2009; 106: 12178-12183.

28. Axerio-Cilies P, Lack NA, Nayana MR, Chan KH, Yeung A, Leblanc E, Guns ES, Rennie PS, Cherkasov A. Inhibitors of androgen receptor activation function-2 (AF2) site identified through virtual screening. Journal of medicinal chemistry. 2011; 54: 6197-6205.

29. Siegel R, Ma J, Zou Z, Jemal A. Cancer statistics, 2014. CA: a cancer journal for clinicians. 2014; 64: 9-29.

30. O'Mahony OA, Steinkamp MP, Albertelli MA, Brogley M, Rehman H, Robins DM. Profiling human androgen receptor mutations reveals treatment effects in a mouse model of prostate cancer. Molecular cancer research : MCR. 2008; 6: 1691-1701.

31. Steinkamp MP, O'Mahony OA, Brogley M, Rehman H, Lapensee EW, Dhanasekaran S, Hofer MD, Kuefer R, Chinnaiyan A, Rubin MA, Pienta KJ, Robins DM. Treatment-dependent androgen receptor mutations in prostate cancer exploit multiple mechanisms to evade therapy. Cancer Res. 2009; 69: 4434-4442.

32. Locke JA, Guns ES, Lubik AA, Adomat HH, Hendy SC, Wood CA, Ettinger SL, Gleave ME, Nelson CC. Androgen levels increase by intratumoral de novo steroidogenesis during progression of castration-resistant prostate cancer. Cancer Res. 2008; 68: 6407-6415.

33. Seruga B, Ocana A, Tannock IF. Drug resistance in metastatic castration-

resistant prostate cancer. Nature reviews Clinical oncology. 2011; 8: 12-23.

34. Lamont KR, Tindall DJ. Minireview: Alternative activation pathways for the androgen receptor in prostate cancer. Mol Endocrinol. 2011; 25: 897-907.

35. Nadiminty N, Gao AC. Mechanisms of persistent activation of the androgen receptor in CRPC: recent advances and future perspectives. World journal of urology. 2012; 30: 287-295.

36. Tran C, Ouk S, Clegg NJ, Chen Y, Watson PA, Arora V, Wongvipat J, Smith-Jones PM, Yoo D, Kwon A, Wasielewska T, Welsbie D, Chen CD*, et al.* Development of a second-generation antiandrogen for treatment of advanced prostate cancer. Science. 2009; 324: 787-790.

37. Attard G, Reid AH, Olmos D, de Bono JS. Antitumor activity with CYP17 blockade indicates that castration-resistant prostate cancer frequently remains hormone driven. Cancer Res. 2009; 69: 4937-4940.

38. de Bono JS, Logothetis CJ, Molina A, Fizazi K, North S, Chu L, Chi KN, Jones RJ, Goodman OB, Jr., Saad F, Staffurth JN, Mainwaring P, Harland S*, et al.* Abiraterone and increased survival in metastatic prostate cancer. N Engl J Med. 2011; 364: 1995-2005.

39. Scher HI, Fizazi K, Saad F, Taplin ME, Sternberg CN, Miller K, de Wit R, Mulders P, Chi KN, Shore ND, Armstrong AJ, Flaig TW, Flechon A*, et al.* Increased survival with enzalutamide in prostate cancer after chemotherapy. N Engl J Med. 2012; 367: 1187-1197.

40. Payton S. Prostate cancer: MDV3100 has antitumor activity in castration-

resistant disease. Nature reviews Urology. 2010; 7: 300.

41. Dehm SM, Tindall DJ. Alternatively spliced androgen receptor variants. Endocrine-related cancer. 2011; 18: R183-196.

42. Tepper CG, Boucher DL, Ryan PE, Ma AH, Xia L, Lee LF, Pretlow TG, Kung HJ. Characterization of a novel androgen receptor mutation in a relapsed CWR22 prostate cancer xenograft and cell line. Cancer Res. 2002; 62: 6606-6614.

43. Ceraline J, Cruchant MD, Erdmann E, Erbs P, Kurtz JE, Duclos B, Jacqmin D, Chopin D, Bergerat JP. Constitutive activation of the androgen receptor by a point mutation in the hinge region: a new mechanism for androgen-independent growth in prostate cancer. International journal of cancer Journal international du cancer. 2004; 108: 152-157.

44. Libertini SJ, Tepper CG, Rodriguez V, Asmuth DM, Kung HJ, Mudryj M. Evidence for calpain-mediated androgen receptor cleavage as a mechanism for androgen independence. Cancer Res. 2007; 67: 9001-9005.

45. Dehm SM, Schmidt LJ, Heemers HV, Vessella RL, Tindall DJ. Splicing of a novel androgen receptor exon generates a constitutively active androgen receptor that mediates prostate cancer therapy resistance. Cancer Res. 2008; 68: 5469-5477.

46. Guo Z, Yang X, Sun F, Jiang R, Linn DE, Chen H, Kong X, Melamed J, Tepper CG, Kung HJ, Brodie AM, Edwards J, Qiu Y. A novel androgen receptor splice variant is up-regulated during prostate cancer progression

and promotes androgen depletion-resistant growth. Cancer Res. 2009; 69: 2305-2313.

47. Hu R, Dunn TA, Wei S, Isharwal S, Veltri RW, Humphreys E, Han M, Partin AW, Vessella RL, Isaacs WB, Bova GS, Luo J. Ligand-independent androgen receptor variants derived from splicing of cryptic exons signify hormone-refractory prostate cancer. Cancer Res. 2009; 69: 16-22.

48. Marcias G, Erdmann E, Lapouge G, Siebert C, Barthelemy P, Duclos B, Bergerat JP, Ceraline J, Kurtz JE. Identification of novel truncated androgen receptor (AR) mutants including unreported pre-mRNA splicing variants in the 22Rv1 hormone-refractory prostate cancer (PCa) cell line. Human mutation. 2010; 31: 74-80.

49. Sun S, Sprenger CC, Vessella RL, Haugk K, Soriano K, Mostaghel EA, Page ST, Coleman IM, Nguyen HM, Sun H, Nelson PS, Plymate SR. Castration resistance in human prostate cancer is conferred by a frequently occurring androgen receptor splice variant. The Journal of clinical investigation. 2010; 120: 2715-2730.

50. Chan SC, Li Y, Dehm SM. Androgen receptor splice variants activate androgen receptor target genes and support aberrant prostate cancer cell growth independent of canonical androgen receptor nuclear localization signal. J Biol Chem. 2012; 287: 19736-19749.

51. Hu R, Lu C, Mostaghel EA, Yegnasubramanian S, Gurel M, Tannahill C, Edwards J, Isaacs WB, Nelson PS, Bluemn E, Plymate SR, Luo J. Distinct transcriptional programs mediated by the ligand-dependent full-length

androgen receptor and its splice variants in castration-resistant prostate cancer. Cancer Res. 2012; 72: 3457-3462.

52. Zhou ZX, Sar M, Simental JA, Lane MV, Wilson EM. A ligand-dependent bipartite nuclear targeting signal in the human androgen receptor. Requirement for the DNA-binding domain and modulation by NH2-terminal and carboxyl-terminal sequences. J Biol Chem. 1994; 269: 13115-13123.

53. Tomlins SA, Rhodes DR, Perner S, Dhanasekaran SM, Mehra R, Sun XW, Varambally S, Cao X, Tchinda J, Kuefer R, Lee C, Montie JE, Shah RB*, et al.* Recurrent fusion of TMPRSS2 and ETS transcription factor genes in prostate cancer. Science. 2005; 310: 644-648.

54. Palanisamy N, Ateeq B, Kalyana-Sundaram S, Pflueger D, Ramnarayanan K, Shankar S, Han B, Cao Q, Cao X, Suleman K, Kumar-Sinha C, Dhanasekaran SM, Chen YB*, et al.* Rearrangements of the RAF kinase pathway in prostate cancer, gastric cancer and melanoma. Nature medicine. 2010; 16: 793-798.

55. Berger MF, Lawrence MS, Demichelis F, Drier Y, Cibulskis K, Sivachenko AY, Sboner A, Esgueva R, Pflueger D, Sougnez C, Onofrio R, Carter SL, Park K*, et al.* The genomic complexity of primary human prostate cancer. Nature. 2011; 470: 214-220.

56. Pflueger D, Terry S, Sboner A, Habegger L, Esgueva R, Lin PC, Svensson MA, Kitabayashi N, Moss BJ, MacDonald TY, Cao X, Barrette T, Tewari AK*, et al.* Discovery of non-ETS gene fusions in human prostate cancer using next-generation RNA sequencing. Genome research. 2011; 21: 56-

67.

57. Rubin MA, Maher CA, Chinnaiyan AM. Common gene rearrangements in prostate cancer. Journal of clinical oncology : official journal of the American Society of Clinical Oncology. 2011; 29: 3659-3668.

58. Reid AH, Attard G, Brewer D, Miranda S, Riisnaes R, Clark J, Hylands L, Merson S, Vergis R, Jameson C, Hoyer S, Sorenson KD, Borre M*, et al.* Novel, gross chromosomal alterations involving PTEN cooperate with allelic loss in prostate cancer. Modern pathology : an official journal of the United States and Canadian Academy of Pathology, Inc. 2012; 25: 902-910.

59. Perner S, Demichelis F, Beroukhim R, Schmidt FH, Mosquera JM, Setlur S, Tchinda J, Tomlins SA, Hofer MD, Pienta KG, Kuefer R, Vessella R, Sun XW*, et al.* TMPRSS2:ERG fusion-associated deletions provide insight into the heterogeneity of prostate cancer. Cancer Res. 2006; 66: 8337-8341.

60. Attard G, Clark J, Ambroisine L, Fisher G, Kovacs G, Flohr P, Berney D, Foster CS, Fletcher A, Gerald WL, Moller H, Reuter V, De Bono JS*, et al.* Duplication of the fusion of TMPRSS2 to ERG sequences identifies fatal human prostate cancer. Oncogene. 2008; 27: 253-263.

61. Fine SW, Gopalan A, Leversha MA, Al-Ahmadie HA, Tickoo SK, Zhou Q, Satagopan JM, Scardino PT, Gerald WL, Reuter VE. TMPRSS2-ERG gene fusion is associated with low Gleason scores and not with high-grade morphological features. Modern pathology : an official journal of the United States and Canadian Academy of Pathology, Inc. 2010; 23: 1325-

1333.

62. Saramaki OR, Harjula AE, Martikainen PM, Vessella RL, Tammela TL, Visakorpi T. TMPRSS2:ERG fusion identifies a subgroup of prostate cancers with a favorable prognosis. Clin Cancer Res. 2008; 14: 3395-3400.

63. Gopalan A, Leversha MA, Satagopan JM, Zhou Q, Al-Ahmadie HA, Fine SW, Eastham JA, Scardino PT, Scher HI, Tickoo SK, Reuter VE, Gerald WL. TMPRSS2-ERG gene fusion is not associated with outcome in patients treated by prostatectomy. Cancer Res. 2009; 69: 1400-1406.

64. Grasso CS, Wu YM, Robinson DR, Cao X, Dhanasekaran SM, Khan AP, Quist MJ, Jing X, Lonigro RJ, Brenner JC, Asangani IA, Ateeq B, Chun SY*, et al.* The mutational landscape of lethal castration-resistant prostate cancer. Nature. 2012; 487: 239-243.

65. Li Y, Alsagabi M, Fan D, Bova GS, Tewfik AH, Dehm SM. Intragenic rearrangement and altered RNA splicing of the androgen receptor in a cell-based model of prostate cancer progression. Cancer Res. 2011; 71: 2108-2117.

66. Watson PA, Chen YF, Balbas MD, Wongvipat J, Socci ND, Viale A, Kim K, Sawyers CL. Constitutively active androgen receptor splice variants expressed in castration-resistant prostate cancer require full-length androgen receptor. Proc Natl Acad Sci U S A. 2010; 107: 16759-16765.

67. Li Y, Hwang TH, Oseth LA, Hauge A, Vessella RL, Schmechel SC, Hirsch B, Beckman KB, Silverstein KA, Dehm SM. AR intragenic deletions linked

to androgen receptor splice variant expression and activity in models of prostate cancer progression. Oncogene. 2012; 31: 4759-4767.

68. Hornberg E, Ylitalo EB, Crnalic S, Antti H, Stattin P, Widmark A, Bergh A, Wikstrom P. Expression of androgen receptor splice variants in prostate cancer bone metastases is associated with castration-resistance and short survival. PloS one. 2011; 6: e19059.

69. Zhang X, Morrissey C, Sun S, Ketchandji M, Nelson PS, True LD, Vakar-Lopez F, Vessella RL, Plymate SR. Androgen receptor variants occur frequently in castration resistant prostate cancer metastases. PloS one. 2011; 6: e27970.

70. Alen P, Claessens F, Verhoeven G, Rombauts W, Peeters B. The androgen receptor amino-terminal domain plays a key role in p160 coactivator-stimulated gene transcription. Molecular and cellular biology. 1999; 19: 6085-6097.

71. Dehm SM, Regan KM, Schmidt LJ, Tindall DJ. Selective role of an NH2-terminal WxxLF motif for aberrant androgen receptor activation in androgen depletion independent prostate cancer cells. Cancer Res. 2007; 67: 10067-10077.

72. Bevan CL, Hoare S, Claessens F, Heery DM, Parker MG. The AF1 and AF2 domains of the androgen receptor interact with distinct regions of SRC1. Molecular and cellular biology. 1999; 19: 8383-8392.

73. Dehm SM, Tindall DJ. Ligand-independent androgen receptor activity is activation function-2-independent and resistant to antiandrogens in

androgen refractory prostate cancer cells. J Biol Chem. 2006; 281: 27882-27893.

74. Zhu P, Baek SH, Bourk EM, Ohgi KA, Garcia-Bassets I, Sanjo H, Akira S, Kotol PF, Glass CK, Rosenfeld MG, Rose DW. Macrophage/cancer cell interactions mediate hormone resistance by a nuclear receptor derepression pathway. Cell. 2006; 124: 615-629.

75. Callewaert L, Van Tilborgh N, Claessens F. Interplay between two hormone-independent activation domains in the androgen receptor. Cancer Res. 2006; 66: 543-553.

76. Hilser VJ, Thompson EB. Structural dynamics, intrinsic disorder, and allostery in nuclear receptors as transcription factors. J Biol Chem. 2011; 286: 39675-39682.

77. Andersen RJ, Mawji NR, Wang J, Wang G, Haile S, Myung JK, Watt K, Tam T, Yang YC, Banuelos CA, Williams DE, McEwan IJ, Wang Y*, et al.* Regression of castrate-recurrent prostate cancer by a small-molecule inhibitor of the amino-terminus domain of the androgen receptor. Cancer cell. 2010; 17: 535-546.

78. Myung JK, Banuelos CA, Fernandez JG, Mawji NR, Wang J, Tien AH, Yang YC, Tavakoli I, Haile S, Watt K, McEwan IJ, Plymate S, Andersen RJ*, et al.* An androgen receptor N-terminal domain antagonist for treating prostate cancer. The Journal of clinical investigation. 2013; 123: 2948-2960.

79. Meimetis LG, Williams DE, Mawji NR, Banuelos CA, Lal AA, Park JJ, Tien

AH, Fernandez JG, de Voogd NJ, Sadar MD, Andersen RJ. Niphatenones, glycerol ethers from the sponge Niphates digitalis block androgen receptor transcriptional activity in prostate cancer cells: structure elucidation, synthesis, and biological activity. Journal of medicinal chemistry. 2012; 55: 503-514.

80. Brand LJ, Dehm SM. Androgen receptor gene rearrangements: new perspectives on prostate cancer progression. Current drug targets. 2013; 14: 441-449.

81. Barfeld S, Itkonen H, Urbanucci A, Mills I. Androgen-regulated metabolism and biosynthises in prostate cancer. Endocrine-related cancer. 2014; 21: T57-66.

82. Culig Z, Santer FR. Androgen receptor signaling in prostate cancer. Cancer metastasis reviews. 2014; 33: 413-427.

83. Helsen C, Van den Broeck T, Voet A, Prekovic S, Van Poppel H, Joniau S, Claessens F. Androgen receptor antagonists for prostate cancer therapy. Endocrine-related cancer. 2014; 21: T105-118.

84. Petrylak DP. Current state of castration-resistant prostate cancer. The American journal of managed care. 2013; 19: s358-365.

85. Sternberg CN, de Bono JS, Chi KN, Fizazi K, Mulders P, Cerbone L, Hirmand M, Forer D, Scher HI. Improved outcomes in elderly patients with metastatic castration-resistant prostate cancer treated with the androgen receptor inhibitor enzalutamide: results from the phase III AFFIRM trial. Ann Oncol. 2014; 25: 429-434.

86. Beer TM, Armstrong AJ, Rathkopf DE, Loriot Y, Sternberg CN, Higano CS, Iversen P, Bhattacharya S, Carles J, Chowdhury S, Davis ID, de Bono JS, Evans CP*, et al.* Enzalutamide in Metastatic Prostate Cancer before Chemotherapy. N Engl J Med. 2014; 371: 424-433.

87. Ryan CJ, Smith MR, de Bono JS, Molina A, Logothetis CJ, de Souza P, Fizazi K, Mainwaring P, Piulats JM, Ng S, Carles J, Mulders PF, Basch E*, et al.* Abiraterone in metastatic prostate cancer without previous chemotherapy. N Engl J Med. 2013; 368: 138-148.

88. Arora VK, Schenkein E, Murali R, Subudhi SK, Wongvipat J, Balbas MD, Shah N, Cai L, Efstathiou E, Logothetis C, Zheng D, Sawyers CL. Glucocorticoid receptor confers resistance to antiandrogens by bypassing androgen receptor blockade. Cell. 2013; 155: 1309-1322.

89. Chang KH, Li R, Kuri B, Lotan Y, Roehrborn CG, Liu J, Vessella R, Nelson PS, Kapur P, Guo X, Mirzaei H, Auchus RJ, Sharifi N. A gain-of-function mutation in DHT synthesis in castration-resistant prostate cancer. Cell. 2013; 154: 1074-1084.

90. Li Y, Chan SC, Brand LJ, Hwang TH, Silverstein KA, Dehm SM. Androgen receptor splice variants mediate enzalutamide resistance in castration-resistant prostate cancer cell lines. Cancer Res. 2013; 73: 483-489.

91. Mostaghel EA, Marck BT, Plymate SR, Vessella RL, Balk S, Matsumoto AM, Nelson PS, Montgomery RB. Resistance to CYP17A1 inhibition with abiraterone in castration-resistant prostate cancer: induction of steroidogenesis and androgen receptor splice variants. Clin Cancer Res.

2011; 17: 5913-5925.

92. Nyquist MD, Li Y, Hwang TH, Manlove LS, Vessella RL, Silverstein KA, Voytas DF, Dehm SM. TALEN-engineered AR gene rearrangements reveal endocrine uncoupling of androgen receptor in prostate cancer. Proc Natl Acad Sci U S A. 2013; 110: 17492-17497.

93. Mateo J, Smith A, Ong M, de Bono JS. Novel drugs targeting the androgen receptor pathway in prostate cancer. Cancer metastasis reviews. 2014; 33: 567-579.

94. Dehm SM, Tindall DJ. Androgen receptor structural and functional elements: role and regulation in prostate cancer. Mol Endocrinol. 2007; 21: 2855-2863.

95. Nyquist MD, Dehm SM. Interplay between genomic alterations and androgen receptor signaling during prostate cancer development and progression. Hormones & cancer. 2013; 4: 61-69.

96. Wright HM, Clish CB, Mikami T, Hauser S, Yanagi K, Hiramatsu R, Serhan CN, Spiegelman BM. A synthetic antagonist for the peroxisome proliferator-activated receptor gamma inhibits adipocyte differentiation. J Biol Chem. 2000; 275: 1873-1877.

97. Nakamuta M, Enjoji M, Uchimura K, Ohta S, Sugimoto R, Kotoh K, Kato M, Irie T, Muta T, Nawata H. Bisphenol a diglycidyl ether (BADGE) suppresses tumor necrosis factor-alpha production as a PPARgamma agonist in the murine macrophage-like cell line, RAW 264.7. Cell biology international. 2002; 26: 235-241.

98. Dworzanski T, Celinski K, Korolczuk A, Slomka M, Radej S, Czechowska G, Madro A, Cichoz-Lach H. Influence of the peroxisome proliferator-activated receptor gamma (PPAR-gamma) agonist, rosiglitazone and antagonist, biphenol-A-diglicydyl ether (BADGE) on the course of inflammation in the experimental model of colitis in rats. Journal of physiology and pharmacology : an official journal of the Polish Physiological Society. 2010; 61: 683-693.

99. Strand DW, Jiang M, Murphy TA, Yi Y, Konvinse KC, Franco OE, Wang Y, Young JD, Hayward SW. PPARgamma isoforms differentially regulate metabolic networks to mediate mouse prostatic epithelial differentiation. Cell death & disease. 2012; 3: e361.

100. Kubota T, Koshizuka K, Williamson EA, Asou H, Said JW, Holden S, Miyoshi I, Koeffler HP. Ligand for peroxisome proliferator-activated receptor gamma (troglitazone) has potent antitumor effect against human prostate cancer both in vitro and in vivo. Cancer Res. 1998; 58: 3344-3352.

101. Yang CC, Wang YC, Wei S, Lin LF, Chen CS, Lee CC, Lin CC. Peroxisome proliferator-activated receptor gamma-independent suppression of androgen receptor expression by troglitazone mechanism and pharmacologic exploitation. Cancer Res. 2007; 67: 3229-3238.

102. Sikka S, Chen L, Sethi G, Kumar AP. Targeting PPARgamma Signaling Cascade for the Prevention and Treatment of Prostate Cancer. PPAR research. 2012; 2012: 968040.

103. Hisatake JI, Ikezoe T, Carey M, Holden S, Tomoyasu S, Koeffler HP. Down-Regulation of prostate-specific antigen expression by ligands for peroxisome proliferator-activated receptor gamma in human prostate cancer. Cancer Res. 2000; 60: 5494-5498.

104. Centenera MM, Gillis JL, Hanson AR, Jindal S, Taylor RA, Risbridger GP, Sutherland PD, Scher HI, Raj GV, Knudsen KE, Yeadon T, Tilley WD, Butler LM. Evidence for efficacy of new Hsp90 inhibitors revealed by ex vivo culture of human prostate tumors. Clin Cancer Res. 2012; 18: 3562-3570.

105. Centenera MM, Raj GV, Knudsen KE, Tilley WD, Butler LM. Ex vivo culture of human prostate tissue and drug development. Nature reviews Urology. 2013; 10: 483-487.

106. Schiewer MJ, Goodwin JF, Han S, Brenner JC, Augello MA, Dean JL, Liu F, Planck JL, Ravindranathan P, Chinnaiyan AM, McCue P, Gomella LG, Raj GV*, et al.* Dual roles of PARP-1 promote cancer growth and progression. Cancer discovery. 2012; 2: 1134-1149.

107. Wang S, Kollipara RK, Srivastava N, Li R, Ravindranathan P, Hernandez E, Freeman E, Humphries CG, Kapur P, Lotan Y, Fazli L, Gleave ME, Plymate SR*, et al.* Ablation of the oncogenic transcription factor ERG by deubiquitinase inhibition in prostate cancer. Proc Natl Acad Sci U S A. 2014; 111: 4251-4256.

108. Puri V, Ranjit S, Konda S, Nicoloro SM, Straubhaar J, Chawla A, Chouinard M, Lin C, Burkart A, Corvera S, Perugini RA, Czech MP. Cidea

is associated with lipid droplets and insulin sensitivity in humans. Proc Natl Acad Sci U S A. 2008; 105: 7833-7838.

109. Simal-Gandara J, Paz-Abuin S, Ahrne L. A critical review of the quality and safety of BADGE-based epoxy coatings for cans: implications for legislation on epoxy coatings for food contact. Crit Rev Food Sci Nutr. 1998; 38: 675-688.

110. Delfosse V, Grimaldi M, le Maire A, Bourguet W, Balaguer P. Nuclear receptor profiling of bisphenol-A and its halogenated analogues. Vitam Horm. 2014; 94: 229-251.

111. Hammarling L, Gustavsson H, Svensson K, Oskarsson A. Migration of bisphenol-A diglycidyl ether (BADGE) and its reaction products in canned foods. Food Addit Contam. 2000; 17: 937-943.

112. Lintschinger J, Rauter W. Simultaneous determination of bisphenol A-diglycidyl ether, bisphenol F-diglycidyl ether and their hydrolysis and chlorohydroxy derivatives in canned foods. Eur Food Res Technol. 2000; 211: 211-217.

113. Agatsuma T, Ogawa H, Akasaka K, Asai A, Yamashita Y, Mizukami T, Akinaga S, Saitoh Y. Halohydrin and oxime derivatives of radicicol: Synthesis and antitumor activities. Bioorgan Med Chem. 2002; 10: 3445-3454.

114. Petersen H, Biereichel A, Burseg K, Simat TJ, Steinhart H. Bisphenol A diglycidyl ether (BADGE) migrating from packaging material 'disappears' in food: reaction with food components. Food Addit Contam Part A Chem

Anal Control Expo Risk Assess. 2008; 25: 911-920.

115. Bakhiya N, Abraham K, Gurtler R, Appel KE, Lampen A. Toxicological assessment of 3-chloropropane-1,2-diol and glycidol fatty acid esters in food. Mol Nutr Food Res. 2011; 55: 509-521.

116. Lavery DN, McEwan IJ. Structural characterization of the native NH2-terminal transactivation domain of the human androgen receptor: a collapsed disordered conformation underlies structural plasticity and protein-induced folding. Biochemistry. 2008; 47: 3360-3369.

117. McEwan IJ. Intrinsic disorder in the androgen receptor: identification, characterisation and drugability. Molecular bioSystems. 2012; 8: 82-90.

118. Kim JB, Wright HM, Wright M, Spiegelman BM. ADD1/SREBP1 activates PPARgamma through the production of endogenous ligand. Proc Natl Acad Sci U S A. 1998; 95: 4333-4337.

119. Guo H, Bazuine M, Jin D, Huang MM, Cushman SW, Chen X. Evidence for the regulatory role of lipocalin 2 in high-fat diet-induced adipose tissue remodeling in male mice. Endocrinology. 2013; 154: 3525-3538.

120. Olson ME, Li M, Harris RS, Harki DA. Small-molecule APOBEC3G DNA cytosine deaminase inhibitors based on a 4-amino-1,2,4-triazole-3-thiol scaffold. ChemMedChem. 2013; 8: 112-117.

121. Brand LJ, Olson ME, Ravindranathan P, Guo H, Kempema AM, Andrews TE, Chen X, Raj GV, Harki DA, Dehm SM. EPI-001 is a selective peroxisome proliferator-activated receptor-gamma modulator with inhibitory effects on androgen receptor expression and activity in prostate

cancer. Oncotarget. 2015;

122. Sharifi N, Gulley JL, Dahut WL. Androgen deprivation therapy for prostate cancer. JAMA. 2005; 294: 238-244.

123. Bastos DA, Dzik C, Rathkopf D, Scher HI. Expanding androgen- and androgen receptor signaling-directed therapies for castration-resistant prostate cancer. Oncology (Williston Park). 2014; 28: 693-699.

124. Yuan X, Cai C, Chen S, Yu Z, Balk SP. Androgen receptor functions in castration-resistant prostate cancer and mechanisms of resistance to new agents targeting the androgen axis. Oncogene. 2013;

125. Yu Z, Chen S, Sowalsky AG, Voznesensky OS, Mostaghel EA, Nelson PS, Cai C, Balk SP. Rapid induction of androgen receptor splice variants by androgen deprivation in prostate cancer. Clin Cancer Res. 2014; 20: 1590-1600.

126. Antonarakis ES, Lu C, Wang H, Luber B, Nakazawa M, Roeser JC, Chen Y, Mohammad TA, Fedor HL, Lotan TL, Zheng Q, De Marzo AM, Isaacs JT*, et al.* AR-V7 and resistance to enzalutamide and abiraterone in prostate cancer. N Engl J Med. 2014; 371: 1028-1038.

127. Ware KE, Garcia-Blanco MA, Armstrong AJ, Dehm SM. Biologic and clinical significance of androgen receptor variants in castration resistant prostate cancer. Endocrine-related cancer. 2014; 21: T87-T103.

128. He B, Lee LW, Minges JT, Wilson EM. Dependence of selective gene activation on the androgen receptor NH2- and COOH-terminal interaction. J Biol Chem. 2002; 277: 25631-25639.

129. Wright PE, Dyson HJ. Intrinsically disordered proteins in cellular signalling and regulation. Nat Rev Mol Cell Biol. 2014; 16: 18-29.

130. Ellis JD, Barrios-Rodiles M, Colak R, Irimia M, Kim T, Calarco JA, Wang X, Pan Q, O'Hanlon D, Kim PM, Wrana JL, Blencowe BJ. Tissue-specific alternative splicing remodels protein-protein interaction networks. Mol Cell. 2012; 46: 884-892.

131. Buljan M, Chalancon G, Eustermann S, Wagner GP, Fuxreiter M, Bateman A, Babu MM. Tissue-specific splicing of disordered segments that embed binding motifs rewires protein interaction networks. Mol Cell. 2012; 46: 871-883.

132. Jenster G, van der Korput HA, Trapman J, Brinkmann AO. Identification of two transcription activation units in the N-terminal domain of the human androgen receptor. J Biol Chem. 1995; 270: 7341-7346.

133. He B, Minges JT, Lee LW, Wilson EM. The FXXLF motif mediates androgen receptor-specific interactions with coregulators. J Biol Chem. 2002; 277: 10226-10235.

134. Callewaert L, Verrijdt G, Christiaens V, Haelens A, Claessens F. Dual function of an amino-terminal amphipatic helix in androgen receptor-mediated transactivation through specific and nonspecific response elements. J Biol Chem. 2003; 278: 8212-8218.

135. Dyson HJ, Wright PE. Coupling of folding and binding for unstructured proteins. Curr Opin Struct Biol. 2002; 12: 54-60.

136. Dogan J, Schmidt T, Mu X, Engstrom A, Jemth P. Fast association and

slow transitions in the interaction between two intrinsically disordered protein domains. J Biol Chem. 2012; 287: 34316-34324.

137. Huggins C, Hodges CV. Studies on prostatic cancer. I. The effect of castration, of estrogen and androgen injection on serum phosphatases in metastatic carcinoma of the prostate. Cancer Research. 1941; 1: 293-297.

138. Yagoda A, Petrylak D. Cytotoxic chemotherapy for advanced hormone-resistant prostate cancer. Cancer. 1993; 71: 1098-1109.

139. Schmid HP, McNeal JE, Stamey TA. Observations on the doubling time of prostate cancer. The use of serial prostate-specific antigen in patients with untreated disease as a measure of increasing cancer volume. Cancer. 1993; 71: 2031-2040.

140. Schmid HP. Tumour markers in patients on deferred treatment: prostate specific antigen doubling times. Cancer Surv. 1995; 23: 157-167.

141. Diamond E, Del Carmen Garcias M, Karir B, Tagawa ST. The evolving role of cytotoxic chemotherapy in the management of patients with metastatic prostate cancer. Current treatment options in oncology. 2015; 16: 324.

142. Zhu ML, Horbinski CM, Garzotto M, Qian DZ, Beer TM, Kyprianou N. Tubulin-targeting chemotherapy impairs androgen receptor activity in prostate cancer. Cancer Res. 2010; 70: 7992-8002.

143. de Leeuw R, Berman-Booty LD, Schiewer MJ, Ciment SJ, Den RB, Dicker AP, Kelly WK, Trabulsi EJ, Lallas CD, Gomella LG, Knudsen KE. Novel Actions of Next-Generation Taxanes Benefit Advanced Stages of Prostate Cancer. Clinical Cancer Research. 2015; 21: 795-807.

144. Berthold DR, Pond GR, Roessner M, de Wit R, Eisenberger M, Tannock AI. Treatment of hormone-refractory prostate cancer with docetaxel or mitoxantrone: relationships between prostate-specific antigen, pain, and quality of life response and survival in the TAX-327 study. Clin Cancer Res. 2008; 14: 2763-2767.

145. Sweeney C, Chen Y-H, Carducci MA, Liu G, Jarrard DF, Eisenberger MA, Wong Y-N, Hahn NM, Kohli M, Vogelzang NJ, Cooney MM, Dreicer R, Picus J*, et al.* Impact on overall survival (OS) with chemohormonal therapy versus hormonal therapy for hormone-sensitive newly metastatic prostate cancer (mPrCa): An ECOG-led phase III randomized trial. J Clin Oncol (Meeting Abstracts). 2014; 32: LBA2-.

146. de Bono JS, Oudard S, Ozguroglu M, Hansen S, Machiels J-P, Kocak I, Gravis G, Bodrogi I, Mackenzie MJ, Shen L, Roessner M, Gupta S, Sartor AO. Prednisone plus cabazitaxel or mitoxantrone for metastatic castration-resistant prostate cancer progressing after docetaxel treatment: a randomised open-label trial. The Lancet. 2010; 376: 1147-1154.

147. Tolis G, Ackman D, Stellos A, Mehta A, Labrie F, Fazekas AT, Comaru-Schally AM, Schally AV. Tumor growth inhibition in patients with prostatic carcinoma treated with luteinizing hormone-releasing hormone agonists. Proc Natl Acad Sci U S A. 1982; 79: 1658-1662.

148. Limonta P, Montagnani Marelli M, Moretti RM. LHRH analogues as anticancer agents: pituitary and extrapituitary sites of action. Expert Opin Investig Drugs. 2001; 10: 709-720.

149. Seidenfeld J, Samson DJ, Hasselblad V, Aronson N, Albertsen PC, Bennett CL, Wilt TJ. Single-therapy androgen suppression in men with advanced prostate cancer: a systematic review and meta-analysis. Ann Intern Med. 2000; 132: 566-577.

150. Moguilewsky M, Bertagna C, Hucher M. Pharmacological and clinical studies of the antiandrogen Anandron. J Steroid Biochem. 1987; 27: 871-875.

151. Sufrin G, Coffey DS. Flutamide. Mechanism of action of a new nonsteroidal antiandrogen. Invest Urol. 1976; 13: 429-434.

152. Furr BJ. Casodex: preclinical studies. Eur Urol. 1990; 18 Suppl 3: 2-9.

153. Group PCTC. Maximum androgen blockade in advanced prostate cancer: an overview of the randomised trials. Prostate Cancer Trialists' Collaborative Group. Lancet. 2000; 355: 1491-1498.

154. Mostaghel EA, Plymate SR, Montgomery B. Molecular pathways: targeting resistance in the androgen receptor for therapeutic benefit. Clin Cancer Res. 2014; 20: 791-798.

155. Chen CD, Welsbie DS, Tran C, Baek SH, Chen R, Vessella R, Rosenfeld MG, Sawyers CL. Molecular determinants of resistance to antiandrogen therapy. Nature medicine. 2004; 10: 33-39.

156. Korpal M, Korn JM, Gao X, Rakiec DP, Ruddy DA, Doshi S, Yuan J, Kovats SG, Kim S, Cooke VG, Monahan JE, Stegmeier F, Roberts TM*, et al.* An F876L mutation in androgen receptor confers genetic and phenotypic resistance to MDV3100 (enzalutamide). Cancer discovery.

2013; 3: 1030-1043.

157. Joseph JD, Lu N, Qian J, Sensintaffar J, Shao G, Brigham D, Moon M, Maneval EC, Chen I, Darimont B, Hager JH. A clinically relevant androgen receptor mutation confers resistance to second-generation antiandrogens enzalutamide and ARN-509. Cancer discovery. 2013; 3: 1020-1029.

158. Chan SC, Dehm SM. Constitutive activity of the androgen receptor. Adv Pharmacol. 2014; 70: 327-366.

159. Barrie SE, Potter GA, Goddard PM, Haynes BP, Dowsett M, Jarman M. Pharmacology of novel steroidal inhibitors of cytochrome P450(17) alpha (17 alpha-hydroxylase/C17-20 lyase). The Journal of steroid biochemistry and molecular biology. 1994; 50: 267-273.

160. Richards J, Lim AC, Hay CW, Taylor AE, Wingate A, Nowakowska K, Pezaro C, Carreira S, Goodall J, Arlt W, McEwan IJ, de Bono JS, Attard G. Interactions of abiraterone, eplerenone, and prednisolone with wild-type and mutant androgen receptor: a rationale for increasing abiraterone exposure or combining with MDV3100. Cancer Res. 2012; 72: 2176-2182.

161. Pejaver V, Hsu WL, Xin F, Dunker AK, Uversky VN, Radivojac P. The structural and functional signatures of proteins that undergo multiple events of post-translational modification. Protein science : a publication of the Protein Society. 2014; 23: 1077-1093.

162. Coffey K, Robson CN. Regulation of the androgen receptor by post-translational modifications. J Endocrinol. 2012; 215: 221-237.

163. van der Steen T, Tindall DJ, Huang H. Posttranslational modification of the

androgen receptor in prostate cancer. Int J Mol Sci. 2013; 14: 14833-14859.

164. Li J, Motlagh HN, Chakuroff C, Thompson EB, Hilser VJ. Thermodynamic dissection of the intrinsically disordered N-terminal domain of human glucocorticoid receptor. J Biol Chem. 2012; 287: 26777-26787.

165. Spolar RS, Record MT, Jr. Coupling of local folding to site-specific binding of proteins to DNA. Science. 1994; 263: 777-784.

166. Altarejos JY, Montminy M. CREB and the CRTC co-activators: sensors for hormonal and metabolic signals. Nat Rev Mol Cell Biol. 2011; 12: 141-151.

167. Baker JM, Hudson RP, Kanelis V, Choy WY, Thibodeau PH, Thomas PJ, Forman-Kay JD. CFTR regulatory region interacts with NBD1 predominantly via multiple transient helices. Nat Struct Mol Biol. 2007; 14: 738-745.

168. Mittag T, Marsh J, Grishaev A, Orlicky S, Lin H, Sicheri F, Tyers M, Forman-Kay JD. Structure/function implications in a dynamic complex of the intrinsically disordered Sic1 with the Cdc4 subunit of an SCF ubiquitin ligase. Structure. 2010; 18: 494-506.

169. Tompa P, Fuxreiter M. Fuzzy complexes: polymorphism and structural disorder in protein-protein interactions. Trends Biochem Sci. 2008; 33: 2-8.

170. Otieno S, Kriwacki R. Probing the role of nascent helicity in p27 function as a cell cycle regulator. PloS one. 2012; 7: e47177.

171. Borcherds W, Theillet FX, Katzer A, Finzel A, Mishall KM, Powell AT, Wu H, Manieri W, Dieterich C, Selenko P, Loewer A, Daughdrill GW. Disorder

and residual helicity alter p53-Mdm2 binding affinity and signaling in cells. Nat Chem Biol. 2014; 10: 1000-1002.

172. Mukherjee SP, Behar M, Birnbaum HA, Hoffmann A, Wright PE, Ghosh G. Analysis of the RelA:CBP/p300 interaction reveals its involvement in NF-kappaB-driven transcription. PLoS Biol. 2013; 11: e1001647.

173. Bienkiewicz EA, Adkins JN, Lumb KJ. Functional consequences of preorganized helical structure in the intrinsically disordered cell-cycle inhibitor p27(Kip1). Biochemistry. 2002; 41: 752-759.

174. Baek S, Kutchukian PS, Verdine GL, Huber R, Holak TA, Lee KW, Popowicz GM. Structure of the stapled p53 peptide bound to Mdm2. J Am Chem Soc. 2011; 134: 103-106.

175. Savkur RS, Burris TP. The coactivator LXXLL nuclear receptor recognition motif. J Pept Res. 2004; 63: 207-212.

176. White JH, Fernandes I, Mader S, Yang XJ. Corepressor recruitment by agonist-bound nuclear receptors. Vitam Horm. 2004; 68: 123-143.

177. Dasgupta S, Lonard DM, O'Malley BW. Nuclear receptor coactivators: master regulators of human health and disease. Annu Rev Med. 2014; 65: 279-292.

178. Mohammed H, Carroll JS. Approaches for assessing and discovering protein interactions in cancer. Molecular cancer research : MCR. 2013; 11: 1295-1302.

179. Mohammed H, D'Santos C, Serandour AA, Ali HR, Brown GD, Atkins A, Rueda OM, Holmes KA, Theodorou V, Robinson JL, Zwart W, Saadi A,

Ross-Innes CS*, et al.* Endogenous purification reveals GREB1 as a key estrogen receptor regulatory factor. Cell reports. 2013; 3: 342-349.

180. Krishnan N, Koveal D, Miller DH, Xue B, Akshinthala SD, Kragelj J, Jensen MR, Gauss CM, Page R, Blackledge M, Muthuswamy SK, Peti W, Tonks NK. Targeting the disordered C terminus of PTP1B with an allosteric inhibitor. Nat Chem Biol. 2014; 10: 558-566.

181. Lao BB, Drew K, Guarracino DA, Brewer TF, Heindel DW, Bonneau R, Arora PS. Rational design of topographical helix mimics as potent inhibitors of protein-protein interactions. J Am Chem Soc. 2014; 136: 7877-7888.

182. Ravindranathan P, Lee TK, Yang L, Centenera MM, Butler L, Tilley WD, Hsieh JT, Ahn JM, Raj GV. Peptidomimetic targeting of critical androgen receptor-coregulator interactions in prostate cancer. Nature communications. 2013; 4: 1923.

183. Pelka P, Ablack JN, Fonseca GJ, Yousef AF, Mymryk JS. Intrinsic structural disorder in adenovirus E1A: a viral molecular hub linking multiple diverse processes. J Virol. 2008; 82: 7252-7263.

184. Hammoudeh DI, Follis AV, Prochownik EV, Metallo SJ. Multiple independent binding sites for small-molecule inhibitors on the oncoprotein c-Myc. J Am Chem Soc. 2009; 131: 7390-7401.

APPENDIX: EPI-001 CHEMICAL SYNTHESIS AND ANALYSIS OF PURITY

General. Chemical reagents were typically purchased from Sigma-Aldrich and used without additional purification unless noted. Bulk solvents were from Fisher Scientific. N,N-dimethylformamide (DMF) was rendered anhydrous by passing through the resin column of a solvent purification system (MBraun). Reactions were performed under an atmosphere of dry N_2 unless noted. Silica gel chromatography was performed on a Teledyne-Isco Combiflash Rf-200 instrument utilizing Redisep R*f* Gold High Performance silica gel columns (Teledyne-Isco). Analytical HPLC analysis was performed on an Agilent 1200 series instrument equipped with a diode array detector and a Zorbax SB-C18 column (4.6 x 150 mm, 3.5 µm, Agilent Technologies). The method started with a 10% CH_3CN (with 0.1% trifluoroacetic acid (TFA)) in H_2O (0.1% TFA), the 10% CH_3CN (with 0.1% TFA) was increased to 15% over 2 minutes, increased to 20 % over 3 more minutes and then increased to 95% CH_3CN (with 0.1% TFA) over 25 minutes. Nuclear magnetic resonance (NMR) spectroscopy employed a Bruker Ascend instrument operating at 500 MHz (for ^1H) and 125 MHz (for ^{13}C) at ambient temperature. Chemical shifts are reported in parts per million and normalized to internal solvent peaks or tetramethylsilane. Mass spectrometry was recorded in positive-ion mode on an Agilent MSD SL Ion Trap.

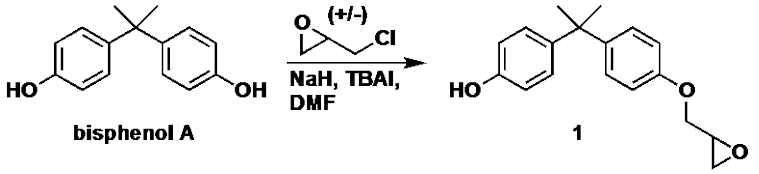

(4-hydroxyphenyl)(4-(oxiran-2-ylmethoxy)phenyl)methanone (**1**). This compound was prepared by modification to the previously reported procedure [REF. A1]. To a stirred solution of NaH (60% dispersion in oil, 1.453 g, 36.331 mmol) in anhydrous DMF (150 mL) at 0 °C was added bisphenol A (4.000 g, 16.514 mmol). The reaction was stirred for 30 min, then tetrabutylammonium iodide (1.220 g, 3.303 mmol) and epichlorohydrin (3.24 mL, 41.3 mmol) was added and the reaction was allowed to warm up to room temperature (rt) over 12 h. The reaction was quenched with water and extracted with ethyl acetate (3 x 50 mL). The organic layer was washed with water (2 x 30 mL), dried over Na_2SO_4, and concentrated *in vacuo*. The crude mixture was purified by silica gel chromatography (gradient CH_2Cl_2 to 10% EtOAc in CH_2Cl_2) to afford **1** (0.580 g, 12% yield) as a clear foam. ^1H NMR (DMSO-d_6): δ 9.15 (s, 1H), 7.09 (d, *J* = 8.5 Hz, 2 H), 6.98 (d, *J* = 8.5 Hz, 2 H), 6.83 (d, *J* = 8.5 Hz, 2 H), 6.64 (d, *J* = 8.5 Hz, 2 H), 4.26 (dd, *J* = 11.5, 2.5 Hz, 1 H), 3.78 (dd, *J* = 11.0, 6.5 Hz, 1 H), 3.29 (br s, 1 H), 2.82 (t, *J* = 4.5 Hz, 1 H), 2.69 (dd, *J* = 5.0, 2.5 Hz, 1 H), 1.55 (s, 6 H). ^{13}C NMR (DMSO-d_6): δ 155.9, 154.9, 143.2, 140.7, 127.4 (2), 127.3 (2), 114.6 (2), 113.8 (2), 68.8, 49.7, 43.8, 41.0, 30.8 (2). MS (m/z) calc'd for $C_{18}H_{20}O_3$ 284.1, found 285.1 $[M+H]^+$.

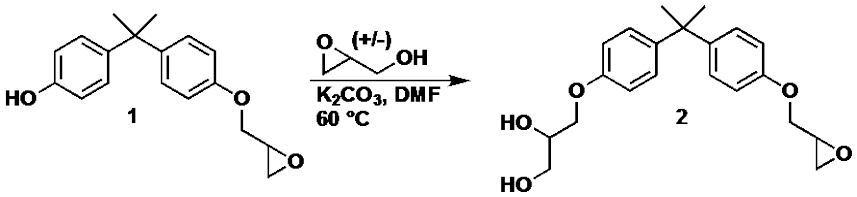

(4-(2,3-dihydroxypropoxy)phenyl)(4-(oxiran-2-ylmethoxy)phenyl)methanone (**2**). This compound was prepared as previously described [REF. 1]. To a stirred solution of **1** (0.493 g, 1.735 mmol) in anhydrous DMF (15 mL) at rt was added K_2CO_3 (0.480 g, 3.469 mmol) and glycidol (0.35 mL, 5.20 mmol). The reaction was stirred at 60 °C for 12 h. The reaction was cooled to rt, quenched with water and extracted with ethyl acetate (3 x 15 mL). The reaction mixture was washed with water (2 x 10 mL), dried over Na_2SO_4, and concentrated *in vacuo*. The crude mixture was purified by silica gel chromatography (gradient 10% EtOAc in CH_2Cl_2 to 50% EtOAc in CH_2Cl_2) to afford **2** (0.258 g, 41% yield) as a clear foam. ^{1}H NMR (DMSO-d_6): δ 7.09 (dd, *J* = 9.0, 7.0 Hz, 4 H), 6.83 (dd, *J* = 14.0, 8.5 Hz, 4 H), 4.89 (d, *J* = 5.0 Hz, 1 H), 4.62 (t, *J* = 5.5 Hz, 1 H), 4.26 (dd, *J* = 11.5, 2.5 Hz, 1 H), 3.94 (dd, *J* = 9.5, 4.0 Hz, 1 H), 3.82-3.74 (m, 3 H), 3.42 (t, *J* = 5.5 Hz, 2 H), 3.30 (br s, 1 H), 2.82 (t, *J* = 4.5 Hz, 1 H), 2.69 (dd, *J* = 5.0, 2.5 Hz, 1 H), 1.57 (s, 6 H). ^{13}C NMR (DMSO-d_6): δ 156.5, 156.0, 143.0, 142.4, 127.4 (2), 127.3 (2), 113.9 (2), 113.8 (2), 69.9, 69.4, 68.8, 62.7, 49.7, 43.7, 41.1, 30.7 (2). MS (m/z) calc'd for $C_{21}H_{26}O_5$ 358.2, found 381.2 $[M+Na]^+$.

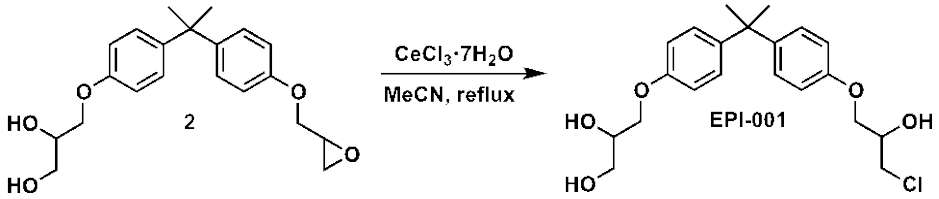

EPI-001. [REF. A1-A4] This compound was prepared by modification to the previously reported procedure [REF. A1]. To a stirred solution of **2** (0.164 g, 0.458 mmol) in CH_3CN (10 mL) was added $CeCl_3$ x $7H_2O$ (0.427, 1.146 mmol) and mixture was heated to reflux for 12 h. The reaction was cooled to rt, excess CH_2Cl_2 was added to the white paste and the cerium salts were removed by filtration. The filtrate was concentrated *in vacuo*. The resulting crude material was purified by silica gel chromatography (gradient 50% EtOAc in CH_2Cl_2 to 100% EtOAc) to afford EPI-001 (0.117 g, 64% yield) as a clear foam. ^{1}H NMR (DMSO-d_6): δ 7.09 (dd, *J* = 8.5, 5.0 Hz, 4 H), 6.82 (t, *J* = 9.5 Hz, 4 H), 5.52 (d, *J* = 5.5 Hz, 1 H), 4.90 (d, *J* = 5.0 Hz, 1 H), 4.63 (t, *J* = 5.5 Hz, 1 H), 4.02-3.99 (m, 1 H), 3.95-3.92 (m, 3 H), 3.82-3.72 (m, 3 H), 3.65 (dd, *J* = 11.0, 5.0 Hz, 1 H), 3.42 (t, *J* = 6.0 Hz, 2 H), 1.57 (s, 6 H) ^{13}C NMR (DMSO-d_6): δ 156.5, 156.1, 142.9, 142.4, 127.4 (2), 127.3 (2), 113.9 (2), 113.8 (2), 69.9, 69.4, 68.8, 68.6, 62.7, 46.8, 41.1, 30.7 (2). MS (m/z) calc'd for $C_{21}H_{27}ClO_5$ 394.2, found 417.2 $[M+Na]^+$.

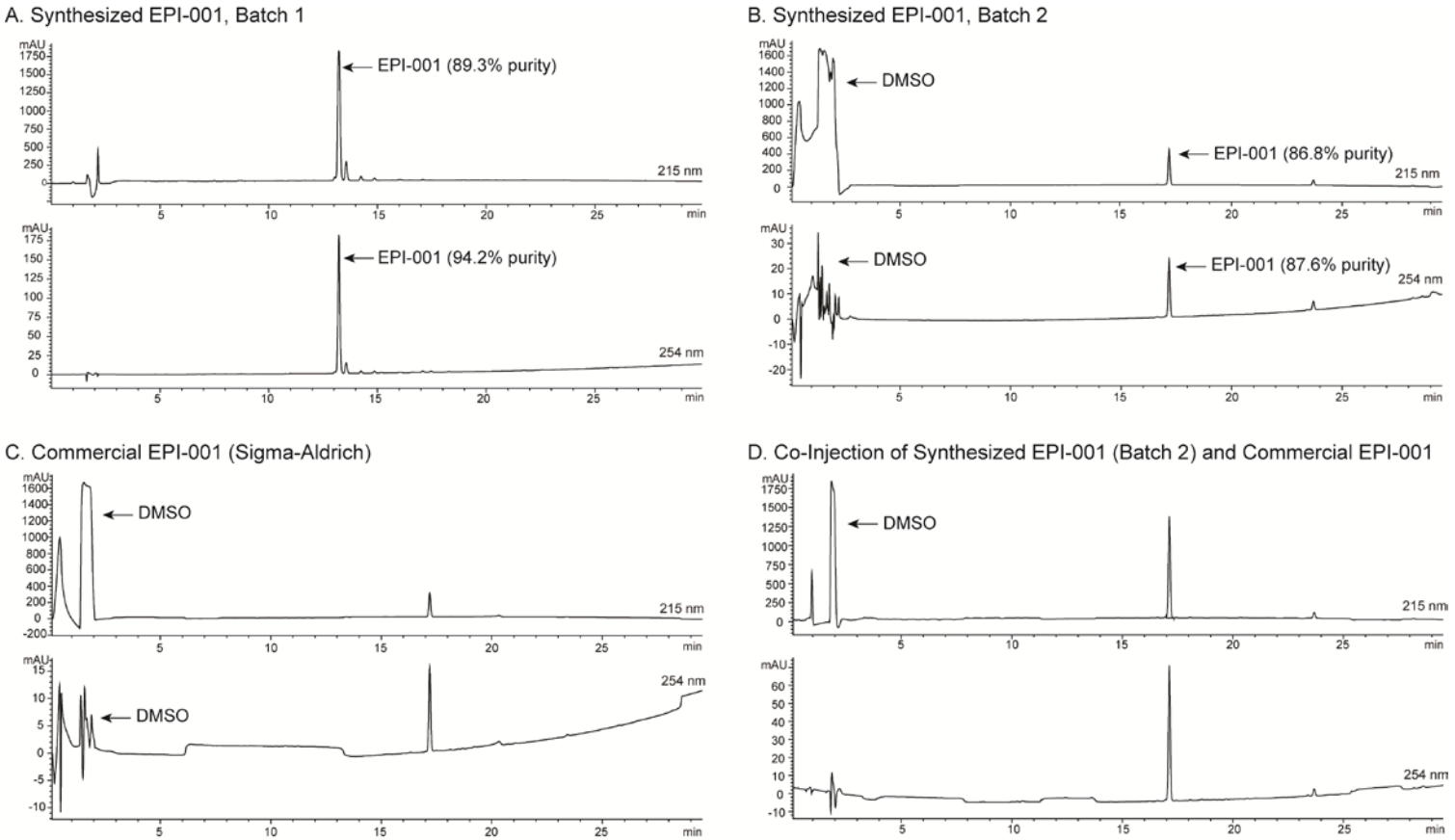

Appendix Figure A1: Analysis of Purity of Synthesized EPI-001 and Commercial EPI-001 (Sigma-Aldrich). Analysis of purity of synthesized and commercial EPI-001 by reverse-phase HPLC. Solutions were monitored at 215 and 254 nm. Please see General section under Synthesis of EPI-001 for HPLC column and elution conditions. Two batches of EPI-001 were synthesized. (*A*) Batch 1 of synthesized EPI-001, which was utilized in this study. (*B*) Batch 2 of synthesized material. (*C*) Analysis of commercial EPI-001 (Sigma-Aldrich Product # 92427). (*D*) Co-injection of synthesized EPI-001 (from panel *B*) and commercial EPI-001 (panel *C*), which further demonstrates the compounds are identical. NOTE: Retention times for synthesized EPI-001, Batch 1 and Batch 2 (panels *A* and *B*) are slightly different because they were analyzed almost two years apart and HPLC column performances vary with use. ^{1}H NMR spectra of batches 1 and 2 are identical.

Appendix Figure A2 (continues)

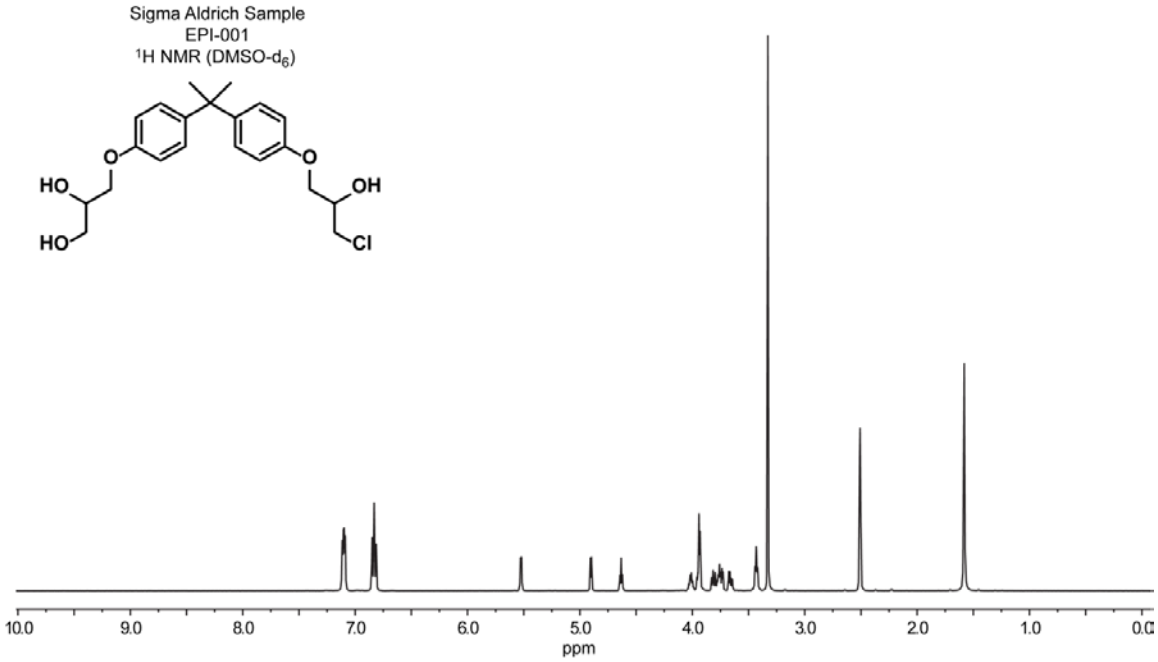

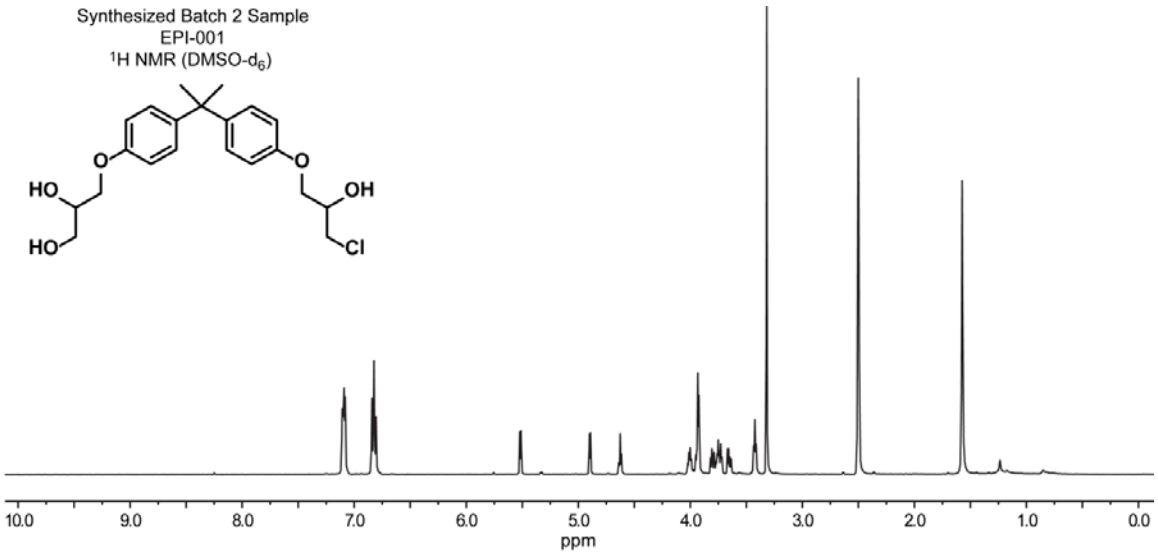

Appendix Figure A2 (Cont.)

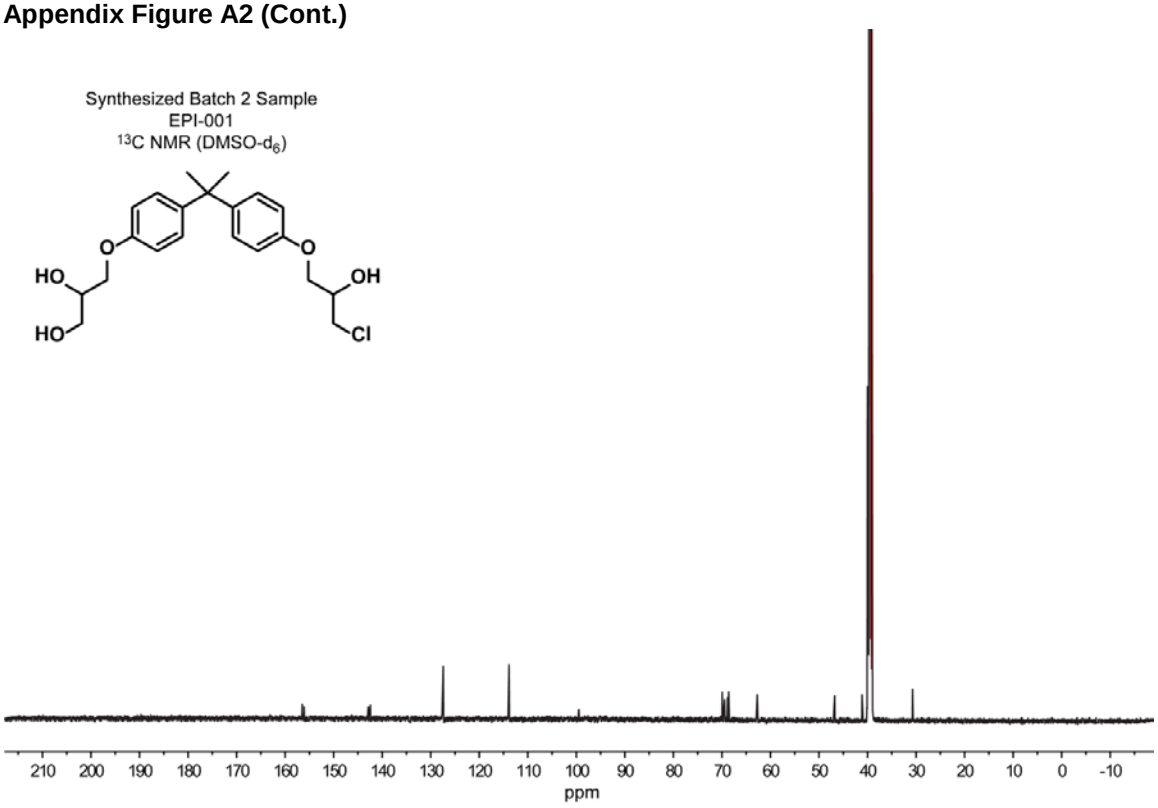

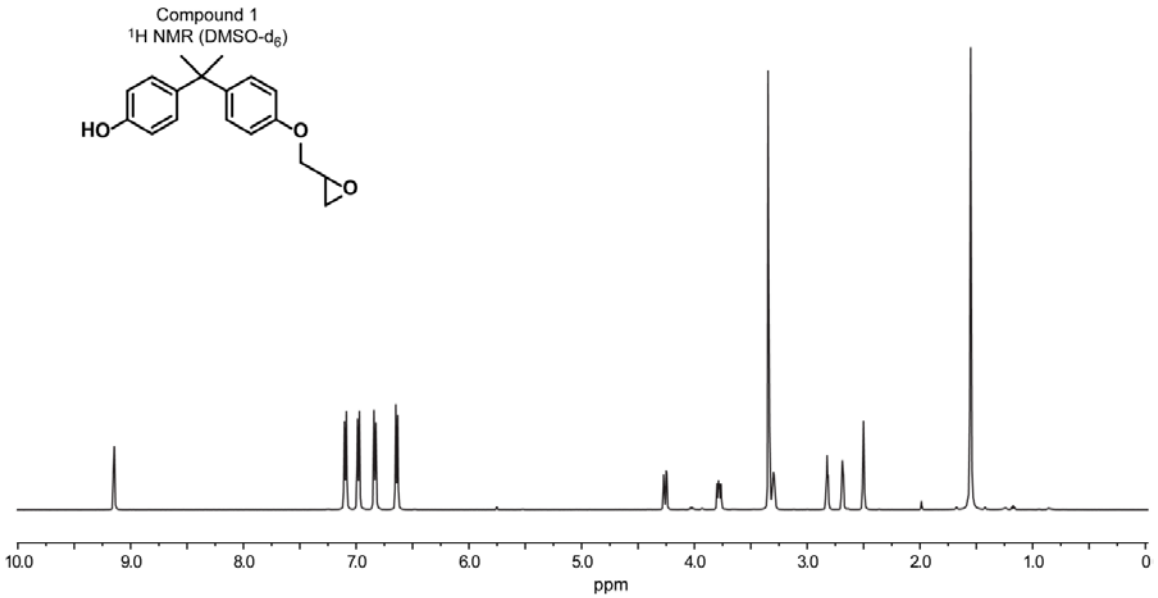

Appendix Figure A2 (Cont.)

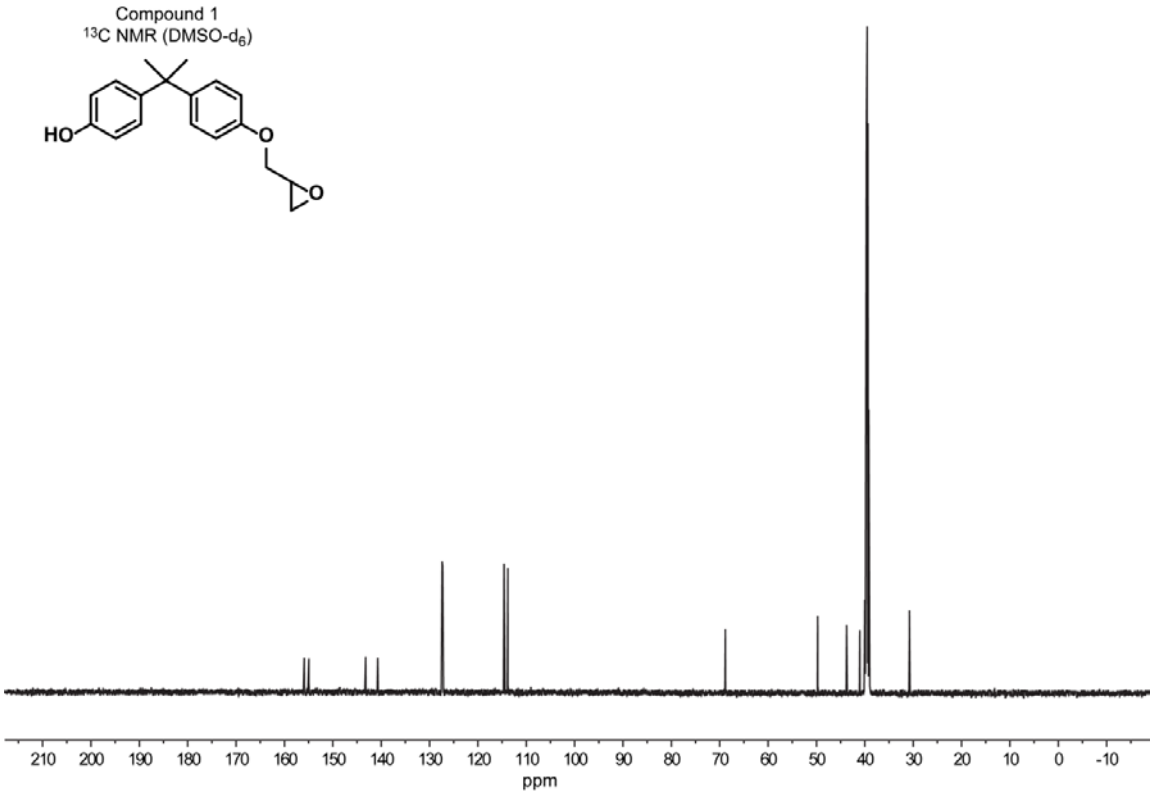

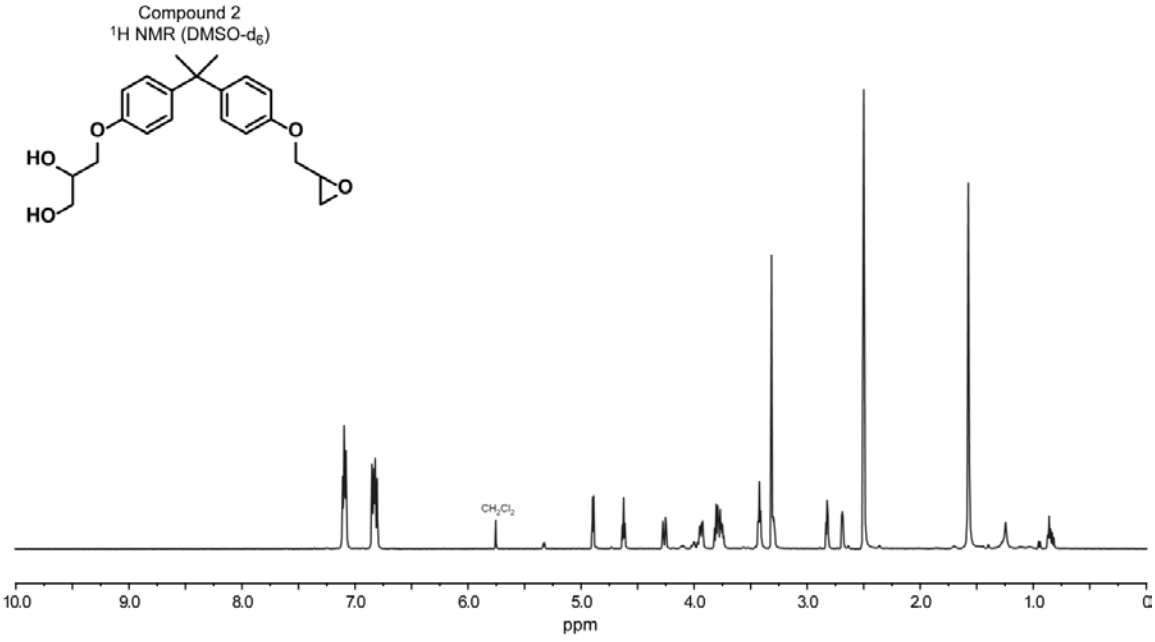

Supplementary Figure S2 (Cont.)

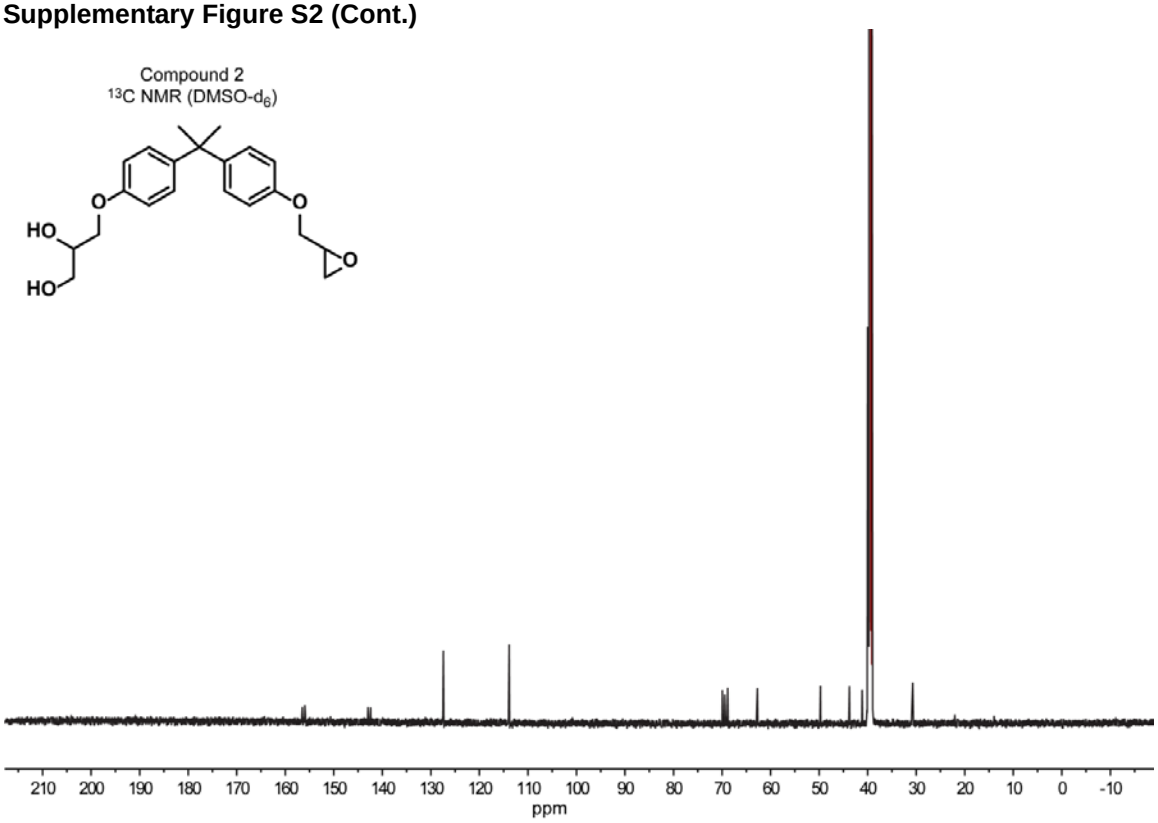

Appendix Figure A2: NMR Spectra of Commercial EPI-001, Synthesized EPI-001 and Reaction Intermediates.

Appendix Figure A3

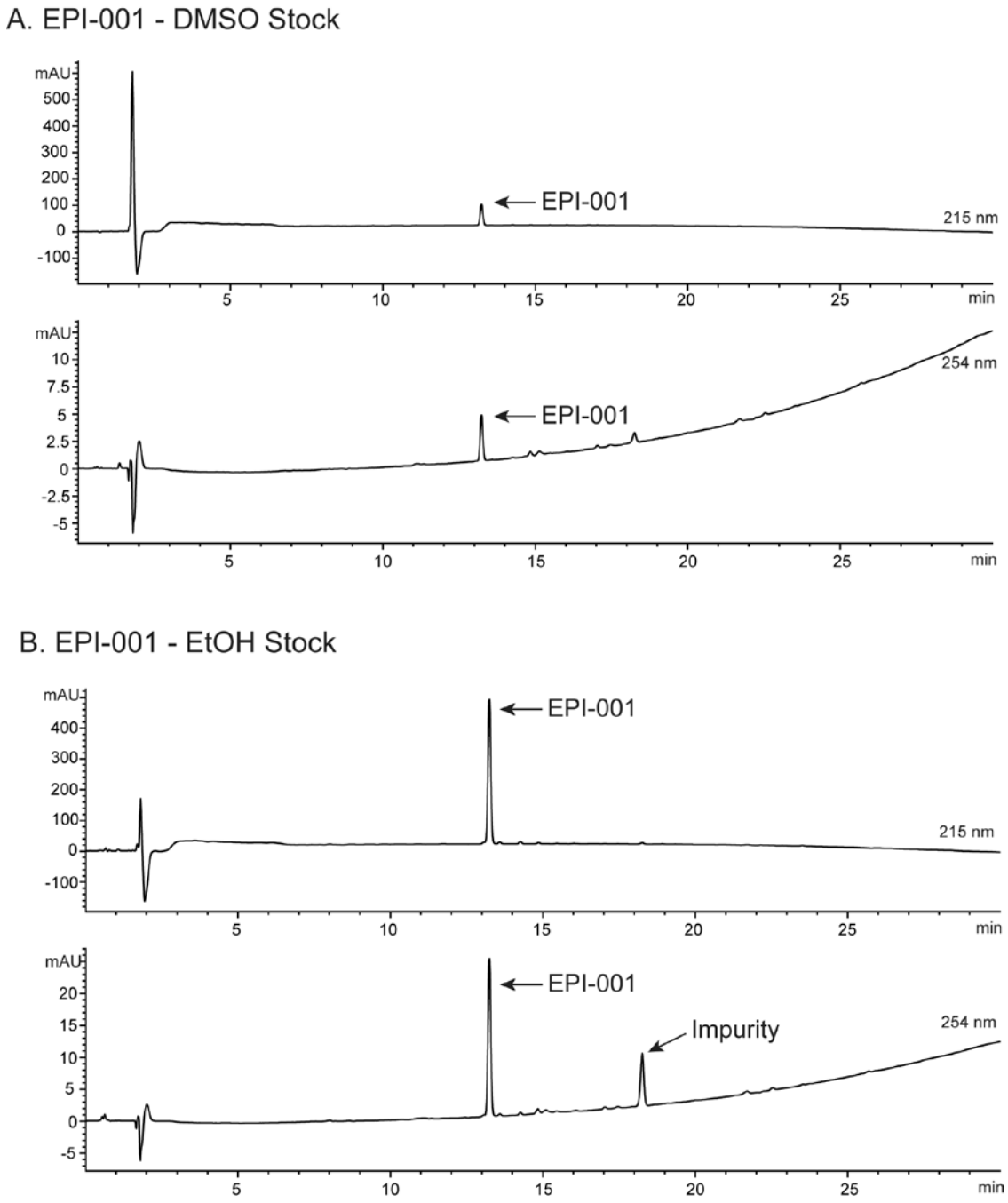

Appendix Figure A3: Stability of EPI-001 Stock Solutions in DMSO and Ethanol. Analysis of purity of EPI-001 solutions prepared in either DMSO (panel A) or EtOH (panel B). Stock solutions were prepared by dissolving lyophilized drug in either EtOH or DMSO at a concentration of 100 mM overnight at 4^{o} C. Stocks were stored at 4^{o} C for up to six months for use in experimentation. A substantial impurity was observed in the 254 nm channel for EPI-001 solutions prepared in EtOH. Following detection of the impurity, all stock solutions were prepared in DMSO and aliquoted for storage at -20^{o} C to prevent decomposition.

APPENDIX REFERENCES

1. Sadar, MD; Mawji, NR; Wang, J; Anderson, RJ; Williams, DE; Leblanc, M. Patent publication WO 2010000066 A1, January 7, 2010. International application PCT/CA2009/000902.
2. Anderson RJ, Mawji NR, Wang J, Wang G, Haile S, Myung J-K, Watt K, Tam T, Yang YC, Bañuelos CA, Williams DE, McEwan IJ, Wang Y, Sadar MD. Cancer Cell 2010; 17:535.
3. Rauter, W.; Dickinger, G.; Zihlarz, R.; Lintschinger, J. Z Lebensm.-Unters.-Forsch A 1999; 208:208.
4. Lintschinger J, Rauter W. Eur. Food. Res. Technol. 2000; 211 211.